CENTRO INTERNACIONAL DE ESTUDOS
DE DOUTORAMENTO E AVANZADOS
DA USC (CIEDUS)

TESE DE DOUTORAMENTO

IN VIVO REPROGRAMMING OF ISCHEMIC BRAIN AS A NEW THERAPEUTICAL WAY AT THE ISCHEMIC STROKE

Ignacio José López Loureiro

ESCOLA DE DOUTORAMENTO INTERNACIONAL

PROGRAMA DE DOUTORAMENTO EN MEDICINA MOLECULAR

SANTIAGO DE COMPOSTELA

2019

USC
UNIVERSIDADE
DE SANTIAGO
DE COMPOSTELA

DECLARACIÓN DO AUTOR/A DA TESE

IN VIVO REPROGRAMMING OF ISCHEMIC BRAIN AS A NEW THERAPEUTICAL WAY AT THE ISCHEMIC STROKE

D./Dna. Ignacio José López Loureiro

Presento a miña tese, seguindo o procedemento axeitado ao Regulamento, e declaro que:

1) A tese abarca os resultados da elaboración do meu traballo.
2) De selo caso, na tese faise referencia ás colaboracións que tivo este traballo.
3) A tese é a versión definitiva presentada para a súa defensa e coincide coa versión enviada en formato electrónico.
4) Confirmo que a tese non incorre en ningún tipo de plaxio doutros autores nin de traballos presentados por min para a obtención doutros títulos.

En Santiago de Compostela, 11 de outubro de 2019

Asdo. Ignacio José López Loureiro

USC
UNIVERSIDADE
DE SANTIAGO
DE COMPOSTELA

AUTORIZACIÓN DO DIRECTOR/TITOR DA TESE

In vivo reprogramming of ischemic brain as a new therapeutical way at the ischemic stroke.

D. José Castillo Sánchez

D. Francisco Campos Pérez

D. Tomás Sobrino Moreiras

INFORMA/N:

Que a presente tese, correspóndese co traballo realizado por D. ***Ignacio José López Loureiro****, baixo a miña dirección, e autorizo a súa presentación, considerando que reúne os requisitos esixidos no Regulamento de Estudos de Doutoramento da USC, e que como director desta non incorre nas causas de abstención establecidas na Lei 40/2015.*

En Santiago de Compostela, 11 de outubro de 2019

Asdo.

José Castillo Sánchez Francisco Campos Pérez Tomás Sobrino Moreiras

USC
UNIVERSIDADE
DE SANTIAGO
DE COMPOSTELA

Conflict of interest

The author and the directors of the work agreed to present the results in this Thesis and declare no conflict of interest.

USC
UNIVERSIDADE
DE SANTIAGO
DE COMPOSTELA

Research stay

During the development of the Thesis the PhD student performed a stay in an international laboratory, in the University of Hamburg, Germany, with the Professor Wolfgang Parak from 15th of January to 15th of July 2019.

USC
UNIVERSIDADE
DE SANTIAGO
DE COMPOSTELA

Funding

This study was supported by the Spanish Ministry of Economy and Competitiveness (SAF2014-56336-R), Xunta de Galicia (Consellería de Educación: GRC2014/027 and Axencia Galega de Innovación), Instituto de Salud Carlos III (PI14/01879), Spanish Research Network on Cerebrovascular Diseases RETICS-INVICTUS (RD16/0019), and the European Union FEDER program.

The sponsors did not participate in study design, collection, analysis, interpretation of the data, writing the report, or the decision to submit the paper for publication.

USC
UNIVERSIDADE
DE SANTIAGO
DE COMPOSTELA

Summary

Tradicionalmente el ictus se ha clasificado como un déficit neurológico inducido por un daño agudo de causa vascular. La consiguiente pérdida neuronal esta comúnmente asociada con un déficit motor y/o cognitivo que puede ser fácilmente detectado por exploración clínica u observado con pruebas de neuroimagen.

Según la Organización Mundial de la Salud (OMS), 15 millones de personas sufren un ictus cada año. Los estudios epidemiológicos indican que un tercio de esas personas mueren, mientras que otro tercio queda en situación de dependencia. Estos datos sitúan al ictus como segunda causa de muerte (11.1% del total de muertes en 2012) y primera causa de discapacidad.

En los países desarrollados de nuestro entorno, las muerte y discapacidad asociada al ictus seguirá incrementando en los próximos años debido al envejecimiento de la población. Estudios recientes han pronosticado un incremento de más del 35% en la incidencia del ictus para 2035. De cumplirse estos pronósticos, Europa tendría que enfrentarse a un coste económico asociado al ictus de 45 billones de euros debido a pérdida de productividad de la población activa, gastos sanitarios e impacto familiar. Este enorme gasto económico y social obliga a la sociedad a hacer un esfuerzo en la investigación

de esta enfermedad para aumentar nuestro entendimiento y poder desarrollar terapias efectivas que minimicen su impacto.

El ictus puede clasificarse en dos grandes grupos (ictus hemorrágico e ictus isquémico) diferenciados por las características que ocasionan el daño vascular. El ictus hemorrágico se caracteriza por una extravasación de la sangre debido a una ruptura del vaso sanguíneo. Es el responsable del 20% de los ictus y está asociado a una mayor mortalidad. Mientras que el ictus isquémico es debido a una isquemia causada por una hipoperfusión del tejido cerebral que puede tener distintos orígenes. El ictus isquémico tiene una mayor importancia social y económica al ser la primera causa de discapacidad permanente. Esto se debe a su baja mortalidad en comparación con el ictus hemorrágico.

El ictus isquémico puede clasificarse en: Aterotrombótico, lacunar, cardioembólico e indeterminado según su etiología.

El daño producido en el ictus isquémico se debe a la obstrucción aguda del flujo sanguíneo cerebral. Esta obstrucción corta el aporte de oxígeno y nutrientes en la zona de irrigación de los vasos afectados. Dentro de la zona afectada se pueden distinguir dos subzonas: 1) el núcleo isquémico, porción de tejido más próxima al vaso sanguíneo y donde la isquemia es más severa. 2)zona de penumbra, la reducción del flujo de sanguíneo es

menos dramática gracias al aporte de la circulación colateral del tejido circundante. El impacto de la isquemia en esta zona dependerá del aporte de la circulación colateral y del tiempo de permanencia de la hipoperfusión. Razón por la cual el tiempo es un factor clave en el tratamiento del ictus.

Varios procesos moleculares se desarrollan en la progresión de la enfermedad a lo largo del tiempo, podemos dividirlos en 4 fases: Hiperaguda (entre los primeros minutos a las primeras 2-3 horas), Aguda (entre las primeras horas y 1-2 días), subaguda (entre el tercer día y las primeras semanas) y tardía (a partir de las 3-4 semanas después del evento isquémico).

En la fase hiperaguda se producen una serie de cambios fisiológicos ligados a la interrupción del flujo de oxígeno: Ruptura de la barrera hematoencefálica, fallo energético, desbalance iónico y excitotoxicidad.

La barrera hematoencefálica está formada por la unión estrecha de las células endoteliales de los capilares cerebrales. Estas células actúan como un filtro que permite la existencia de un microambiente extracelular único del sistema nervioso cerebral que es imprescindible para la función de las células cerebrales. A pesar del que la principal función de la barrera recae en las células endoteliales, la formación y función de la barrera depende de la relación de varios tipos celulares entre los que

destacan: células endoteliales, pericitos, astrocitos, neuronas y microglía. A esta interacción estructural y funcional se la conoce como unidad neurovascular.

Tan pronto como como comienza el evento isquémico, los cambios de presión sanguínea dañan las células endoteliales y resienten la funcionalidad de la barrera hematoencefálica. Este daño a su vez se ve acrecentado por el déficit de nutrientes y desencadena una extravasación de sustancias de la sangre al parénquima, incrementando el daño causado por la hipoxia.

El daño causado por la hipoxia se sucede a varios niveles. En primer lugar, la reducción de los niveles de ATP compromete el funcionamiento de las bombas iónicas que mantienen los potenciales de membrana. La entrada masiva de calcio y cambio osmótico producido por el desbalance iónico activan las rutas de señalización apoptóticas de la célula. Paralelamente la despolarización debida al desajuste iónico produce la liberación masiva de glutamato, neurotransmisor excitador que va a incrementar la despolarización de las neuronas circundantes mediante la activación de los receptores NMDA y AMPA en un proceso denominado excitotoxicidad.

En la fase aguda (2-3 horas después del evento isquémico) se produce un incremento del estrés oxidativo que excede los mecanismos antioxidantes celulares. La producción de estrés

oxidativo se debe al incremento de las especies reactivas del oxígeno en los procesos de respiración anaerobia ligados a la hipoxia y a la disfunción mitocondrial. Este desajuste de los niveles de especies reactivas de oxígeno afecta a proteínas, lípidos y ácidos nucleicos. Por lo tanto, tiene un gran impacto en la actividad enzimática, metilación del ADN y peroxidación lipídica. El mal funcionamiento de estos procesos desencadena una respuesta apoptótica en la célula.

En esta fase también comienza la respuesta inflamatoria asociada al daño isquémico. En condiciones de isquemia se activa la población de microglía y comienza la producción de moléculas proinflamatorias que producen la activación de la respuesta inflamatoria en la zona lesionada. Esta señalización atrae a células del sistema inmune (neutrófilos y macrófagos) no presentes en el sistema nervioso central en condiciones fisiológicas que van a acrecentar todavía más la respuesta inflamatoria.

Ya en la fase subaguda (primeros días después del evento isquémico) comienza una proliferación de los astrocitos que rodean la zona dañada. Esta respuesta, es conocida como gliosis reactiva. Los astrocitos de las áreas circundantes a la zona isquémica sufren un proceso de desdiferenciación caracterizado por una rápida división, cambios morfológicos (hipertrofia) y la

sobreexpresión de la proteína ácida fibrilar glial (GFAP). Este proceso de rápida división de los astrocitos va a culminar en la formación de la cicatriz glial, una barrera de astrocitos cuyo rol es aislar la zona de la lesión para evitar la extravasación de sustancias tóxicas al tejido sano.

En la fase tardía (semanas después del evento isquémico) continua la formación de la cicatriz, fibroblastos procedentes de los vasos dañados y de las meninges proliferan por la zona lesionada secretando moléculas de matriz para rellenar los espacios dejados por las células muertas, formando la llamada cicatriz fibrótica.

Durante esta fase los procesos más agudos descritos en fases precias se reducen drásticamente y comienzan a activarse los procesos reparadores: angiogénesis, neurogénesis y neuroplasticidad. Sin embargo, estos procesos (poco eficaces en mamíferos) no son capaces de regenerar la zona dañada ni (en la mayoría de los casos) recuperar la función que desempeñaban esas áreas cerebrales ahora desaparecidas. Es por ello que el desarrollo de terapias que ayuden a limitar el área afectada por la lesión y/o ayuden a la neuroreparación, son claves para el futuro de nuestra sociedad.

En la actualidad los profesionales sanitarios solo disponen de dos tratamientos para el ictus isquémico. Uno farmacológico, el

activador del plaminógeno tisular (tPA) y otro mecánico, la trombectomía. Ambos son tratamientos neuroprotectores que solo son eficaces si son aplicados en fase aguda (primeras horas tras el ictus isquémico). Estas limitaciones temporales son las responsables de que pocos pacientes se puedan beneficiar de estos tratamientos. Es por lo tanto imprescindible para la sociedad el dotar a los profesionales sanitarios de nuevos tratamientos que puedan ser usados con efectividad en fases más tardías de la enfermedad.

En los últimos años se ha hecho un gran esfuerzo por desarrollar terapias regenerativas. Estas terapias se basan en el uso de fármacos, terapia celular y nuevas técnicas de reprogramación celular para tratar de recuperar la zona de la lesión.

Las técnicas de reprogramación celular son las más novedosas y prometedoras de entre las técnicas neuroreparadoras. Esta tecnología permite la transformación de una célula madura en otro tipo celular. Esto permite abrir nuevos horizontes en numerosas enfermedades, en la actualidad esta terapia se está aplicando a cerebro, corazón, ojos, etc.

Dentro de la reprogramación podemos distinguir entre la reprogramación de células pluripotentes y la reprogramación directa. La primera está basada en la obtención de células pluripotentes mientras que la segunda se refiere al cambio

fenotípico entre tipos celulares sin pasar por el estado de pluripotencia. Al saltarse el estado de pluripotencia también se solventan los problemas de seguridad y éticos que acompañan al uso de las células pluripotentes inducidas. Esto le otorga una importante ventaja para el desarrollo de terapias traslacionales.

Para llevar a cabo la reprogramación (tanto la reprogramación de células pluripotentes como la reprogramación directa) es necesario inducir un cambio de la expresión génica de la célula. Esto se puede hacer por diferentes vías: usando factores de transcripción, RNAs de interferencia o pequeñas moléculas.

Los factores de transcripción son el método más empleado para llevar a cabo la reprogramación celular. Estos factores inducen la transcripción de RNA mensajeros clave para el proceso de cambio de tipo celular.

Los RNA de interferencia son moléculas de RNA que por complementariedad de bases inducen la degradación de RNA mensajeros. Esto permite la modificación de la expresión de la célula de una forma similar al uso de los factores de transcripción.

Las pequeñas moléculas son compuestos químicos que tienen la capacidad de activar o inhibir determinadas rutas de señalización. La modificación de las rutas de señalización celular

condiciona a la célula a un cambio de la expresión génica y por consiguiente un cambio de su fenotipo celular.

De entre estos mecanismos de reprogramación celular el primero y más común es el uso de los factores de transcripción. Sin embargo, también es el menos traslacional ya que para su vectorización eficiente es necesario el empleo de un virus que los exprese endógenamente en la célula diana. Los virus pueden inducir una expresión estable en la célula, tienen una baja toxicidad y pueden ser eficientemente vectorizados a la célula diana por distintas estrategias (promotores, cápsides, etc). Aunque esta metodología es muy eficiente en investigación, su traslación a la clínica presenta grandes inconvenientes.

Por ello, los ARN interferentes y pequeñas moléculas son las estrategias más prometedoras en la investigación traslacional. Ya que tienen la ventaja de que pueden ser eficientemente encapsulados en otras plataformas más seguras, baratas y eficientes (como las nanopartículas). De entre estas dos estrategias traslacionales, cabría destacar el uso de los RNA por su potencial especificidad en el silenciamiento de ARNs. Mientras que las pequeñas moléculas actúan a un nivel mucho más general en la modificación de rutas de señalización, activando y/o inhibiendo receptores. El uso de los RNA interferentes está asociado a una modulación más fina y

controlada de los patrones de expresión celulares. Los RNA interferentes y nuevas plataformas de vectorización como las nanopartículas, abren un nuevo campo de desarrollo de alternativas con múltiples posibilidades terapéuticas.

En los últimos años se están desarrollando interesantes estrategias para el tratamiento del ictus isquémico basadas en la reprogramación directa. De entre ellas podemos destacar el aprovechamiento de la proliferación de la gliosis reactiva en la zona peri-infarto para llevar a cabo reprogramación de los astrocitos y convertirlos en una población de neuronas o neuroblastos que pueda tener un impacto positivo en la recuperación de la zona dañada por la isquemia. En esta estrategia se aprovecha por una parte la gran proliferación celular que ocurre en un área localizada al lado de la zona lesionada y, por otra parte, las características inmaduras de los astrocitos en proliferación. En teoría estos astrocitos serían más susceptibles de llevar a cabo los procesos de reprogramación ya que ellos mismos sufren un proceso de reprogramación endógena en su transformación de astrocito maduro con una baja tasa de proliferación a astrocito reactivo.

En este sentido, recientemente se ha descubierto una estrategia basada en el silenciamiento de la ruta de señalización NOTCH1 en astrocitos para su conversión en células progenitoras

neurales. Sin embargo, los hallazgos realizados hasta ahora utilizando esta estrategia se basan en el uso de ratones transgénicos, muy útiles para el descubrimiento de nuevas posibilidades terapéuticas pero cuyos resultados tienen escaso valor traslacional. Es por ello necesario el desarrollo de un estudio que evalúe las posibilidades terapéuticas de este nuevo posible tratamiento, sin perder de vista la traslacionalidad.

Basándonos en la estrategia de silenciamiento de NOTCH1 descrita previamente, fue hipotetizado que el uso de pequeños RNAs de interferencia contra la ruta de señalización NOTCH1 podría inducir una reprogramación *in vitro* de los astrocitos en un proceso mediado por la sobreexpresión de la proteína ASCL1. También se hipotetiza que la reprogramación *in vivo* de astrocitos de la cicatriz glial influencia la recuperación del daño isquémico en un modelo animal de isquemia cerebral. Finalmente, también se hipotetiza que el uso de plataformas de liberación alternativas a los virus, como las nanocapsulas de sílice, podrían mediar una liberación efectiva de los RNAs *in vitro*.

Para testar estas hipótesis se han desarrollado los siguientes objetivos:

-Optimización de un cultivo de astrocitos para la realización de los experimentos *in vitro.*

-Búsqueda del tratamiento más efectivo para el silenciamiento de la ruta de señalización NOTCH1.

-Estudio de la efectividad del silenciamiento de la ruta de señalización Notch en la reprogramación de astrocitos.

-Estudio de la evolución de la cicatriz glial durante los primeros días de evolución de un modelo animal de infarto cerebral.

-Estudio del efecto de la expresión de los siRNAs contenidos en un vector viral en el silenciamiento de la ruta de señalización NOTCH1.

-Comprobar el efecto del silenciamiento de la ruta de señalización NOTCH1 en la recuperación de un modelo animal de isquemia cerebral.

-Sintetizar y caracterizar las nanocapsulas de sílice para su potencial uso como agente de transfección.

-Comprobar la habilidad de las nanocapsulas para liberar su carga dentro de los astrocitos.

Nuestros resultados *in vitro* mostraron que en ambos tratamientos (RNAs contra *Rbpj* y *Hes1*) la inhibición de la ruta de señalización NOTCH1 estaba asociada con un incremento en la expresión del RNA mensajero del factor pro-neurogénico *Ascl1*. Sorprendentemente, la inhibición de *Hes1*, pese a ser

menos eficiente que la inhibición de *Rbpj*, inducía un mayor incremento en la expresión de *Ascl1*. Paradójicamente, los resultados muestran que la sobreexpresión del ARN mensajero de *Ascl1*, no induce una sobreexpresión de la proteína ASCL1. Es más, en el tratamiento contra *Rbpj* incluso inhibe la expresión de ASCL1 a 72h. Estos resultados parecen sugerir que ASCL1 presenta una tasa de recambio baja y que su incremento de expresión podría producirse más allá de los 7 días (tiempo máximo del seguimiento). Otra posibilidad sería que ASCL1 estuviera sometida a un fuerte regulamiento postranscripcional que inhibiera el incremento de la síntesis proteica.

En los experimentos de formación de neurosferas con los tratamientos inhibidores para NOTCH1 no se encontró diferencias significativas en el número de neurosferas del grupo tratado comparado con el grupo control. Esto podría deberse a un efecto tóxico del agente de trasnfección (lipofectamina) que impidiera observar el efecto del tratamiento. Otra posibilidad es el estado inmaduro del cultivo de astrocitos (de origen fetal) favorezca la desdiferenciación espontanea de las células en un medio libre de FBS.

Los estudios *in vivo* no muestran una reducción del volumen de infarto ni mejora en la ejecución de los test funcionales en el grupo tratado comparado con el grupo control. Tampoco se

observó un incremento del marcador característico de neuroblastos (DCX) en estudios proteicos o de inmunofluorescencia. Varios factores pueden estar influenciando estos resultados. Por una parte, la pequeña zona de difusión del virus dificulta la obtención de unos resultados claros en el estudio proteico. Por otro lado, el tiempo de seguimiento (21 días) quizá sea demasiado escaso para la obtención de marcadores positivos de neuroblastos. En futuros experimentos sería conveniente extender el tiempo del seguimiento y evaluar marcadores de neurogénesis más tempranos como ASCL1.

Para tratar de realizar un enfoque traslacional, diseñamos, caracterizamos y empleamos una plataforma de liberación alternativa para el tratamiento basado en ARNs. Estas nanocapsulas demostraron una gran eficacia en su habilidad para internalizarse en el interior celular y liberar el tratamiento en el interior de la célula. La evaluación del silenciamiento debido al ARN introducido dentro de las nanopartículas, probó la efectividad de esta estrategia. Este dato abre una nueva vía para el uso de plataformas alternativas al uso de los virus para la vectorización de tratamientos basados en ARNs.

Teniendo en cuenta los resultados expuestos anteriormente pudimos concluir lo siguiente:

1. El tratamiento con el RNA silente para Rbpj induce la sobreexpresión de Ascl1 a través de la inhibición de la ruta de señalización de NOTCH1 durante 7 días.
2. El tratamiento con el RNA silente para Hes1 induce la sobreexpresión de Ascl1 a través de la inhibición de la ruta de señalización de NOTCH1 durante 7 días.
3. El RNA contra Hes1 ha demostrado ser más efectivo que el RNA contra Rbpj en la sobreexpresión de Ascl1.
4. El tratamiento con RNA silentes no ha demostrado una reprogramación de los astrocitos in vitro.
5. Los astrocitos reactivos de la cicatriz glal desarrollan su máxima expresión a las 72 horas del modelo de isquemia cerebral. La gliosis se mantiene al menos hasta los 7 días.
6. El tratamiento con RNAS vectorizados con AAV5 no reveló una reducción del volumen de infarto o mejora funcional.
7. Las capsulas de sílice biodegradables son capaces de entrar en la célula a través de endocitosis.
8. El tratamiento encapsulado en las nanopartículas induce una reducción de expresión del gen diana, abriendo nuevas posibilidades terapéuticas para su uso como vector de tratamientos en la isquemia cerebral.

USC
UNIVERSIDADE
DE SANTIAGO
DE COMPOSTELA

Agradecimientos

Se suele decir que los agradecimientos son la parte más personal de la tesis, donde debes plasmar la gratitud hacia todo el equipo que ha contribuido al desarrollo del trabajo y a tu formación como investigador. Siguiendo un sabio consejo, intentaré no extenderme demasiado ni pasarme de sentimental.

En primer lugar, tengo que agradecer a mis directores de tesis la oportunidad de trabajar en este laboratorio. Su dedicación ha permitido dotar a este trabajo de infraestructura, reactivos y salario. José Castillo, Tomás Sobrino, Francisco Campos, gracias por formar a un equipo tan extraordinario y hacerme partícipe de él.

Gracias Ramón y Pablo, esta tesis no habría sido posible sin vosotros. Sois una fuente de buenos consejos (científicos y no científicos).

Joserra, tú eres el cerebro del equipo ¿Qué más puedo decir? Me has ayudado siempre con buenos consejos y buenas acciones. Gracias por no perder la paciencia y estar siempre disponible.

Gracias Andrés, Esteban y Alba, de vosotros he aprendido no solo a ser un investigador (o intentarlo), sino otras cosas mucho

más importantes. No podríais ser más distintos, pero a la vez encajar de una forma tan perfecta. Sois un ejemplo y una guía para todos, ha sido un placer teneros de maestros.

María, cuando entré en el laboratorio tú me enseñaste los primeros pasos de esta carrera que es la tesis. Gracias por tener tanta paciencia conmigo.

Gracias Bárbara por tus sinceros consejos, cuánta razón tenías.

Gracias Juan por tener ese humor tan genial y, junto con Ramón, hacernos pasar tan buenos ratos.

Clara, gracias por todo lo que me has ayudado. Tengo que dar gracias también a la normativa que te obligó a cursar un máster (sin necesitarlo) y que hizo posible que nos encontráramos.

Héctor, empezamos juntos y acabamos juntos (aún duramos…). Ha sido un placer compartir este camino contigo y gracias por tus lecciones de latín.

Manuel y Dopico, a lo largo de la historia los triunviratos no siempre acabaron bien. Sin embargo, puedo decir que vosotros habéis sido un apoyo imprescindible para mí dentro y fuera del laboratorio (y pensar que en la carrera me caíais mal).

Compañeros: Vanesa, Tania, Fernando, Uxía, Adrián, Paulo, Ana, Elena, Marta, Antía. No me llega la extensión de esta tesis para

mostraros mi agradecimiento. Siempre habéis estado disponibles para ayudar en cuestiones científicas y no científicas. Ha sido un placer compartir esta experiencia con vosotros. Sin duda, hacéis de este desfiladero que es la tesis, un camino mucho más ameno. Gracias por dotar, a este espacio físico que es el laboratorio, de un ambiente de trabajo tan agradable.

Gracias a mis amigos Alberto, Jaime, Andrés, Ricky y Marcote. Aunque entre amigos sobran los agradecimientos, me habéis ayudado siempre y cuento con que lo sigáis haciendo, gracias.

Gracias también a Jimmy y a Seijo porque fueron los que me motivaron, hace ya muchos años, a intentar entender cómo funcionan las cosas.

Muchas gracias a los clínicos del grupo, Miguel, Manuel, Susana, Emilio, Iria, María, Isabel, Clara, Juan, Aida y Gema, vosotros siempre habéis dado un punto de vista distinto y necesario a la actividad investigadora de este equipo.

Gracias, Wolfgang Parak y Neus Feliu por acogerme en vuestro laboratorio. Gracias también a todos los compañeros de Hamburgo: Germán, Michele, Manuel, Tim, Shati, Heiko, Yalang, Yang, Marvin, Martin, Marten, Saad y a todo el equipo.

Gracias a mi familia, papá, mamá, Paula y a los abuelos. Lo que me habéis enseñado vale más que cualquier tesis o

conocimiento. La educación que me habéis inculcado es el tesoro más valioso que tengo, gracias.

Gracias M. porque tú has sido, mi directora de tesis, mi amiga, mi compañera y mi psicóloga. Me has apoyado y ayudado en todo, compartido momentos alegres y tristes, pero siempre siendo un pilar fundamental en la felicidad de mi día a día.

“No hay felicidad o infelicidad en este mundo; sólo hay comparación de un estado con otro. Solo un hombre que ha sentido la máxima desesperación es capaz de sentir la máxima felicidad. Es necesario haber deseado morir para saber lo bueno que es vivir”

Alejandro Dumas

“Cuando emprendas tu viaje a Ítaca
pide que el camino sea largo.
Lleno de aventuras, lleno de experiencias”

Constantino Cavafis

“Donde no falta voluntad siempre hay un camino”

J.R.R. Tolkien

USC
UNIVERSIDADE
DE SANTIAGO
DE COMPOSTELA

Index

USC
UNIVERSIDADE
DE SANTIAGO
DE COMPOSTELA

LIST OF ABBREVIATIONS AND ACRONYMS

AAV: Adeno-associated viruses

Ad: Adenoviruses

AIF: Apoptosis-inducing factor

AMPA: α-amino-3-hydroxy-5-methyl-4-isoxazol propionic acid

AMPArs: α-amino-3-hydroxy-5-methyl-4-isoxazol propionic acid receptors

Apaf-1: Apoptotic protein-activating factor-1

ATP: Adenosine tri-phosphate

AU: Arbitrary units

BBB: Blood-brain barrier

BDNF: Brain-derived neurotrophic factor

CBF: Cerebral blood flow

CCA: Common carotic artery

COX-2: Cyclooxigenase-2

CNS: Central Nervous System

DAMPs: Danger-/damage-associated molecular patterns

DIV: Days *in vitro*

DISC: Death-inducing signalling complex (p31)

dsDNA: double-stranded DNA

ECA: External carotid artery

ECM: Extracellular matrix

ESCs: Embryonic stem cells

FA: Flip angle

FGF: Fibroblast growth factor

FOV: Field of view

G-CSF: Granulocyte-colony stimulating factor

GFAP: Glial fibrillary protein

HDAC: histone deacetylase

HIF1: Hypoxia-inducible factor-1

HIV: Human immunodeficiency virus

HRE: Hypoxia response element

ICA: Internal carotid artery

ICAM-1: Intercellular adhesión molecule-1

IDLVs: Integration-deficiente lentiviral vectors

IGF-1: Insulin growth factor-1

IFN-γ: Interferon gamma

IL-1: Interleukin-1

IL-4: Interleukin-4

IL-6: Interleukin-6

IL-8: Interleukin-8

IL-10: Interleukin-10

IL-12: Interleukin-12

IL-23: Interleukin-23

iPSCs: Induced pluripotent stem cells

miRISC: miRNA induced silencing complex

MLV: Murine leukemia virus

MMPs: Matrix metalloproteinases

MNCs: Marron-nuclear cells

MSME: Multi-slide multi-echo

mPTP: Mitochondrial permeability transition pore

MCA: Middle cerebral artery

MSCs: Mesenchymal stem cells

NECD: Notch extracellular domain

NICD: Notch intracellular domain

NMDA: N-methyl-D-aspartate glutamatergic

NMDArs: N-methyl-D-aspartate glutamatergic receptors

NO: Nitric oxide

NOS: Nitric oxide synthase

ODD: Oxygen-dependent degradation domain

OMM: Outer mitochondrial membrane

PDE5: Phosphodiesterase 5

PEG: Polyethylene glycol

RARE: Rapid Acquisition with Refocused Echoes

RPE: Retinal pigment epithelial

RNS: Reactive nitrogen species

ROS: Reactive oxygen species

r-tPA: Recombinant tissue plasminogen activator

SGZ: Subgranular zone of the dentate gyrus

SSRIs: Selective serotonin inhibitors

ssRNA: single-stranded RNA

SVZ: Subventricular zone of the lateral ventricles

SW: Spectral bandwidth

Tc: T cytotoxic lymphocytes

TE: Echo time

Th: T helper lymphocytes

tMCAO: Transitory middle cerebral artery

TR: Repetition time

Treg: T regulatory lymphocytes

TIA: Transient ischemic attack

TNF: Tumour necrosis factor

TNFrs: Tumour necrosis factor receptors

VCAM-1: Vascular cell adhesion molecule-1

VEGF: Vascular endothelial growth factor

1.Introduction

1.1. Stroke

1.1.1. Definition

Classically, stroke has been defined as a neurological deficit induced by an acute focal injury in the central nervous system (CNS) due to vascular cause. The consequent alterations of normal cerebral blood flow usually lead to an injury to the surrounding neural tissue. The resulting loss of neural function is commonly associated with the impairment of cognitive and/or motor behaviour in patients. Thus, it can be easily detected by clinical exploration or observed by neuroimaging techniques[1][2].

The term "Stroke" was coined by William Cole in its work "*A Physico-Medical Essay Concerning the Late Frequencies of Apoplexies*" (1648). However, since long before him Hippocrates had used the term "apoplexy" for describing this disease in 400 BC. The definition of stroke disease has evolved during human history, changing along with a better understanding of the disease. Nevertheless, popular culture is still using the term introduced by Hippocrates to refer about this disease[3].

1.1.2. Epidemiology

According to the World Health Organization (WHO), 15 million people suffer a stroke every year worldwide. Epidemiological studies suggest that 5 million of these would probably die from this cause and another 5 million are likely to be permanently disabled. These data reveal that stroke is becoming the second leading cause of mortality (11.1% of total deaths by 2012) after heart disease and the main cause of long-term disability. Therefore, stroke should be considered as a costly disease from the human, familial and societal perspectives[4][5][6].

In developed countries as in the case of the European Union nations, the consequences of stroke-related death and disability will be dramatically increased in the near future due to the ageing of the population. According to recent studies, the number of stroke events is expected to increase from 613,000 per year in 2015 to 820,000 by 2035. It means an increase of more than 35%, despite of the healthy lifestyle, reduced risk factors and improved treatments. Economically, Europe would be facing a €45 billion-cost of stroke in less than two decades, mostly related to losses in productivity, the spending in health care and the impact on familial lifestyle[7][8].

1.1.3. Classification of stroke

Focusing on the nature of the lesion, stroke can be classified in two main groups, named ischemic and haemorrhagic stroke. The differences between them rely on the characteristics of the blood flow disturbance.

However, alternative classifications of this cerebrovascular disease can be used considering other parameters such as stroke subtype, progression profile, neuroimaging properties, size and the mechanisms of induction and aetiology[9][10].

1.1.3.1 Haemorrhagic stroke

The haemorrhagic stroke consists of blood extravasation as a result of the breakage of a blood vessel. The consequent bleeding, which can take place in brain parenchyma, ventricular or subarachnoid space, produces an increased intracranial pressure and cell toxicity resulting in cell death and the later loss of brain function.

The most frequent causes of haemorrhagic stroke include: arteriolar hypertensive disease (30–60%), amyloidal angiopathy (10–30%), drugs (among them, anticoagulation treatments are the most significant 1–20%), and vascular structural lesions (3–8%). Other less frequent causes are toxics such alcohol and

cocaine and brain tumours, among others. In about 5-20% of the cases, the underlying cause remains undetermined[11][2].

Haemorrhagic stroke account for less than 20% of all strokes and it is commonly associated to a higher mortality. It should be noted that this classification only includes the haemorrhages caused by vascular events (i.e. non-traumatic blood vessel rupture) and thus, the traumatic haemorrhages cannot be defined as strokes[11][12].

1.1.3.2 Ischemic stroke

The ischemic stroke is the most prevalent type of stroke, representing about the 80% of all strokes. Although ischemic stroke is associated with a lower mortality rate when compared to haemorrhagic subtype, it remains the main cause of permanent disability owing to its higher incidence and improved survival rate[8].

The term “ischemic stroke” can be referring to global or focal ischemia. The global ischemia is related to a hipoperfusion of all brain tissue, mostly induced by cardiac arrest [13]. On the other hand, focal brain ischemia defines an ischemic condition restricted to a certain area of the brain. Within this division, it is also possible to differentiate between transient ischemic attack

(TIA) and cerebral infarction. TIA is defined as a focal cerebral dysfunction originated by an arterial thrombus or embolism and it is often, associated to a pre-existing arterial, cardiac or hematologic disease. Although its symptoms normally disappear after less than an hour, TIA patients present a higher risk of subsequent stroke and other vascular episodes, being the outcome of each patient extraordinarily variable. On the other side, the cerebral infarction is a lesion caused by an intense or prolonged ischemia in which the loss of functional neural tissue is irreversible and it is followed by clinical symptoms and abnormalities in neuroimaging tests[9][14][15].

On the basis of aetiology and clinical presentation, the cerebral infarction can be divided in the different ischemic stroke subtypes presented below:

- *Atherothrombotic* infarctions account for the 20% of cerebral infarctions and they are generally accompanied by middle or large sized infarcts with cortical, subcortical, carotid or vertebro-basilar topography. In these patients, the presence of one or several cerebrovascular risk factors coincides with clinically generalized atherosclerosis, or the demonstration of occlusion or stenosis (>50% occlusion or <50% plus two or more

vascular risk factors) in cerebral arteries, with an established correlation to the patient's clinic.

- *Lacunar* infarction or small vessel disease represents the 25% of ischemic strokes and it is characterized by a small sized infarct (<15 mm of diameter), localized in the distribution territory of the penetrating arterioles. Although micro-atheromatosis and lipohialinosis of penetrating arterioles are the most frequent pathologic substrate in lacunar infarcts, other less frequent potential causes include cardiac embolism, arterial embolism, infectious arthritis or prothrombotic state.

- *Cardioembolic* infarctions reach close to the 20% of overall ischemic events and they generally include medium (1,5-3 cm of diameter) or large (>3 cm of diameter) sized infarcts, with the onset of symptoms frequently starting during early morning awakening. It is also imperative the presence of a demonstrated embolic origin as well as, the absence of significant concomitant arterial occlusion or stenosis.

- The etiology of the remaining 30-35% cerebral infarctions is considered to be *undetermined* with brain infarcts of

medium or large size with more than two potential etiologies or unknown origin.

1.1.2. Biochemistry of cerebral ischemia

The acute obstruction of a brain artery instantaneously prevents normal blood flow and oxygen from reaching the corresponding irrigation area (focal ischemia). However, the interruption of the blood supply is not homogeneous and it may vary depending on the occluded vessel, collateral ramification of the vessels or occlusion type[9].

Two regions can be distinguished within the infarct region: 1) the ischemic core, which is the portion of tissue closest to the affected blood vessel and where the ischemia becomes severe, and 2) the ischemic penumbra, where the reduction of blood flow supply is less noticeable, thanks to the blood flow from collateral arteries of the non-ischemic neighbour tissue. The impact of brain ischemia will depend on the extent to which the artery is occluded and the duration of a diminished blood flow, which is the reason why timing is a key parameter in successful stroke diagnosis and treatment[16].

Shortly after the onset of brain ischemia, the interruption of oxidative phosphorylation processes and the deficient

production of adenosine tri-phosphate (ATP) trigger a cascade of molecular events initiated with an energetic failure in cells. The dysfunction of sodium-potassium-ATPase pumps and other mechanisms involved in ATP production generally lead to the cessation of transmembrane ionic gradients. The resulting energetic imbalance is one of the pivotal factors which contribute to the physiopathology of stroke (i.e. cell death in the ischemic core, particularly if the vascular occlusion is sustained after few minutes)[17][18].

Therefore, a new scenario arises as the entrance of sodium, chloride and calcium into the cell cytoplasm causes an extreme depolarization both in neurons and glial cells [19]. At the same time, the release of potassium from cells induces a sudden increase of its extracellular levels[20]. As a consequence of the energetic failure and the associated ionic changes, it is originated an increment in glutamate, which causes the hyperexcitability of N-methyl-D-aspartate glutamatergic (NMDA) receptors (NMDAr), and of α-amino-3-hydroxy-5-methyl-4-isoxazol propionic acid (AMPA) receptors (AMPArs), which in turn enhances the initial increase of intracellular calcium[21][22][23].

The increase of intracellular calcium levels does not exclusively depend on the activation of glutamate receptors, but also on the stimulation of Ca^{2+} voltage-dependent channels. This induced

hyperexcitability causes a depolarization phenomenon in the periphery of the infarct, what it contributes to an even higher cellular energy consumption while the membrane tries to re-polarize itself[24][25].

The combination of an increase in intracellular calcium levels, acidosis and peri-infarct depolarization contributes to promote the ischemic damage [26][27]. During the artery reperfusion that follows an ischemic episode, the generation of free radicals occurs. Free radicals are highly reactive species that can be originated in several stages of brain ischemia. In first place, the oxygen reactive species (ROS) can be either generated by the metabolism of arachidonic acid or by the activity of neuronal nitric oxide (NO) synthase (NOS). During intermediate stages, free oxygen radicals are provided by the infiltration of neutrophils in the ischemic area. At later stages, these highly reactive species are produced via the synthesis and activation of inducible NO synthase enzymes (iNOS) and cycloxigenase-2(COX2). These dysfunctions at the molecular level are followed by neuroinflammation processes and apoptotic cell death which contribute to the worsening and the extension of the lesion [28][29]

Even considering the above-mentioned molecular disturbances as typical features of stroke, ischemic cellular death can take

place in two different manners. Necrosis in the core region of the lesion zone is the most common, with cells first undergoing morphological changes and finally cell lysis which also provokes neuroinflammation [30]. On the other hand, apoptotic processes are typical from (i.e. programmed cell death) the region surrounding the core region and they can be observed when energy-dependent intracellular mechanisms are activated, leading to cell degradation[23][31].

1.1.3. Physiopathology of ischemic stroke

Ischemic stroke is a dynamic process, consisting on a fast-developing acute phase, followed by a slow or delayed process of reparation (**Figure 1**). To comprehensively describe the molecular and cellular mechanisms underlying ischemic stroke, they were grouped under four temporal phases: hyperacute (first minutes to hours), acute (first hours to days), subacute (first weeks) and delayed (first months after ischemic event).

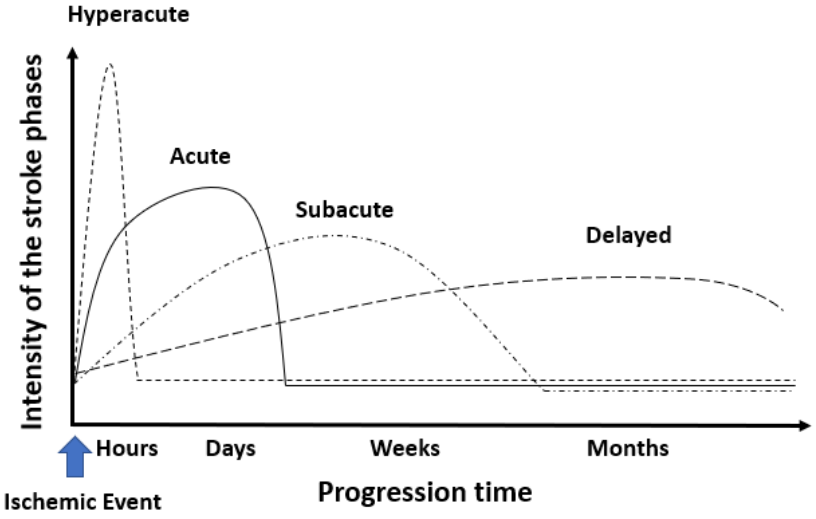

Figure 1. Temporal profile of physiopathological processes induced by cerebral ischemia. Self-created figure.

1.1.3.1. Hyper acute phase

Hyper acute phase includes the cellular and biochemical changes that take place just after blood flow interruption, from the first minutes to the first 2-3 hours of injury evolution. The main physiopathological events concern the blood-brain barrier (BBB) disruption, the energetic failure, the ionic imbalance and the resulting excitotoxicity and endoplasmic reticulum stress.

1.1.3.1.1. Blood-Brain Barrier disruption

The CNS provides an enabling biochemical microenvironment for cell survival and for the transmission of electrical and chemical signals between neurons. The particularity of this environment is preserved through the presence of the BBB that, acting as a selective filter, maintains a stable scenario for functional nervous cells. The BBB also has a critical role in ion regulation, neurotransmitters compartmentalization and protein and neurotoxin isolation outside the CNS[32].

In the mammalian brain, the endothelial cells that form the walls of the capillaries reduce their permeability when entering the CNS so that they increase their selectivity to give rise to the BBB. The barrier acts as a physical barrier (i.e. tight junctions between cells that limit the molecular exchange between the lumen and the parenchyma), a transport barrier (i.e. enhancing the specific transport of solute flux), and as a metabolic barrier (i.e. enzymes metabolizing molecules in transit). The barrier function is not static, but can be modulated and regulated, both in physiological and pathological conditions as in the ischemic stroke [33].

Despite of the alleged key role of the endothelial cells in the BBB formation and function, the role of the BBB depends on the crosstalk between endothelial cells, pericytes, astrocytes, neurons and microglia. This functional and structural interaction

is called neurovascular unit (**Figure 2**) [34]. Both, pericytes (a fibroblast-like cells with contractile capacity) and glial cells, surround the vessels giving structural and nutritional support to the BBB while neuronal signalling inform about nutrient or oxygen specific requirements. Microglia, for its part, has key immunoregulatory functions[35][36].

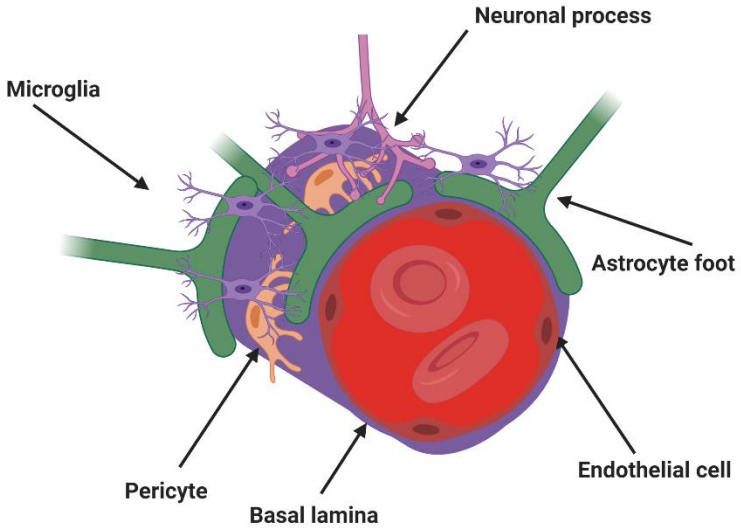

Figure 2. Schematic representation of the neurovascular unit. Self-created figure using biorender academic license.

The neurovascular unit is considerably vulnerably to a stroke-induced damage. As soon as the ischemic event starts, the changes in blood pressure that take place in the affected vasculature immediately injure the endothelium and

intercellular junctions. In addition, the subsequent lack of O_2 and nutrients undermine the BBB integrity leading to an increased paracellular and transcellular permeability (**Figure 3**).

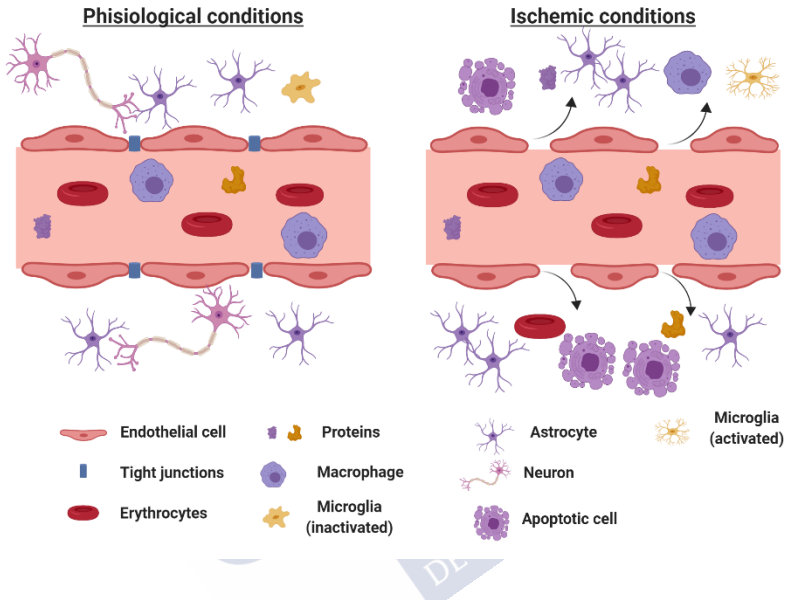

Figure 3. Blood-brain barrier in physiological and ischemic conditions. Self-created figure using Biorender academic license.

Therefore, in an ischemic context, the extravasation of blood cells, chemicals and fluids into brain parenchyma is produced because of the forementioned BBB impairment. Brain homeostasis is then disrupted and the massive entrance of water through disturbed aquaporins and other intercellular damaged junctions provoke the formation of a vasogenic edema.

Other consequences do not take long to appear: the enclosed neural microenvironment virtually disappears due to the uncontrolled entrance of ions, proteins and neurotoxic substances. The infiltration of leukocytes gives rise to an exacerbated neuroinflammatory response. Taken together, these phenomena aggravate brain injury and increase the risk for haemorrhagic transformation[37][38].

To sum up, the BBB disruption in two stages. In the first one (i.e. early disruption), the altered blood pressure and nutrient depletion damage the endothelial cells which mainly constitute the BBB. In the late disruption stage, highly reactive species such as ROS activate the matrix metalloproteinases (MMPs). These enzymes are capable of degrading collagen and laminin in the basal lamina and ultimately disrupt the integrity of BBB. Indeed, late disruption is the natural consequence of a complex scenario in which neuroinflammation, cell necrosis, metalloproteinases and alterations in gene expression contribute to increase the BBB permeability[39].

1.1.3.1.2. Energy failure

The CNS requires a huge energetic demand to sustain neuronal activity. The oxygen consumption of the brain is very high relative to its weight (the brain consumes approximately 20% of the total oxygen intake). This is understandable given its increased metabolism and the need to maintain membrane potentials, a process energetically expensive but indispensable to ensure cellular excitability. In physiological conditions, neurons and glial cells obtain their energy from aerobic glucose metabolism, or in extreme cases, from the aerobic metabolism of ketonic bodies. Nonetheless, during an ischemic event, the levels of O_2 and glucose fall below their desirable ranges, even reaching critical limits due to the interruption of blood supply. Anaerobic metabolism is not as efficient as the aerobic one and the available glucose in the brain is rapidly depleted. The main repository for glycogen storage is found in astrocytes, also phosphocreatine can provide a short-term energy reserve. However, in contrast to what happens in the liver, the brain has not as much storage capacity so that in a very brief period of time (as short as two minutes) a mismatch between ATP use and production leads to loss of membrane potentials and activation of cell death pathways[40][41][42].

1.1.3.1.3. Ionic imbalance

The Na^+/K^+ ATPase is responsible for the maintenance of Na^+ ions outside the cellular membrane and K^+ inside the cytoplasm. Nevertheless, the reduction in ATP synthesis disables this cationic pump and the polarity of cell membrane cannot be preserved, allowing Na^+ and Cl^- to penetrate the cell. This overall ionic imbalance, causes cellular depolarization, increased osmolality and an easier entrance of water into the cell producing cell swelling (**Figure 4**). Moreover, the Na+ imbalance blocks the Na+/Ca2+ exchange protein, responsible for the Ca2+ movement outside the cell, causing a Ca2+ accumulation inside the cytoplasm. The higher concentration of Ca2+ in the intracellular space promotes the activation of the apoptotic route and it also may produces the cell necrosis [43].

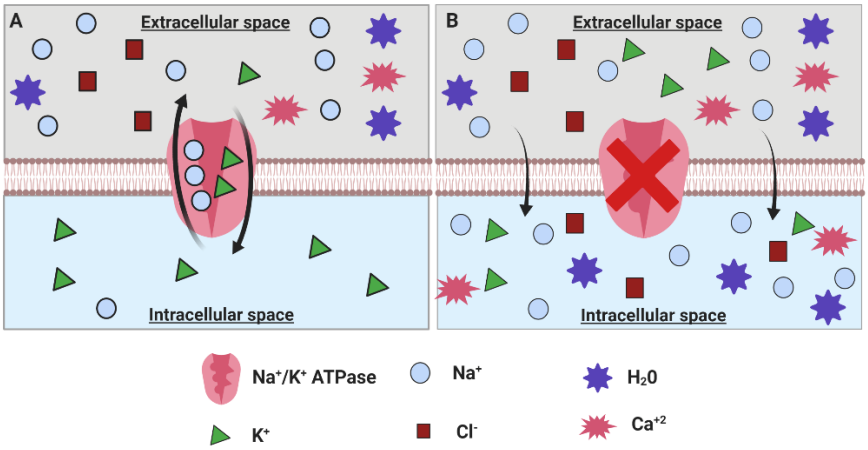

Figure 4. (A) In physiological conditions, the presence of ATP allows the Na^+/K^+ ATPase to maintain Na^+ in the extracellular space and K^+ in the cytosol. However, in ischemic conditions**. (B)** the lack of O2 produce a drop in ATP levels, Na^+ is accumulated in the cytosol facilitating the entrance of Cl^-, water and Ca^{+2}. While water produce cell swelling, Ca^{+2} activates apoptotic pathways. Self-created figure using Biorender academic license**.**

1.1.3.1.4. Excitotoxicity

Glutamate is the most abundant excitatory neurotransmitter in the brain, and it exerts its action through two main types of receptors, named ionotropic receptors (i.e. ligand-gated ion channels) and metabotropic receptors (G-protein coupled receptors). The release of glutamate by neurons is affected by the cellular depolarization due to the $Na^+/K^+/Ca^{2+}$ imbalance that accompanies the ischemic episode. Under these conditions, the

glutamate is released in large amounts, overloading physiological levels and thus becoming toxic [44].

The glutamate-associated excitoxicity in stroke can be partly explained by the overstimulation of N-methyl-D-aspartate receptors (NMDAr) and alpha-amino-3-hydroxy-5-methylisoxazole-4-propionate receptors (AMPAr) at the postsynaptic level. The activation of these non-selective ionotropic receptors allows the Na^+ and Ca^{2+} cations to enter the postsynaptic neuron where they will induce a process of depolarization. This contributes to calcium overload which in turn activates calcium-dependent enzymes, increasing the levels of highly reactive species provoking a signalling cascade which results in cell death[45][42](**Figure 5**).

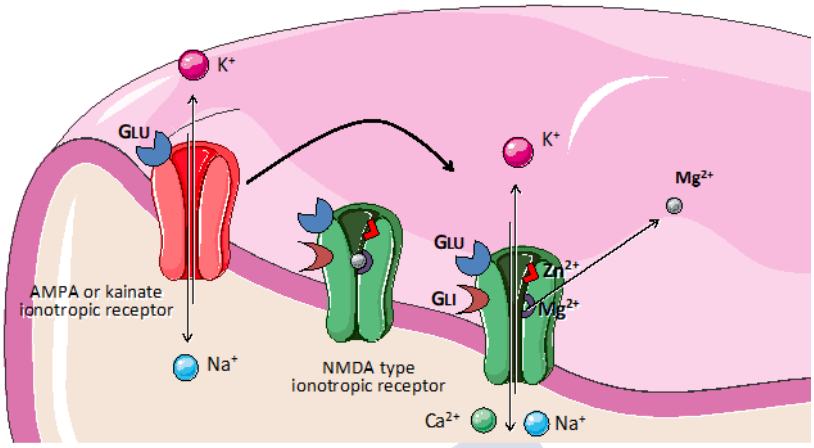

Figure 5. Role of glutamate on the stimulation of AMPA and NMDA receptors during cerebral ischemia. Self-created image using elements with a creative commons license.

1.1.3.2. Acute phase

The acute phase begins 2-3 hours after stroke, and it develops during the next few days post ischemic episode. This phase is physiopathologically characterised by severe oxidative and nitrosative stress and associated mitochondrial dysfunction and a subsequent transcriptional response which can lead to apoptosis and early neuroinflammation [43].

1.1.3.2.1. Oxidative and nitrosative stress

Under physiological conditions, cells naturally produce ROS and reactive nitrogen species (RNS). Although these molecules are biologically active and at low concentrations, they are even necessary for certain cell processes, the reactive species can be very harmful at higher concentrations. Therefore, the cell has antioxidant mechanisms which allows for a perfect balance between its synthesis and elimination[44].

However, in the ischemic condition that follows a stroke, the increased production of ROS and RNS reaches levels that exceeds the antioxidant mechanisms of the cell to counteract the oxidative damage. Proteins, lipids and nucleic acids are affected so that several regulatory processes such as enzymatic activity, DNA methylation and lipid peroxidation are compromised and lead to the activation of apoptotic pathways[44][39].

In ischemia, the most relevant source of ROS comes from O_2 and H_2O_2, two highly reactive species produced by dysfunctional mitochondria and an anaerobic metabolism. Simultaneously, it is observed an increased production of peroxynitrite ($ONOO^-$, the most abundant RNS) from the reaction between NO and O_2. NO production is commonly linked to the activation of nNOS due to the Ca^{2+}which enters the cell and activates NMDAr during the

excitotoxicity process. On balance, the ATP depletion, the presence of ROS and high cytosolic Ca^{2+} concentrations induce the opening of mitochondrial permeability transition pore (mPTP) enabling the water and large ions to freely enter the mitochondria. The water intake produces osmotic swelling and thus the rupture of the outer mitochondrial membrane (OMM) and cytochrome C release. In these circumstances the cell can easily undergo necrosis or apoptosis death depending on the extent of damage and on the caspase pathway activation death by either necrosis or apoptosis depending on the damage level and caspase pathway activation[42][46][47].

Since that the neural tissue in the ischemic core is virtually irrecoverable, it may be reasonable to focus therapeutic efforts on the penumbral tissue. Nonetheless, several technical hurdles must be assessed. In first place, the high toxicity produced by oxidative and nitrosative stress drastically limits the survival of penumbral tissue. During ischemia, this tissue is hypo-perfused, then presenting lower levels of O_2 and glucose. Although cells can face these conditions, the reduction in the activity of mitochondrial complex I causes the impairment of electron transport chain. Therefore, when the blood flow is restored, the damaged cells receive high doses of O2 which provoke the saturation of mitochondrial respiratory chain. This is unable to

adequately respond to this stimulus because of the previously described complex I malfunction. The dysfunctional mitochondria is the scenario where uncoupled reactions and subsequent production of ROS takes place, being the main source of oxidative stress and cell toxicity linked to reperfusion[48].

1.1.3.2.2. Transcriptional regulation

The neural tissue response to ischemic stroke include, among other processes, a modification of transcriptional patterns partly induced by ion imbalance, ATP depletion and reactive species production. On the one side, this response includes the expression of antioxidant-related genes, the activation of p53 and an unfolded protein-mediated response. On the other side, there is a translation inhibition through which the translational machinery is arrested and the constitutively expressed mRNAs are silenced. This response aims at a triple effect on repairing the cell damage. Ideally, this would reduce the cell damage, clear the toxic substances produced by it and repair the cell. In fact, this response can lead to cell survival and reset the cell state to a pre-injury behaviour if the severity of the lesion is moderate. However, it also could lead to cell death if the activated

mechanisms are not strong enough to counteract the existing damage[49].

Likewise, the so-called response linked to hypoxia-inducible factor (HIF1) accounts for other relevant mechanism implied in counteracting the ischemic stimulus. H1F1 is a heterodimeric transcription factor composed by a constitutively expressed subunit (HIF1β) and an oxygen-regulated subunit (HIF1α). Under normoxic conditions, the oxygen-dependent degradation domain (ODD) of HIF1α is prolyl hydroxylated and therefore marked to be degraded in proteasomes. Under hypoxic conditions, the ODD of HIF1α dimerizes with HIF1β and the complex is then translocated into the nucleus to activate the transcription of target genes with an hypoxia response element (HRE). HIF1 is also known by its association with ischemic toleration phenomena and by its implications in neuroinflammation via NF-κβ[50][51][52].

1.1.3.2.3. Apoptosis

Although necrotic cell death is typical in the tissue located in the ischemic core, the penumbral tissue does not immediately undergo necrosis but a fine tuning between stress and repair mechanisms takes place and ultimately decides the fate of these

cells. If the balance leans forward the restoration of blood flow and functional recovery, cells will probably survive. On the contrary, cells go through programmed cell death, also known as apoptosis[53].

Apoptosis is an energy-dependent cascade which arises as the result of two principal pathways, named extrinsic and intrinsic pathways **(Figure 6)**[54].

The *extrinsic pathway* is initiated by the extracellular signalling which follows an injury and that activates 'death receptors' in the cellular membrane. These receptors belong to the tumour necrosis factor receptors (TNFRs) family and they join several protein adapters to form the death-inducing signalling complex (DISC), responsible for caspase-8 activation. Caspase-8, by its part, activates caspases 3 and 7 which in turn cleave structural proteins and enzymes to promote cell death[54][55][56].

The *intrinsic pathway* is, on the contrary, intracellularly induced when Ca^{2+} accumulates in the cytosol and activates the proapoptotic member of the Bcl-2 family, BID. BID interacts with other proapoptotic proteins as BAD and BAX, causing mitochondrial dysfunction (i.e. opening of mPTP and release of cytochrome C and apoptosis-inducing factor (AIF) to the cytosol). Once in the cytosol, cytochrome C binds to the apoptotic protein-activating factor 1 (Apaf-1) and procaspase 9 to form the

apoptosome. Caspase 9 results activated and in turn activates caspase 3 that cleaves essential structural proteins and enzymes for cell survival[54][55].

Both pathways are closely connected at multiple points and mutually converge at the end of the cascade. For example, BID protein can be activated in the intrinsic pathway but it can also be activated by the caspase-8 from the extrinsic pathway. In any case, both cascades end with DNA fragmentation, cytoskeletal and nuclear proteins degradation, the formation of apoptotic bodies and ultimately phagocytosis in a complex process mediated by caspase 3[56].

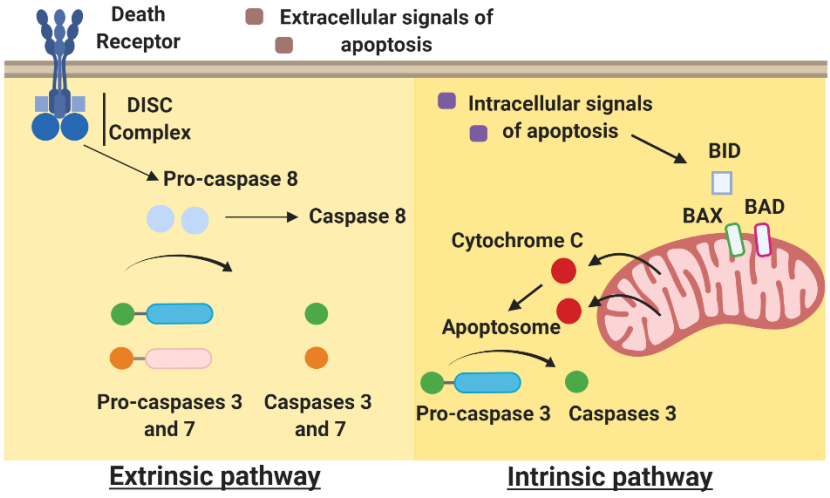

Figure 6. Extrinsic and Intrinsic pathway of apoptosis. Self-created figure using Biorender academic license.

1.1.3.2.4. Inflammation

Neuroinflammation is one of the most complex components of the pathological scenario found after a stroke. In the acute phase, the resident phagocytic cells (i.e. microglia and macrophages) are responsible for the clearance of dead cells and its associated debris. During the first hours after stroke, the neutrophils are recruited towards the lesion site thanks to the expression of several markers such as E-selectin, vascular cell adhesion molecule-1 (VCAM-1) and intercellular adhesion molecule-1 (ICAM-1) by endothelial cells. At the same time, neutrophils, as well as microglia and macrophages, release proinflammatory cytokines (TNF-α, IL-6, IL-8) which contribute to neutrophil and leucocyte further recruitment. Additionally, the endothelial cells also release ROS and NOS, playing a part in the spreading of the inflammatory response. [57][58][59].

Neuroinflammation is a complex process whereby the presence of an injury is detected, and it triggers a signalling cascade which include the releasing of pro-inflammatory substances. Nevertheless, at the same time, it also limits the extent to which this inflammatory response could damage the nearby tissue via anti-inflammatory signals. The balance between pro-inflammatory and anti-inflammatory responses is a promising target for future therapeutic approaches aiming at limiting

stroke damage. In animal models, pro-inflammatory stimuli are typically associated to worse prognosis and anti-inflammatory responses to a better recovery from stroke. Surprisingly, anti-inflammatory treatments had no beneficial effect in ischemic stroke patients[60].

Microglia mediates the “early inflammatory response” that is activated due to the presence of ROS, cell debris and damage-associated signalling. The early inflammatory process begins with intracellular molecules which work as danger-/damage-associated molecular patterns (DAMPs) and can activate microglial receptors. Microglia then undergoes a series of morphological and functional changes as a result of its activation. Typically, these cells switch from a ramified morphology displaying long processes to an ‘activated state’ characterised by an amoeboid morphology. The activated state of microglia can be polarized to the M1 (pro-inflammatory/destructive) phenotype or alternatively to M2 (anti-inflammatory/neuroprotective) phenotype due to different signals. M1 phenotype, as well as macrophages, promote the release of pro-inflammatory molecules like tumour necrosis factor-alpha (TNF-α) and cytokines like interleukins 1, 6, 12 or 23 (IL-1, IL-6, IL-12, IL-23) or oxidative metabolites like NO. These molecules enhance the recruitment of circulating immune

cells through the expression of VCAM and ICAM in endothelial cells. In contrast, activated M2 microglia expresses anti-inflammatory molecules like interleukin 10 (IL-10), CD206 or arginase 1[57][61].

Interestingly, recent studies have dismantled this classical division in two well establish phenotypes, suggesting that both phenotypes are extremely plastic and thus, different intermediate phenotypes are possible. In the acute phase, the signalling from the damaged tissue greatly unbalances the microglial phenotype towards M1 phenotype. However, at longer time periods, M2 activity may play a role in the brain recovery of normal function[59][62].

1.1.3.3. Subacute phase

The subacute phase concerns the physiopathological mechanisms that take place in the first days after the ischemic insult. At this time point, the immune response has a critical role in the prognosis of ischemic stroke patients.

1.1.3.3.1 Delayed immune response

After the first few days after stroke, the innate immunity response gives way to the adaptive immunity response over the course of the next few days and weeks. T lymphocytes, also known as T cells, are in charge of executing the adaptive response after receiving the pro-inflammatory signals released by microglia and macrophages. T cells are capable of originating and sustaining a complex immunity response through their subtypes T helper (Th; $CD4^+$ cells) and T cytotoxic (Tc; $CD8^+$ cells)[63][59].

According to their cytokine release profile, Th cells can be subdivided in Th1, Th2 and regulatory T cells (Treg). Th1 cells release pro-inflammatory cytokines such as interferon gamma (IFN-γ) while Th2 cells release anti-inflammatory molecules like IL-4 and IL-10. On the other side, Treg cells exert an immunosuppressive action by limiting the brain injury after stroke [63].

Tc cells are responsible for inducing apoptosis in target cells since they can release several enzymes involved in the formation of membrane pores and apoptosis induction (perforin, granizymes and granulysin)[63].

However, the inflammatory response to ischemia is often associated to a systemic depletion of lymphocytes (lymphopenia) and reduced T cell responsiveness several hours after ischemic damage. At the same time, an autoimmune response to CNS antigens is triggered, exacerbating the secondary injury to CNS. Altogether, the systemic immunosuppression and autoimmunity increase the vulnerability to nosocomial bacterial infection and thus the mortality rate[59][63].

1.1.3.3.2 Lesion scar (glial scar)

As previously described, the breakdown of the BBB results in an impaired homeostasis inside the CNS parenchyma due to the entrance of blood and serum components (IL-1, fibrinogen, endothelin 1, among others). In order to avoid the affectation of the healthy surrounding tissue caused by the BBB breakage, glial cells surround the injured tissue to create a glial scar[64][65].

During the subacute phase, the scar is mainly composed of astrocytes, microglia and glial precursor cells which rise their number after the ischemic insult (Figure 6). These cells become activated, expressing and releasing a wide range of bioactive molecules implied in neuroinflammation, BBB repair and

neuroprotection processes [66] **(Figure 6)**. In the initial development of the glial scar, astrocytes are the most abundant cell type within the lesion scar. They undergo a process called astrogliosis whereby the mature resident astrocytes, revert to a previous, more immature state in response to tissue injury. These immature astrocytes, also known as 'reactive astrocytes' become hypertrophic and exhibit thicker process and higher glial fibrillary acidic protein (GFAP) expression[66].

Apparently, the glial scar exerts a protective effect, acting as a physiological barrier against injury progression. This could help to preserve healthy tissue from the damage induced by the severe neuroinflammation at the lesion core. However, this initial protective role could be negative in the long term since the physical barrier entraps dystrophic axons and sharply limits their ability to regenerate over long distances[67].

1.1.3.4. Delayed phase

In the several weeks since the ischemic insult, the acute and subacute physiopathological characteristics tend to be less apparent. In parallel, the regenerative mechanisms that were slowly arising in the damaged area, finally emerge. During the

delayed phase, the lesion scar becomes chronic while the regenerative processes acquire importance[65].

1.1.3.4.1. Lesion scar (fibrotic scar)

In this phase, the fibroblasts from damaged meninges and nearby vessels invade the lesion. Fibroblasts proliferate and secrete several extracellular matrix (ECM) molecules to fill the space left by cell loss caused by the ischemic insult. These cells constitute the fibrotic scar [66]. Only one or two weeks after stroke, the damaged area presents a mature lesion scar formed by a glial scar in the penumbra surrounding the fibrotic scar which fills the injured tissue in the core area (**Figure 7**)[65][68].

Nevertheless, the collagen secreted by fibroblasts could form a physical barrier that could impede the entrance of new axons into the injured area. This fact could explaining, at least in part, the absence of neuroregenerative processes inside the mammalian CNS[65].

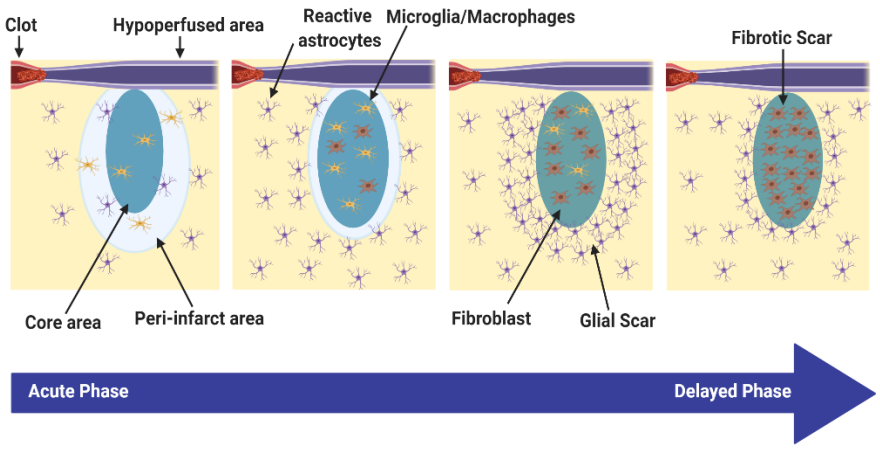

Figure 7. Glial scar progression after ischemic injury. Self-created figure using Biorender academic license.

1.1.3.4.2. Tissue reparation

The damage induced by an ischemic stroke triggers a response aimed at repairing the lesion. However, this reaction is counterbalanced by the pro-inflammatory microenvironment caused by cell death, macrophage infiltration and microglial activation which take place during the acute and subacute phases. Surprisingly, anti-inflammatory drugs did not improve the brain recovery in ischemic patients. In fact, the particular nature of the proinflammatory state contributes to eliminate damaged cells and to remove cell debris from the ischemic core. Thus, the total blockage of pro-inflammatory state would abolish

its critical role in limiting the lesion area and protecting the homeostasis of healthy tissue[69].

In the delayed phase, the lesion is contained inside the glial scar, so that the risk of affecting healthy tissue with debris or apoptotic signal is reduced. Consequently, the pro-inflammatory state is stabilized, and the anti-inflammatory state acquires a prominent position in the enhancement of repair processes, namely angiogenesis, neurogenesis and neuroplasticity[65].

- **Angiogenesis**: The beginning of angiogenesis can be placed in the acute phase when pericytes first separate from endothelial cells. Then, damaged endothelial and perivascular cells secrete angiopoietin-2 which contributes to disrupt old vessels, leaving the endothelial cells free to undergo cellular division. Endothelial proliferation is constantly stimulated by growth factors such as VEGF and fibroblast growth factor (FGF). Parallel to vascular development, the remodeling of the ECM occurs in a process mediated by several MMPs. During the first days after stroke, the angiogenic signaling promotes the neovascularization of the damaged region. This will provide oxygen and nutrients to the injured tissue, thus improving endothelial, glial and neuronal survival. Moreover, angiogenesis also helps to remove

tissue waste. Angiogenesis persists along the first weeks and although it seems to peak around 2 weeks after injury, there is not consensus about its temporal profile[70].

Even though angiogenesis is generally considered a protective mechanism, it must be tightly regulated. Otherwise, an excess in vascular permeability or in the proteases released to help RCM remodeling could lead to a worsening of the secondary injury to ischemia, increasing the edema and parenchymal deterioration[70].

- **Neurogenesis** After brain ischemia, neurogenesis is increased in the two well-establish neurogenic niches in the adult mammalian brain, namely the subventricular zone of the lateral ventricles (SVZ) and the subgranular zone of the dentate gyrus (SGZ). Recent studies suggest that a group of newly generated neuroblasts in the SVZ changes their tropism and migrate to the injured areas. However, the capability of these cells to integrate and generate functional circuits is still controversial since they tend to differentiate into $GABA^+$ interneurons. It has been also suggested that the neuroblasts found in the

cortex could partly arise from a hypothetical local neurogenesis. Moreover, the survival of these neuroblasts in the injured region is currently under debate since these cells usually degenerate soon after differentiation[71][72][73][74][75].

- **Neuroplasticity**: represents the third mechanism contributing to the repair of the injured area in the chronic phase. Under the term of neuroplasticity are englobed the processes of synaptic remodeling and axonal outgrowth which may be the primarily responsible for motor, sensitive and cognitive improvement in stroke patients[76][77].

1.1.4. Therapeutic options in ischemic stroke

Pharmacological or mechanical (thrombectomy) thrombolysis are the strategies that report higher benefits for the patient, in terms of neurological outcome. The most common thrombolytic agent is the recombinant tissue plasminogen activator or rt-PA, an enzyme involved in the clot degradation of the occluded vessel. The thrombectomy is a technique, which allows the extraction of the thrombus by a mechanical device. Both therapies have pushed for the creation of stroke units inside

hospitals, which have improved the management of stroke patients. Nevertheless only 3-7% of stroke patients are currently treated by these procedures in most developed countries. Such reduced numbers may be due to different factors, including the narrow therapeutic window and the high risks of haemorrhage transformation[78].

Other several strategies have been considered to effectively reduce the ischemic lesion in the different phases of stroke evolution. According to their target, these approaches can be divided in three categories: neuroprotective, anti-inflammatory and reparative strategies[79].

1.1.4.1. Neuroprotective strategies

The hyperacute and acute phases importantly determine the magnitude of the initial ischemic lesion. Therefore, the approaches focused on these time points should have the strongest therapeutic potential. These strategies are also known as 'neuroprotectants' as its main role is to protect neural brain cell populations from the initial ischemic damage, without affecting the subsequent tissue reperfusion. Thus, these strategies are designed to antagonize, interrupt or at least slow down the physiopathological processes of ischemic injury. In the

90s, the unravelling of the molecular mechanisms underlying cerebral ischemia led to the development of neuroprotectant agents. Although promising in preclinical studies, none of these alternatives obtained positive results in clinical trials. This failure could be partly explained by the fast-developing nature of the events taking place during the hyper acute phase which drastically reduces the available time window and counteract their great therapeutic potential[80].

Despite of the discouraging translational results, the neuroprotection-based strategies are a flourishing field of research. Currently, the most promising neuroprotective therapies target the following ischemic mechanisms:

- **Ca+2 dysregulation:** The blockade of Ca 2+ channels is one of the most promising therapies. Nimodipine – a blocker of L-type voltage-gated Ca2+ channels – reduces the entrance of Ca2+ into the cell, thus limiting the excitotoxicity-associated damage. Furthermore, it has vasoactive properties which are used to prevent uncontrolled vasoconstriction (i.e. vasospasm) after subarachnoid hemorrhages. Unfortunately, after a large number of preclinical studies, nimodipine has not shown any benefit in cerebral ischemia[80][79]. Alternatively, Mg2+ has been tested as a Ca2+ competitor which

interferes with Ca2+ channels, reducing its uncontrolled release and blocking NMDA channels. Up to now, Mg2+ has showed encouraging results and it is currently being tested in clinical trials[81].

- **Neurotransmitters homeostasis:** Reducing glutamate excitotoxicity via modulating NMDA and AMPA glutamate receptors had positive results in animal models. Nevertheless, the glutamate receptors antagonism did not exhibit the same effect on patients. The side effects derived from reducing the glutamate transmission throughout the brain could be masking the beneficial effects of glutamate beneficial effects of this treatment[79][80]. A great alternative could be to focus on a direct reduction of brain glutamate via a grabbing system. By lowering the systemic blood glutamate levels, the transport of glutamate will be forced from the brain to the blood through the BBB. This transport occurs in favor of its concentration gradient so that this approach constitutes an attractive strategy to clear the glutamate excess in the brain and to reduce its excitotoxicity[82], [83]

  On the other side, GABA is the main inhibitor neurotransmitter in the brain and thus, it is a very

interesting target for counteracting glutamate excitotoxicity. GABA agonists such as Diazepam has been tried in clinical studies with negative results [80]. By its part, the anesthetic gas xenon that works as a NMDA blocker at low concentrations showed promising results in animal models and it is currently under study in patients with global brain ischemia produced by cardiac arrest[84].

- **Death signalling pathways:** In animal models, anaesthetics and anticonvulsant drugs (i.e. pentobarbital, sevoflurane, isoflurane and ketamine, among others) have showed pro-survival potential. Once again, the leap to clinics failed to exhibit positive results Besides, the use of anesthetics in neurological patients raises several risks derived from clinical management[79][85].

- **Antioxidants:** As one of the main causes involved in the cell death which follows ischemia, oxidative stress emerges as another interesting target for neuroprotective approaches. NXY-059, one of the most studied synthetic antioxidants, showed encouraging results, reducing brain infarct by 66% in animal models

and improving the functional outcome of patients. However, in a second clinical trial, the results were discouraging[80]. Uric acid, by its part, has also showed positive results in stroke experimental models. Indeed, a recent clinical trial assesses whether uric acid would improve functional outcomes at 90 days post-acute ischemic stroke in patients. Uric acid proved to be safe but barely efficient since it did not improve the percentage of patients with excellent outcome after stroke when compared to placebo. Currently, other antioxidant alternatives such as vitamin E are under study[86].

- **Others:** A precursor in the phosphatidylcholine synthesis named citicoline has been tested as a potential stabilizing agent of cell membranes. Despite the early encouraging results in small studies, this drug failed to be beneficial in larger randomized trials[80].

Regardless of the initial pessimism that these negative results arose, the study on the search for new neuroprotective strategies led to a better understanding of the molecular mechanisms underlying ischemic injury. Accordingly, it has been recently proposed a preventive role

of neuroprotective agents for those patients at a high risk of stroke[87]. This reinterpretation could allow for the recycling of those neuroprotective candidates that were discarded due to their short therapeutic window.

1.1.4.2. Anti-inflammatory strategies

Both early and delayed inflammation are attractive targets for therapeutic approaches since they provide a longer therapeutic window and thus, an increased usability. Likewise, as they act as key regulators of cell survival and repair mechanisms, its proper regulation could lead to a smaller, more controlled initial damage which usually results in a better outcome. The main goal of anti-inflammatory and immunomodulatory therapies is to limit the entrance of neutrophils and to potentiate the anti-inflammatory phenotypes (i.e. macrophages and microglial M2 phenotype). Also, targeting the blockade of T cells migration during delayed inflammation revealed controversial results, even in preclinical studies. Other important target in immunomodulatory studies is the blockade of IL-1 receptors which partially interrupts the pro-inflammatory cascade[88].

The potential of minocycline – a microglial inhibitor – to reduce microglial activation has been tested without significant

beneficial effects on patients when compared to placebo. Other compounds aimed at reducing lymphocyte infiltration via the blockade of CD11b, CD18 or ICAM-1 showed encouraging results in animal models of ischemic stroke but failed to reproduce the same effect on clinical trials. The use of mouse monoclonal antibodies to block the target molecules led to the activation of adaptive responses which could overshadow the protection provided by these therapies. Humanized antibodies arises then as a promising alternative for the coming trials[89].

Other approaches target the lymphocyte infiltration and release from the generating niches. Natalizumab, a monoclonal antibody against α4-β1 integrin, did not show a significant reduction in lesion volume of treated patients but could improve the outcome in small lesions. Fingolimod is a modulator of lymphocyte behaviour and it can decrease lymphocyte liberation from the lymph nodes. Preliminary results in patients with both ischemic and haemorrhagic strokes showed promising results[89].

1.1.4.3. Reparative therapies

The reparative therapies aim at recovering the injured tissue and are usually focused on the delayed phase. Nevertheless, an

increasing body of evidence suggests that the anticipation to the acute or subacute phases is essential.

- **Pharmacological approaches:** Several drugs which were initially designed for other pathologies have been tested in the context of cerebral ischemia. For example, a group of classical antidepressants, the selective serotonin reuptake inhibitors (SSRIs), has demonstrated to promote neural plasticity in stroke animal models and to improve the motor recovery in the long term in patients. Moreover, phosphodiesterase 5 (PDE5) inhibitors, firstly designed to treat erectile dysfunction due to its vasodilatory properties, improved neurological recovery since it promotes neurogenesis, angiogenesis and synaptogenesis in experimental studies and in a preliminary clinical trial. However, further studies are required to confirm its therapeutic effect[77].

  Other specific approaches are being developed. Nogo-A inhibits neurite outgrowth and its blockage by specific antibodies and pharmacological antagonists showed an improved synaptic plasticity in preclinical studies. A humanized antibody to Nogo-A has been developed and

its safety has already been tested but not yet its therapeutic potential[77].

- **Growth factors:** can stimulate endogenous mechanisms of brain repair such as angiogenesis, neurogenesis and synaptic plasticity. VEGF, BDNF, granulocyte-colony stimulating factor (G-CSF) or insulin growth factor-1 (IGF-1) have been tested in preclinical and clinical studies. G-CSF demonstrated to have anti-apoptotic, immunomodulatory and regenerative effects in preclinical studies but in patients, this approach did not yield any significant results. Also, observational studies in patients have related increased VEGF levels to microbleeds[77][90].

- **Cell therapies:** aim at using cells from different origins to replace the damaged tissue or as a source of immunomodulatory molecules and growth factors which would enhance the endogenous repair mechanisms of the brain. Nowadays, the injection of cells into the brain parenchyma could be replacing the dead cells or more likely, inducing immunomodulatory potentiating effects. These cells are usually obtained from fetal or embryonic sources, but they also could be extracted from adult

tissues, such as bone marrow, in which case these cells are multipotent stem cells or lineage-specific cells. In cell-based therapies, the marron-derived mononuclear cells (MNCs) and mesenchymal stem cells (MSCs) are the most recurrent cell types. Preliminary studies have proved their safety, but their therapeutic effects remain controversial[77].

- **Cell reprogramming:** is becoming an increasingly attractive alternative for the treatment of ischemic stroke. This new technology allows for the transformation of a cell type to another thanks to the overexpression of certain transcription factors that change cell phenotype. In recent years, the injection of these cells intracerebrally has been proved to be beneficial for functional recovery in animal models. It has been suggested that several mechanisms as trophic actions, modulation of inflammation, angiogenesis promotion and cellular and synaptic plasticity may be responsible for this improvement[91].

1.1.4.4. Multifactorial therapies

More often than not, the therapies designed to treat stroke aims at a single target, even though they can indirectly affect another secondary mechanism. Nonetheless, several therapies could influence multiple factors at the same time being melatonin administration and hypothermia the most remarkable.

Melatonin is a hormone mainly secreted by the pineal gland and it is known its role in the regulation of circadian rhythms. This hormone can scavenge highly reactive species and possesses immunomodulatory and anti-apoptotic properties. These characteristics make it very attractive as therapeutic compound in stroke treatment. In fact, melatonin has proved to regulate Ca^{2+} levels and to reduce apoptosis via inhibition of the mpTP formation in preclinical studies. At the same time, it regulates NO synthesis and cytokines release which in turn controls pro-survival signalling pathways [92]. Although less studied, it has been proposed a role for melatonin in the delayed phase after ischemic stroke when it could be promoting neuroplasticity processes[93].

In conclusion, the new therapies which arise to treat ischemic stroke are very limited in their leap to clinic with a very low percentage of the initial candidate molecules achieving the clinical use.

1.2. Cell reprogramming

1.2.1. Definition

As previously described, cell reprograming is a newly generated tool which allows to dedifferentiate mature cells to induce pluripotency or multipotency. However, this technology also enables the transformation of a mature cell type into another cell type. This opens new horizons in the field of repair mechanisms with plenty of applications in several diseases. To date, it has been tested to treat brain, heart and eye diseases, among others[94].

1.2.2. Historical perspectives

Beyond its therapeutic potential, cell reprograming has dismantled one of the most well-established dogma of developmental biology that states that the cell fate and its differentiation potential is largely determined by the lineage history of that specific cell. In general, the cell identity is remarkably stable and only stem/multipotent/pluripotent cells retains the ability to give rise to another cell types. This fact was described by Conrad Waddington as a ball rolling down through

a “developmental” landscape from an undifferentiated stem or progenitor cell state to a physiologically mature state[94][95].

While Waddington advocated his doctrine, Gurdon suggested that the differentiated cells were plastic and could be reprogrammed to alternative cell fates in 1962. Gurdon’s experiments demonstrated that nucleus from *Xenopus laevis* gut were able to develop new individuals when they were transfected into enucleated oocytes. This revealed for the first time the potential of cytoplasm molecules to induce the reprogramming of differentiated nucleus. Nearly 30 years after, a myoblast cDNA encoding the transcription factor MyoD was able to directly transform fibroblasts into myoblasts, without an intermediate pluripotent state before assuming their new fate.[96] In 1996, one of the major milestones of cell reprogramming was achieved with the birth of Dolly the sheep. Wilmurt and collaborators transferred the nuclei of epithelial cells into enucleated of oocytes, making a significant shift from *Xenopus* to mammalian cloning[97][95].

In the last decade, several experiments explored the ability of other factors to induce cell reprogramming. Little success was achieved until 2006, when Yamanaka stablished a cocktail of a few cell fate-changing transcription factors that profoundly reverted somatic cells to a state of pluripotency. As a result, the

notion that cell fate is mutable and malleable finally took hold as this combinatorial approach paved the way for the next experiments in cell reprogramming[98].

1.2.3. Classification of reprogramming methodologies

The boom of cell reprogramming in the last decades led to a wide range of suitable alternatives for modifying cell fate. Due to their novelty, a consensual classification of the reprogramming methodologies is still lacking and the bibliography in this respect remains controversial. In this work, we have divided these methodologies in two groups: reprogramming to induced pluripotent stem cells (iPSCs) and direct reprogramming, also known as transdifferentiation[97][99][100].

1.2.3.1 Reprogramming to iPSCs

Pluripotent stem cells are defined as those capable of undergoing self-renewal and giving rise to the three germinal layers. Until recently, the embryonic stem cells (ESCs) from the inner cell mass of the blastocyst were the main source of the pluripotent stem cells used in research. They represent a

powerful system to study the gene expression patterns and subsequent physiological processes which take place during development. However, technical (immune reject, impurity of population obtained after proliferation and differentiation) and ethical issues derived from the use of human embryos emerged when they were applied to clinical studies[101].

In 2006, a ground-breaking publication by Yamaka completely redefined the stem cell biology field since his team achieved for the first time the dedifferentiation of adult somatic cells (mouse fibroblasts) to pluripotent stages due to the expression of specific proteins using four transcription factors (Sox2, Oct4, Klf4 and c-Myc)[102].

iPSCs are an invaluable tool in studying the pathogenesis of human genetic diseases and in testing improved drugs (**Figure 8**). Their capacity to differentiate into specific cell types was first tested in a clinical trial in Japan in 2014. iPSCs-derived retinal pigment epithelial (RPE) sheets were used to treat neovascular age-related macular degeneration. Since then, several clinical trials using iPSCs are underway in the treatment of diabetes mellitus and spinal cord injury[101][103][104].

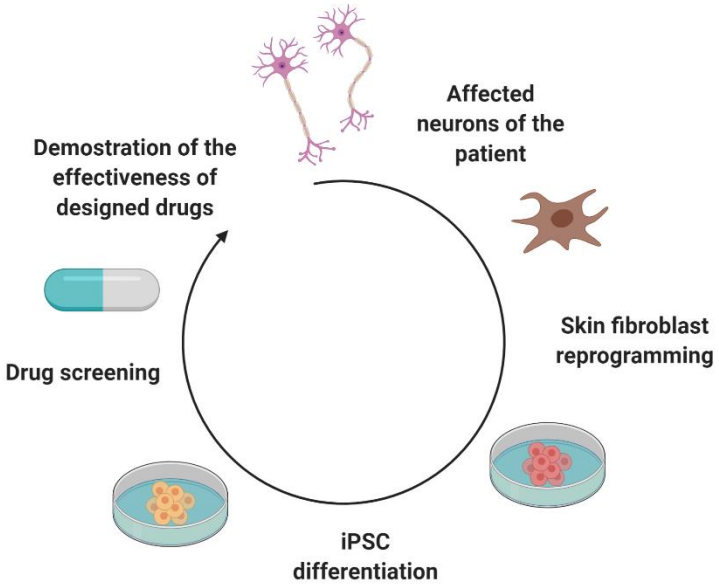

Figure 8. Schematic Flow-chart of the drug discovery process using iPSCs. Self-created figure using Biorender academic license.

These clinical trials had to overcome three main limitations of using iPSCs in clinical applications:

- Viral transfection, safety versus efficacy. Most iPSCs-derived techniques make use of integrative systems such as retroviral and lentiviral delivery that efficiently enables the integration of viral transgenes in several cell types. However, the integration of viral transgenes into cell genome raises concerns about the safety of these vectors. In contrast, new no-integrative viruses like adenovirus, sendai virus, plasmids, Cre-LoxP and

inducible lentivirus as well as non-viral alternatives such as proteins, small RNAs and small molecule compounds open new possibilities to create safer iPSCs-based technologies[97][105].

- Epigenetic memory retention in reprogrammed cells. Genomic-wide profiling of ESCs and iPSCs has identified over a thousand differentially methylated regions caused by an inefficient silencing of the somatic cell genes (i.e. epigenetic memory) or by an acquisition of a new methylation pattern (i.e. epigenetic mutation)[97][105].

- Tumorigenicity: iPSCs present a higher frequency of 'sub chromosomal copy number variations. Also, multiple passages of iPSCs could lead to oncogene duplication and the silencing of tumour suppressor genes. Besides, it has been demonstrated that iPSC-derived chimeras develop tumours either due to a failure in demethylating pluripotency genes or due to the reactivation of oncogenes c-Myc and Klf4[97][105].

1.2.3.1 Direct reprogramming (transdifferentiation)

The dedifferentiation plus subsequent differentiation processes to transform either ESCs or iPSCs into a new mature cell type are expensive and time consuming. Moreover, the safety and ethical issues previously described that accompany this process provide further need to search an alternative. Direct reprogramming, also known as transdifferentiation, arose as an alternative which avoids the 'pluripotency step'. Basically, this technology allows a somatic cell to transform in another type of somatic cell thanks to the activation of some 'master control genes' to guide the cell toward the desired cell type. As opposed to iPSCs reprogramming, the epigenetic information is not erased to attain a pluripotent 'ground state'[97][106][107].

This technology was initially developed *in vitro* to bypass the tumorgenicity problems associated to pluripotency. Recent studies have reported possible *in vivo* transdifferentiation using cocktails of small molecules or miRNAs pools[97].

1.2.4. Ways to reach reprogramming

For reprogramming a cell, many different alternatives have been discovered in the last years that can be used for inducing pluripotency or direct reprogramming.

1.2.4.1 Transcription factors

Probably, the most frequent technique for cell reprogramming involves the forced expression of transcription factors, which will induce a modified expression of key mRNAs that in turn will change the cell fate. In 1987, David *et al*. were able to transform mouse fibroblast into cardiomyocytes for the first time thanks to cDNA encoding the transcription factor c-Myc[96].

Nearly two decades later, Yamanaka developed a cocktail of transcription factors (OSKM) that bears his name. This cocktail can induce pluripotency in differentiated cell. Since then, researches have been searching for transcription factor pools that could be useful for the reprogramming of cell types with therapeutic interest (cardiomyocytes, neurons, neuroblasts, myocytes, macrophages, etc.). It should be noted that the effectivity of transcription factors could depend on their delivery vector. For example, differences between the usage of plasmids or different viral vectors have been reported[108]

1.2.4.2. Interference RNAs

Interference RNAs are non-coding RNAs that regulate gene expression by degrading mRNA. Among the several types of interference RNAs, two should be highlighted by its considerably

greater capacity to regulate cell fate: miRNAs and siRNAs[109][110].

1.2.4.2.1. miRNAs

miRNAs have an endogenous origin and they are firstly transcribed by RNA polymerase II/III into long, primary transcripts called pri-miRNAs which are in turn cut and processed to give rise to short pre-miRNAs. After being translocated to the cytoplasm, pre-miRNAs are transformed into short, double-stranded miRNA molecules of 22-nucleotide length by the DICER enzyme. One of the strands (the guide strand) is complementary to a target mRNA molecule and it is recruited to form the miRNA-induced silencing complex (miRISC) responsible for mRNA degradation[111].

miRNAs bind target mRNA by an unperfected match so that they may interact to different mRNAs and thus possibly affects more than one cellular pathway[112].

The same strategy is also used to find useful miRNAs for transdifferentiating experiments. With this information, researchers may use miRNA also for converting one cell type to another differentiated cell. The comparison between miRNAs expressed by pluripotent and differentiated cells made possible

to identify potential useful miRNAs for cell reprogramming. Some of the discovered miRNAs increase the reprogramming efficiency of transcription factors (miRNA-291-3p, miRNA-294 and miRNA-295) while others induce pluripotency by themselves (miRNA-302/367 cluster)[112].

Following the same strategy, useful miRNAs for transdifferentiation have been found. It has been reported their use for obtaining neurons (miRNA-9/9* and miRNA-124) and cardiomyocytes (miRNA-1, miRNA-133, miRNA-208 and miRNA-499). The reprogramming of astrocytes and fibroblasts is particularly appealing for regenerative therapies in ischemic stroke[113][114].

miRNAs could have a double effect on iPSCs reprogramming and transdifferentiation. On one hand, they could be targeting a large repertoire of genes related to the cell fate. On the other, they could be acting as epigenetic regulators involved in chromatin remodelling. Thus, miRNAs constitute a powerful tool in reprogramming approaches since they both improve the efficiency of existing strategies and are a new way of achieving reprogramming[113].

1.2.4.2.2. siRNA

siRNAs are the defenders of genome integrity in response to foreign or invasive nucleic acids which can have their origin in viruses, transposons or transgenes. It is their capability to degrade target mRNAs which make them an attractive therapeutic tool for their use in cancer, genetic diseases and regenerative medicine[115].

Initially, long, linear, perfectly base-paired doble-strand RNAs are synthetized and later processed by the DICER enzyme in a manner similar to miRNAs. The resulting siRNAs are recruited, and they induce the silencing effect through RISC complex[115].

The use of siRNA opens a new concept for cell reprogramming. Instead of changing the transcription regulatory networks (by transcription factors or miRNAs), siRNA can silence a specific pathway. This alternative allows to improve the understanding of molecular pathways involved in cell reprogramming. In addition, the specific activity of siRNA could avoid the side effects of other treatments[116].

Despite these therapeutic advantages, siRNAs only have been used in a few studies when compared to miRNAs. This can be easily explained if we consider that miRNAs can simultaneously modulate several molecular pathways. This synergic activity may

improve its efficacy as a treatment. By its part, the use of siRNAs may require a deeper understanding of the involved molecular pathways than miRNAs do. Furthermore, siRNAs could complement or even improve miRNA treatments. A good example is the transdifferentiation of fibroblasts to cardiomyocytes by a pool of miRNAs (miRNA-1, miRNA-133, miRNA-208 and miRNA-499). When a siRNA was used to silence the same pathway affected by the pool of miRNAs, an overexpression of cardiomyocytes markers is achieved but there was no transdifferentiation from fibroblasts to cardiomyocytes. Interestingly, the combination of both strategies led to a more efficient transdifferentiation. These data revealed that miRNA pool was affecting more than one molecular pathway since the siRNA on its own did not induce a complete transdifferentiation[117].

Encouragingly, siRNAs have been successfully used in other works where the silencing of an alternative splicing of TAF4 (subunit of transcription factor TFIID) was able to transform facial dermal fibroblasts into melanocyte-like (iMel) cells[116].

1.2.4.3. Small molecules

The usage of transcription factors as the prevailing strategy for cell reprogramming must face several challenges in terms of efficiency, safety and *in vivo* delivery[118][119].

An alternative approach that would be the use of small molecules for cell reprogramming. The so-called small molecules are small chemical compounds that target signalling pathways, epigenetic modifications and metabolic processes. The first works in the field tested the efficacy of histone deacetylase (HDAC) inhibitors such as valproic acid (VPA)[120]. More recently, the interest has been focused on molecules with inherent reprogramming capacities.[119] Zhang and collaborators, for example, demonstrated that a cocktail of 9 molecules were able to reprogram human astrocytes into neurons in only 8-10 days. The small size of these molecules enables their encapsulation and vectorization which is a clear advantage for their *in vivo* use[121].

Transcription factors, interference RNAs and small molecules are different strategies capable of efficient cell reprograming. Regardless of their intrinsic efficacy and safety, the delivery method also influences these parameters.

1.2.5. Delivery strategies for cell reprogramming

1.2.5.1. Viral Vectors

The natural ability of viruses to infect cells and to use cell machinery to replicate their own genetic material is the basis for the usage of viral vectors. The artificial modification of the virus structure allows for the replacement of viral replicative material with mRNA encoding reprogramming transcription factors or interference RNAs. This methodology is highly attractive to *in vivo* approaches because of the infectious capacity of the viruses and the long-term expression of the genes contained in the same. Viral vectors can be subdivided in integrative and non-integrative viral vectors[122].

1.2.5.1.1. Integrative virus

Integrative viruses insert their genetic material inside the host cell, promoting the long-term viral expression since the viral material replicates at the same rate that host genetic material does. This methodology allows for the inheritance of viral insert by daughter cells. However, the integrative strategy presents an associated risk related to the possible insertion of genetic material in an essential sequence of the host cells. In that case, the high risk in terms of mutagenesis can lead to genotoxicity,

cell malfunction, cancerous behaviour or even death. In fact, the first clinical trials in which integrative viruses were used showed genotoxicity associated to insertional mutagenesis. Although clinically effective, the risk of mutagenesis is a great limitation for the clinical use of this strategy. Integrative viruses are mainly composed by for viruses from the *Retroviridae* family and they are widely used in basic research and clinical trials[123].

1.2.5.1.1.1 Retroviruses

Retroviruses are single-stranded RNA (ssRNA) viruses capable of creating a double-stranded DNA (dsDNA) which can be then stably integrated into the host genome and replicated along with it Retroviruses possess a characteristic three-layered structure with a genome-nucleoprotein complex and several molecules as reverse transcriptase, integrase and proteases in the inner layer. This structure is enclosed within a capsid which is in turn surrounded by a matrix protein layer. Outside it, a lipid envelope with surface glycoproteins is responsible for the virus tropism[124][125].

Two members of the *Retroviridae* family are particularly interesting in gene therapy and cell reprogramming: gamma-retroviruses (murine leukemia virus, MLV) and lentiviruses

(human immunodeficiency virus, HIV). Lentiviruses are the only ones capable of infecting non-dividing cells since they can cross the nuclear membrane. The usage of gamma-retroviruses, by its part, remains restricted to gene transfer into hematopoietic cells[124][125].

1.2.5.1.2. Non-integrative virus

In contrast to integrative viruses, the non-integrative viruses present a reduced risk of genotoxicity so that they offer a safer alternative to integrative viruses. Additionally, these vectors can provide stable transgene expression in quiescent cells. However, the trade-off of non-integrative viruses is the need for repeated transductions in order to achieve long-term expression in proliferating cells[126].

The most commonly used non-integrative viruses are adenoviruses (Ad), adeno-associated viruses (AAV) and Integration-Deficient Lentiviral Vectors (IDLVs)[126].

1.2.5.1.2.1. Adenoviruses (Ad)

Adenoviruses (Ad) are a family of dsDNA-genome viruses with an icosahedral non-enveloped capsid [126]. This capsid determines

the Ad serotype, being the Ad2 and Ad5 serotypes the most commonly used in research [127]. The capsid is also related to the viral tropism so that researchers have been trying to modify this capsid to develop viral vectors against specific cell types such as cancer cells [128].

Unfortunately, adenoviral vectors tend to trigger innate and adaptive responses in the infected tissue. Recently, several studies aimed at solving the adenoviral-associated immunogenicity by co-expressing the viral construct together with miRNA-122a which inhibits the expression of the viral gene E4 that is linked to hepatotoxicity and immune system activation[129].

1.2.5.1.2.2. Adeno-associated (AAV)

The AAV-viruses are non-enveloped viruses that package a linear ssDNA genome[130]. They need a helper virus (often adenovirus) for their replication.[122] Although AAV-viruses are naturally integrative virus, the depletion of certain viral sequences (*rep* and *cap* genes) prevents the adenoviral vector from its integration in the host genome[126].

Their relatively frequent use in clinical trials can be explained due to their low immunogenicity and great tropism for specific cell

types. The latter depends on the viral serotype – at least 12 different serotypes have been identified to date. Since each one of them 'prefers' to infect given cell types, the viral vectorization against one cell type can be easily accomplished[126].

Their numerous serotypes, their tropism and low immunogenicity as well as the long-term expression of the insert have turned these vectors in one of the best candidates for translational medicine. Consequently, several clinical trials are being developed using AAV-viruses for multiple diseases such as blindness, haemophilia, Alzheimer's disease, Parkinson's disease, hepatitis, etc[122].

1.2.5.1.2.3. Integration-Deficient Lentiviral Vectors (IDLVs)

Lentiviruses-based vectors are characterised by a stable genomic expression of the viral insert. Nevertheless, as it was previously described, several disadvantages linked to integration limit their applicability. In order to address this problem, the IDLVs were designed to eliminate the lentiviral integrase responsible for the integration. This was challenging since this enzyme is also involved in the reverse transcription and nuclear import. Specific point mutations into the integrase sequence led to a disrupted

integrative function without affecting its other roles in the viral vector[131].

The resulting lentiviral vector is not able to integrate in the host genome but generates an episome which mediates a transient transduction in dividing cells and a stable expression in quiescent cells[126].

1.2.5.2. Nanoparticles

Nanoparticles are defined as those which have a size within the nanometre range (1 – 1,000 nm) [132]. This definition therefore encompasses particles with a variety of sizes, shapes and suitable materials. In consideration of their small size, nanoparticles are ideal candidates for their usage as a drug delivery system. Furthermore, nanoparticles are extremely adaptable to their desired used. They can be functionalized with different compounds (antibodies, aptamers, polyethylene glycol) in order to reduce their immunogenicity or to enhance their targeting or internalization to a specific the cell. Their role as nanocarriers enhaces the drug efficiency, reducing the effective dose and thus avoiding side effects[133].

Given their high degree of variability, the biodegradable polyelectrolyte/silica microcapsules are of special interest since

they can be customized with different functionalities. These are susceptible to be externally activated with the application of light, magnetic fields, an ultrasounds, chemically induced temperature, pH or salinity. The activation of the nanoparticle would trigger the cargo release. The most obvious advantage of these particles is their biodegradable composition which enables the capsule degradation by the cell and enhancing their biocompatibility. It has also been demonstrated that these nanoparticles can escape from the lysosome in which are encapsulated inside the cell so that the release of the cargo can take place inside the cytosol[130]. Altogether, these properties make these particles highly for medical applications[122]. This strategy has been recently tested in reprogramming fibroblasts to iPSCs via the encapsulation of the Yamanaka's factor Oct4[134].

1.2.6. Cell reprogramming in brain repair

The human brain is an isolated structure with a very low recovery potential after damage. Providing that it has always been a particularly difficult tissue to repair, in-depth research in ischemic stroke has focused on different strategies: neurotrophic factors, cell grafts, the recruiting of endogenous

stem cells and the modification of inflammatory and glial response. Notwithstanding these efforts, none of them have resulted in a translational treatment for stroke patients[135].

Cell reprogramming arises then as a promising alternative in the treatment of ischemic stroke. The ultimate aim would be the creation of neural cells capable of integrating into the neuronal circuits of the damaged areas.[99] Parenchymal astrocytes from the glial scar have been highlighted as a potential source for reprogrammable cells given their relative abundance and proximity to the injured area. Indeed, the most recent studies suggest that reactive glia possess a stem cell-like phenotype which could enable the reprogramming step[135].

Within this research line, some efforts have been already made towards the reprogramming of the glial scar. In 2010, Heinrich and collaborators reprogrammed astrocytes *in vitro* by forcing the expression of the transcription factors Neurog2 and Dlx2 via viral vectors. As expected, the use of different transcription factors will induce a determined neuronal phenotype. In this work, Neurog2-induced reprogramming led to the formation of glutamatergic neurons while Dlx2 reprogrammed astrocytes to GABAergic neurons[136][137].

Similar studies tested the astrocyte reprogramming potential using miRNAs [138] and small molecules [139][140].

Additionally, the *in vivo* reprogramming of astrocytes opens a new translational perspective for the treatment of ischemic stroke and other neurological conditions [141][142]. Magnusson and collaborators have suggested the existence of a latent neurogenic program in reactive astrocytes that could be activated by brain damage. The transcription factor Ascl1 may be an important mediator in the neurogenic program in astrocytes. Thus, it is not a coincidence that Ascl1 has been already tested for obtaining neurons [143]. These preliminary results endorsed the idea of using astrocytes not only to create new healthy neural cells but also to activate their intrinsic neurogenic program to repair the damaged brain[144]. Also, it seems reasonable toassume that Ascl1 and thus, the Notch signalling pathway are involved in the astrocyte reprogramming to neurons[143].

1.2.6.1. ASCL1 and NOTCH1 signalling pathway

Notch signalling is an evolutionarily conserved pathway which regulates cell-fate determination during development and maintains adult tissue homeostasis. Notch receptors are single-pass transmembrane proteins composed of functional extracellular (NECD), transmembrane (TM), and intracellular (NICD) domains. After Notch-1 activation, the NCID is

translocated into the nucleus where is associated to RBPJ protein to activate the transcription of the HES family-related genes. This is known as the 'canonical' Notch pathway. HES proteins are related to the inhibition of Ascl1 expression so that the modulation of NOTCH1 pathway could be a promising target for astrocyte reprogramming strategies[145] (**Figure 9**).

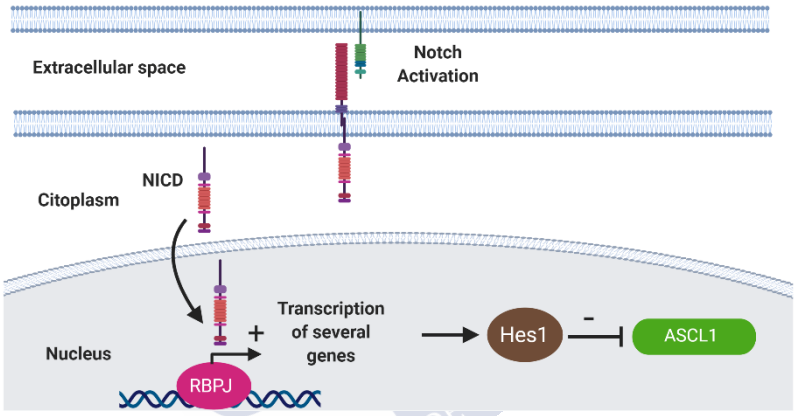

Figure 9. NOTCH1 signaling pathway. Self-created image using Biorender academic license**.**

USC
UNIVERSIDADE
DE SANTIAGO
DE COMPOSTELA

2.Hypothesis & Justification

Stroke is the world's second leading cause of death and the first one in terms of permanent disability. Several drugs have proved to be efficient in animal models, but they failed in clinical trials. The lack of a safe and efficient pharmacological treatment for stroke patients lays the foundation for new therapeutic possibilities. Among them, cell reprogramming is a new promising regenerative approach that has already obtained hopeful results in the generation of functional neuronal cells *in vivo*. Even then, it is necessary to put more effort in the search for translational reprogramming strategies and their implementation as regenerative therapy. Among the reprogramming strategies, silencing of NOTCH1 pathway seems to be one of the most promising and translational treatments.

Therefore, in this study, it was hypothesized that the use of small interference RNAs against the NOTCH1 signalling pathway could induce the *in vitro* reprogramming of astrocytes in a process mediated by the transcription factor ASCL1. We also hypothesize that *in vivo* astrocyte reprogramming from the glial scar could be achieved using interference RNAs via viral vectors, influencing the recovery from the ischemic damage in animal models of cerebral ischemia. Finally, we also hypothesize that

biodegradable silica capsules could mediated a safe and effective delivery of siRNAs, opening new possibilities for a safe reprogramming therapy.

3.Objectives

This works aimed at studying the possible neurorepair effects of inhibiting the NOTCH1 signalling pathway in astrocytes, both *in vivo* and *in vitro.* Here, this work also aims to study the effectivity of a potential translational delivery of siNRAs by nanoparticles. To achieve these main objectives, three specific aims has been proposed.

- To study the *in vitro* reprogramming capacity of siRNA treatment to inhibit NOTCH1 signaling, which in turn would cause an overexpression of Ascl1.
- To study the *in vivo* reprogramming capacity of siRNAs expressed by viral vectors in the peri-infarct region *in vivo* in an animal model of ischemic stroke and to explore whether this strategy improves animal recovery.
- To study the feasibility of a possible translational approach by means of nanoparticle delivery of siRNAs

.

USC
UNIVERSIDADE
DE SANTIAGO
DE COMPOSTELA

4.Section I. siRNAs for *in vitro* reprogramming

4.1. Hypothesis

Recent works regarding cell reprogramming support the therapeutic potential of this strategy in brain repair. Besides, it has been demonstrated that the inhibition of Notch-1 signalling pathway is a robust method for reprogramming astrocytes. Then, we postulate that the inhibition of this pathway by using siRNAS may efficiently reprogram cortical astrocytes *in vitro*.

4.2. Objectives

In this section, we aimed to assess the reprogramming capacity of siRNA administration. Thus, our main goals were:

- To optimize a cortex astrocyte culture for the *in vitro* experiments.
- To find the most effective treatment for silencing the Notch pathway.

- To study the effectivity of silencing Notch pathway in reprogramming cortical astrocytes.

4.3. Material and Methods

4.3.1. Primary cortex astrocyte culture

T-75 flasks were coated with 10 mL of poly-D-Lysine 0,01 mg/mL the day before culture. After overnight incubation, flasks were washed twice with PBS. The dissection was carried out in a fresh Petri dish using cold PBS to prevent cell death. Four P1 mice pups c57bl/6 (from Central Animal House of Universidade de Santiago de Compostela (USC), Spain) were used in each culture. In this regard, experimental protocols and animal handling were approved by the chief of the Servizo provincial da Gandaría of the territorial department of Consellería de medio Rural e do Mar of province of A Coruña, being the main responsible PhD Francisco Campos Pérez. The animal experiments were conducted under the procedure number: 15010/2019/004 according to the Spanish and EU rules (86/609/CEE, 2003/65/CEE, 2010/63/EU, RD 1201/2005 and RD 53/2013). All procedures were carried out in the Health Research Institute of Santiago de Compostela (IDIS), with the registration number: ES1507802928[01].

In brief, mice were decapitated after washing heads with EtOH at 70%. The skin was then removed with tweezers to expose the skull. Once removed, brains were transferred to a fresh Petri dish. Hemispheres were separated following the midline and meninges were easily recognized thanks to profuse vascularization and then removed. Other brain areas like midbrain and diencephalon were discarded.

Cortex were washed with PBS and enzymatically digested with 3 mL of trypsin (Thermo-Scientific, U.S.A.) at 37 °C for 10 min. Additional mechanical disaggregation was achieved by pipetting. The tissue was then incubated with 60µL of DNase solution (5mg/mL) (Sigma-Aldrich, U.S.A.) at 37 °C for 5 min. Complete medium was used to inactivate trypsin and cells ere centrifuged at 300 g for 5 min at RT. Pellet was resuspended in 5 mL of complete medium, DMEM (Thermo-Scientific, U.S.A) containing 10%FBS (Thermo-Scientific, U.S.A), and filtered through a 70 µm cell strainer (CLS431751, Corning, U.S.A). Once filtered, cell suspension was centrifuged (300 g for 5 min at RT) and resuspended in 3 mL of complete medium. Cells were counted on a haemocytometer and seeded at 20,000 cell/cm^2 in T-75 flask.

At 7 days *in vitro* (DIV) astrocytes are a confluent monolayer. Cultures were shaken in an orbital shaker at 250-300 rpm for 15

h to increase culture purity since due to their adherent properties, astrocytes will attach to the bottom of the flask while microglia and oligodendrocytes will be discarded. Flasks were then washed with PBS and shaken manually for one additional minute. Cells were split using 3 mL of trypsine and 70µL of DNAse for 5 min. Trypsine was inactivated by adding 6 mL of complete medium. Cells were then centrifuged at 300 g for 5 minutes at RT. Cells were counted and reseeded at 20,000 cells/cm^2. At 18-21 DIV, confluent cultures are ready for being split into six-wells plate dishes (Corning, U.S.A). Cells should be confluent and ready for splitting to plate dishes. Experiments were performed when cells reached a confluent monolayer at 28-30 DIV.

4.3.2. Flow cytometry for astrocyte culture characterization

Flow cytometry was used to characterize the astrocyte population in culture. P2 cells were trypsinizated and centrifuged at 300 g for 5 min at RT and then permeabilized and fixes using the BD Cytofix/Cytoperm™ (554714, BD, U.S.A). Approximately 100,000 cells were added to each cytometry tube. Antibodies for GFAP, GLAST and proper isotype control for GFAP were individually incubated (**Table1**). Manufacturer

instructions were followed for incubation and blocking protocol for each antibody. Samples were injected into a FACS DIVA flow cytometer 6.0.3 (BD, U.S.A.). A minimum of 10,000 events were recorded per sample.

Table 1. Antibodies used in Flow cytometry experiments.

Antibody	**Dilution**	**Reference**	**Commercial**
Mouse anti-GFAP	1:11	130-105	Miltenyi Biotec, Germany
Mouse Isotype control GFAP	1:11	130-104	Miltenyi Biotec, Germany
Mouse anti-Glast	1:11	130-095	Miltenyi Biotec, Germany

4.3.3. Transfection experiments for *in vitro* reprogramming

Following manufacturer instructions, siRNA (**Table2**) was incubated with Lipofectamine siRNAiMAX (Thermo-Scientific, U.S.A) (5 µL/well) in OptiMEM medium (Thermo-Scientific, U.S.A) for 10 min. Then, siRNA and lipofectamine were added to cells until the desired concentration of siRNA (1.6 nM, 16 nM or 32 nM). Experiments were performed in a 6 well-plate so that 3

wells were used for quantitative polymerase chain reaction (qPCR) assays and 6 wells were used for Western Blot (WB) experiments. At the end of the follow-up period, cell pellet was stored at -80 °C until their use.

Different siRNA (**Table2**) concentrations were assessed (1.6 nM, 16 nM, 32 nM) to determine their knockdown capacity at 72h following manufacturers recommendation. The most effective concentration of siRNA was then used to evaluate the knockdown expression of Notch1 pathway and the subsequent increase in Ascl1 expression after 7 days. *Gapdh* siRNA was used as positive control for the transfection process (1,6 nM or 16 nM/well) at 72h.

Table 2. Commercial siRNA purchased for the experimets.

siRNA	**Reference**	**Commercial**
***Gapdh* positive control**	4390850	Thermo-Scientifc, U.S.A.
Scramble negative control	4390844	Thermo-Scientifc, U.S.A.
Rbpj	s72809	Thermo-Scientifc, U.S.A.
Hes1	s67462	Thermo-Scientifc, U.S.A.

4.3.4. Quantitative PCR

The *Gapdh, Rbpj*, *Hes1* and *Ascl1* mRNA expression was evaluated by qPCR. Frozen cell pellets were directly submerged in lysis buffer. RNA extraction was performed using a commercial column-based kit (GeneJET Gel Extraction Kit, (Thermo-Scientific, U.S.A) following manufacturer instructions. The final RNA quantity and quality were spectrophotometrically assessed by Nanodrop (Thermo-Scientific, USA). Only samples with 280/260 and 260/230 ratios over 1.7 were included in further experiments. A total amount of 1 µg of RNA was used for retrotranscription into cDNA using the GoScript™ Reverse Transcription System (Promega, U.S.A).

In short, 1 µg RNA was diluted in RNase-free water containing 0.5 µg of random primers to a final volume of 11 µL. This mix was incubated for 5 min at 70°C allowing the secondary structures of RNA to unwind. The mix was then rapidly cooled down in ice for 10 min. Reverse transcription mix was composed by 4 µL of reaction buffer (5x), 2 µL of $MgCl_2$ (2.5 mM final concentration), 1 µL of dNTPs (0.5 nM of each nucleotide final concentration) and 1 µL of GoScript™ reverse transcriptase. The final volume of 20 µL was incubated for 5 min at 25 °C allowing annealing and for 60 min at 42 °C allowing the extension of the cDNA strand. The final product was diluted at 1:5 in RNase free water.

Finally, gene target expression (*Rbpj*, *Hes1* and *Ascl1*) and the reference gene *RPL13* were studied by qPCR using the GoTaq qPCR masterMix (Promega, USA) and Mx3005P qPCR system (Agilent Technologies, U.S.A). Briefly, a total volume of 2µL of diluted cDNA was mixed with 3.5µL of nuclease free water, 0.5 µL of 10mM specific primers (0.25µL for each sense) (**Table3**) and 6µL of GoTaq® qPCR Master Mix (2X), obtaining a total final reaction volume of 12µL. Reactions were performed by triplicate in 96 well plates.

Table 3. Primer sequences used for the PCR purchased to Sigma-Aldrich, U.S.A.

Primer	Sense	Antisense
Rbpj	CCTGTGCCTGTCGTAGAAAGT	GTTTCGGCTTCTACATCCCCA
Ascl1	GAATGGACTTTGGAAGCAGGATG	CATTTGACGTCGTTGGCGAG
Hes1	GAAGAGGCGAAGGGCAAGAA	GGAATGCCGGGAGCTATCTTT
Rpl13	CGGAGGGGCAGGTTCTAGTA	GTACAACCACCACCTTTCGG

4.3.5. Western blot

Protein was extracted in a total volume of 100 µL cold RIPA buffer (Thermo-Scientific, U.S.A) cointaining protease inhibitors (11697498001, Roche, Switzerland). Disaggregated pellets were incubated for 15 min in ice and then centrifuged at 20,000 g for

30 min. Protein content of the lysates was assessed using the BCA Protein Assay Kit (Thermo-Scientific, U.S.A).

A total amount of 30 µg of protein was subjected to SDS PAGE using Criterion gels 4-15% (Biorad, U.S.A) with a fixed voltage of 140 V (180 mA). Proteins were then transferred to a PVDF membrane (Millipore, U.S.A) usting a Trans-Blot semi-dry system (Biorad, U.S.A) with a limited voltage of 25 V and 180 mA for 2 h. After blotting, membranes were blocked with 5% BSA in Tris-Chloride buffer containing 0.1% Tween 20 (TBST) (Sigma-Aldrich, U.S.A) for 1 h. Primary antibodies were incubated overnight in agitation following manufacturer instructions (**Table 4**).

Secondary antibodies were incubated in agitation for 1 h at RT. Finally, HRP activity was revealed using PierceTM ECL Western Blotting Substrate (Thermo-Scientific, U.S.A) and detected by Chemidoc (Biorad, U.S.A). WB results were analysed using ImageJ (Rasband, U.S.A). The expression of target proteins is relativized to the Histone 3 expression levels of each sample. The average of sample values of each group was normalized to this control.

Table 4. Antibodies used in western blot

Antibody	Dilution	Reference	Commercial
Mouse anti-RBPJ	1:400	G3893	Sigma, U.S.A.
Mouse anti-Hes1	1:400	Ab2597	Abcam, U.K.
Rabbit anti-ASCL1	1:400	ab52642	Abcam, U.K.
Rabbit anti-Histone13	1:400	ab93157	Abcam, U.K.
Rabbit anti-Mouse HRP	1:200	P0260	Dako, U.S.A.
Goat anti-Rabbit HRP	1.200	P0448	Dako, U.S.A.

4.3.6. In vitro reprogramming experiments

Astrocyte cultures were split 3 days after the siRNA treatment and seeded at 5,000 cells/cm2. Cells were then cultured in reprogramming medium (DMEM/F12 supplemented with B27, N2, FGFb, EGF) (**Table 5**). Two weeks after, neurospheres were observed in these cultures.

Table 5. Recipe of reprogramming medium

Compound	Quantity	Reference	Commercial
DMEM	40%	41965	Thermo-Scientific, U.S.A.
F12	40%	11765	Thermo-Scientific, U.S.A.
Neurobasal	20%	21103049	Thermo-Scientific, U.S.A.
B27	200µL	17504044	Thermo-Scientific, U.S.A.
N2	400µL	17502001	Thermo-Scientific, U.S.A.
FGFb	20ng/mL	40-33	Peprotech, U.S.A.
EGF	20ng/mL	315-09	Peprotech, U.S.A.

4.3.7. Evaluating Neurosphere properties

Primary neurospheres were mechanically disaggregated by pipetting. The resulting cell suspension was seeded in a 96-well plate at (5,000 cel/cm^2). The neurosphere forming potential (number of neurospheres/100 seeded cells) of these cells was assessed after 10 DIV.

4.3.8. Immunofluorescence

Primary neurospheres were collected and mechanically disaggregated by pippeting. The resulting cell suspension was

reseeded at 5,000 cel/cm^2 in reprogramming medium and allow to grow neurospheres (i.e. secondary neurospheres). In differentiation assays, secondary neurospheres were allowed to grow in DMEM (Thermo-Scientific, U.S.A) supplemented with 10% FBS (Thermo-Scientific, U.S.A) for 2 weeks. After 10 DIV, secondary neurospheres were passed to a coverslip glass coated with Poly-D-Lysine (A-003-E, Sigma-Aldrich). Neurospheres were then fixed with 4% formaldehyde (VWR, U.S.A.) and 5% BSA (Sigma-Alrich, U.S.A) was used as blocking solution for 1 h. Primary antibodies were incubated overnight at 4 °C. Secondary antibodies were incubated for 1h at RT and subsequently streptavidin was added for 30 min (**Table 6**). Hoechst (1:6,000) (Invitrogen, U.S.A) was used for 10 min for nuclei staining. Photographs were taken in a Leica DMI 6000 B microscope with the software LAS AF 1.0.0 (Leica Microsystems, Sweden).

Table 6. Antibodies used in the immunofluorescence protocol.

Antibody	Dilution	Reference	Commercial
Mouse anti-GFAP	1:400	G3893	Sigma-Aldrich, U.S.A.
Mouse anti-B3tubulin	1:400	657404	Biolegend, U.S.A.
Rabbit anti-S100B	1:400	ab52642	Abcam, U.K.
Rabbit anti-Nestin	1:400	ab93157	Abcam, U.K.
Horse anti-Mouse Dy488 Horse	1:200	DI-2488	Vector, U.K.
Horse anti Mouse Biotinylated	1.200	BA-2001	Vector, U.K.

4.3.9. Statistics

All data are presented as the mean and standard error of the mean (mean ± SEM). One-way analysis of variance (ANOVA) followed by post-hoc Bonferroni evaluation was used for multiple groups to determine significant differences. Student´s t-test was used to test the differences between two groups. Statistical significance was set as *P<0.05; **P<0.01; ***P<0.001. The statistical analysis was conducted using GrapPad Prism 7.0.

4.4. Results

4.4.1. Characterization of astrocyte cell culture using Flow cytometry

The expression of astrocyte markers in culture was assessed by flow cytometry using GFAP and Glast antibodies as astrocyte markers in order to determine the culture purity. GFAP marker was expressed in 88.7% ± 5.89 of the cells in culture. Glast was expressed by 70.5% ± 5.4 of cells in culture **(Figure 10)**. The high expression of both astrocytic markers accounts for a highly enriched cortex astrocyte culture, essential requirement for subsequent *in vitro* reprogramming studies.

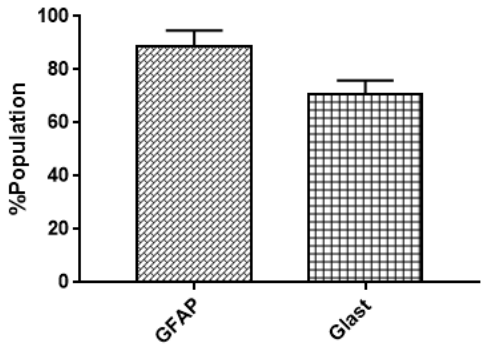

Figure 10. Expression of GFAP and Glast in a passage 2 cortical astrocyte culture (n=3 cultures). Data are showed as mean ± SEM.

4.4.2. Dose-response experiments with siRNAs.

Dose-response experiments were performed at 72h to determine the optimal dose of siRNAs needed to maximize the knockdown of (*Rbpj* and *Hes1*) in the cell culture of astrocytes. Transfection conditions were firstly assessed with a positive control *Gapdh* siRNA and lipofectamine as transfection reagent by measuring the mRNA levels by qPCR using the mRNA levels of RPIL3 as a reference. This experiment showed a high effectivity of the tested transfection conditions since both doses (1.6 nM and 16 nM) of *Gapdh* siRNA achieved a marked knockdown of the target mRNA. At the lowest dose (1.6 nM), *Gapdh* expression falls to 6.69 ± 1.39%, while the highest dose (16 nM) reduces the *Gapdh* expression to 3.58± 0,58% compared to control (100%) (all $p<0.0001$) **(Figure 11).** No statistical differences were found between the two tested doses of *Gapdh* siRNA.

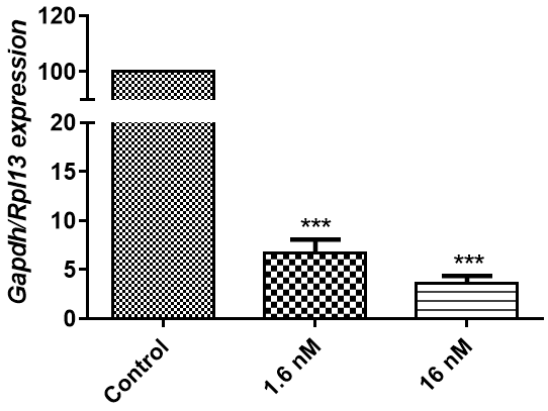

Figure 11. Expression of *Gapdh* mRNA at 72 hours after the treatment with different doses of *Gapdh* siRNA. *Gapdh* expression was relativized to Rpl13 expression and normalized to the expression in control cells. Data are show as mean ± SEM. ***P<0.001 (n=3 per group).

Suitable transfection conditions were then used to reduce *Rbpj* expression. In this case, a statistically significant difference was observed between the 1.6 nM dose of *Rbpj* siRNA (22.18 ± 2.14%) and the higher 16 nM dose (13.17 ± 1.5%) when compared to non-treated controls. The higher dose of 16 nM *Rbpj* siRNA was then considered as the optimal dose for subsequent experiments (**Figure 12**).

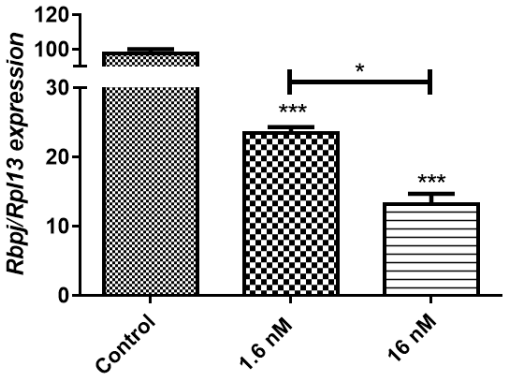

Figure 12. Expression of *Rbpj* mRNA at 72 hours after the treatment with different doses of Rbpj siRNA. Rbpj expression was relativized to *Rpl13* expression and normalized to the expression in control cells. Data are show as mean ± SEM. *P<0.05; ***P<0.001 using 1-way ANOVA followed by the post hoc Bonferroni test (n=3 per group).

On the other hand, the Hes1 siRNA treatment, we observed that 16nM dose (71±4.8%) was statistically less effective than 32 nM dose (43±11.5%). Therefore, the higher dose of 32 nM Hes1 siRNA was our choice for the subsequent experiments (Figure **13**).

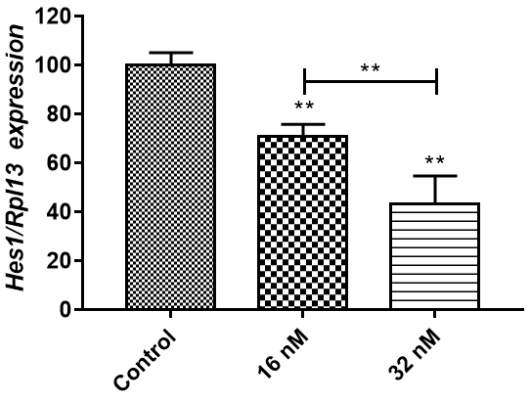

Figure 13. Expression of *Hes1* mRNA at 72 hours after the treatment with different doses of *Hes1* siRNA. *Hes1* expression was relativized to Rpl13 expression and normalized to the expression in control cells. Data are show as mean ± SEM. **P<0.01 using 1-way ANOVA followed by the post hoc Bonferroni test (n=3 per group).

4.4.3. *In vitro* treatment with siRNAs.

Once we have tested the *Rbpj* and *Hes1* siRNAs conditions to downregulate their mRNA targets, we assessed variations in Ascl1 expression due to siRNAs treatment. These variations could be an expected feature of the inhibition of the Notch1 signalling pathway achieved by *Rbpj* and *Hes1* siRNAs.

4.4.3.1. Effect of *Rbpj* siRNA treatment in *Rbpj* mRNA and protein expression

A *Rbpj* siRNA dose of 16 nM reduced the *Rbpj* mRNA expression in an enriched astrocyte culture from postnatal cortex. Data from qPCR assays revealed that *Rbpj* siRNA at this optimal dose reduced mRNA expression from 24h to 7 days. The temporal profile of *Rbpj* mRNA showed an inverted bell-shaped curve with the maximal inhibition occurring at 72h. At 24h, the *Rbpj* mRNA expression is reduced to the 70% (29.68 ± 2.07%) respect to the non-treated controls, that represents the 100% of the *Rbpj* mRNA expression. The inhibition percentage slightly increased at 48 h (20.52 ± 3.28%) and reached its maximum point at 72h (14.36 ± 1.66%). At 96h, mRNA inhibition starts to decrease (16.36 ± 2.21%) and this tendency is sustained until at least 7 days (24.27 ± 1.55%).

Interestingly, all groups presented a knockdown of *Rbpj* expression ($p<0.001$) when compared to untreated control cells. Statistically significant differences were found between groups at 24h and 72h ($p<0.01$) and 96 h ($p<0.05$) group (**Figure 14**). This experiment indicates that *Rbpj* siRNA can induce an 80% of

knockdown of the *Rbpj* mRNA expression which can be sustained for at least one week in astrocyte cultures (**Figure 11**).

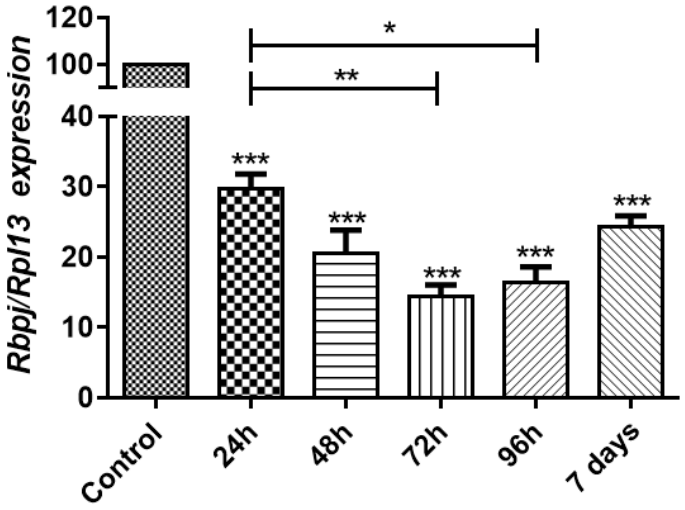

Figure 14. Expression of Rbpj mRNA at different times using 16 nM of Rbpj as treatment. Rbpj expression was relativized to Rpl13 expression and normalized to the expression in control cells. Data are show as mean ± SEM. *P<0.05; **P<0.01; ***P<0.001 (n=3 per group).

As a result of the knockdown of *Rbpj* mRNA, we evaluated the expression of RBPJ protein at 72 hours (maximum inhibition point) and 7 days (longest timepoint effect) by western blot. Results demonstrated that siRNA treatment also induced a statistically different downregulation of the RBPJ protein at 72 h (23.20% ± 3.9) and at 7 days (15.10% ± 4.9) when compared to non-treated controls. No significant differences were found between these two groups (72 and 7 days) (**Figure 15**)

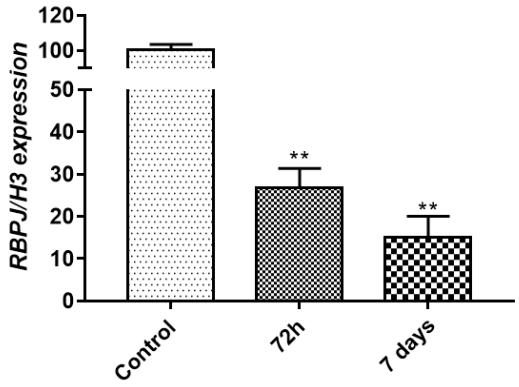

Figure 15. Expression RBPJ protein at 72 hours and 7 days using 16 nM of Rbpj siRNA as treatment. RBPJ expression was relativized to Histone3 expression and normalized to the expression in control cells. Data are show as mean ± SEM. **P<0.01 (n=3 per group).

4.4.3.2. Effect of *Hes1* siRNA treatment in *Hes1* mRNA and protein expression

The treatment with 32 nM *Hes1* siRNA induced a reduction of 60% (43.02% ± 9.5) in the *Hes1* target mRNA at 72h, while this silencing was reduced after 7 days, and the mRNA expression was 70.9± 9.5% (**Figure 16**). This data revealed a great difference with the results achieved by *Rbpj* siRNA treatment where less amount of treatment achieved a higher knockdown of the siRNA. Unfortunately, due to technical problems (several antibodies were tested and none of them has worked, *data not shown*), we

were not able to evaluate the effect of knockdown of *Hes1* expression in HES1 protein.

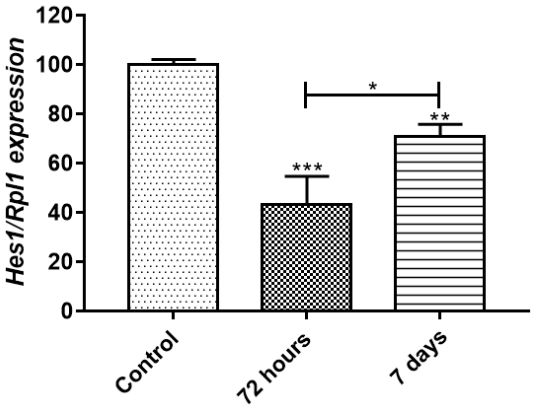

Figure 16. Expression of Hes1 mRNA at 72 hours and 7 days using 32 nM of Hes1 siRNA as treatment. Hes1 expression was relativized to Rpl13 expression and normalized to the expression in control cells. *P<0.05 **P<0.01; ***P<0.001 (n=3 per group).

4.4.3.3. Ascl1 expression variations associated to siRNAs treatment

To test that we are effectively targeting the NOTCH1 pathway, we studied the variations in the down-stream protein ASCL1.

4.4.3.3.1. *Rbpj* siRNA treatment

Rbpj siRNA effectively reduced *Rbpj* mRNA expression and RBPJ protein levels. Regarding the levels of *Ascl1* associated to the NOTCH1 signaling pathway, we observed an increase in *Ascl1* mRNA levels in *Rbpj* siRNA treated cells when compared to control. At 24 h, *Ascl1* mRNA presented a 1.5 ± 0.2-fold-increase, and this increase in *Ascl1* mRNA was continued over tie with an expression at 48h of 1.59 ± 0.07, at 72h 1.8 ± 0.2, at 96h 1.91 ± 0.12 and 1.92 ± 0.9 at 7 days (**Figure 17**). These results confirmed that changes in *Rbpj* mRNA expression could directly modify the *Ascl1* mRNA expression 7 days after treatment.

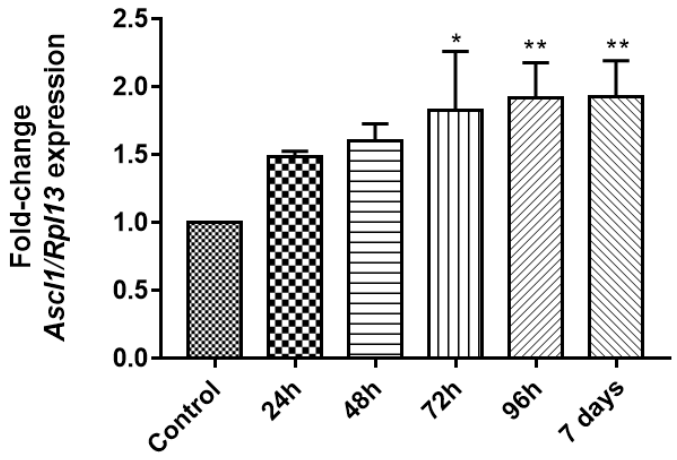

Figure 17. Expression of Ascl1 mRNA after Rbpj siRNA treatment. Ascl1 expression was relativized to Rpl13 expression and normalized to the expression in control cells. Data are show as mean ± SEM. *P<0.05; **P<0.01; using 1-way ANOVA followed by the post hoc Bonferroni test (n=3 per group).

Paradoxically, the increment in Ascl1 mRNA expression did not lead to a protein overexpression but to a reduction in the ASCL1 protein levels at 72 hours (50.83 ± 18.75%) compared to control. Despite this reduction at 72 hours, the protein levels reached control expression at 7 days (101.1 ± 3.13%). There was a statistical difference between 72 hours and control group and between 72h and 7 days group. The reduced expression at 72 h suggest that the siRNA treatment could induce some short-time protein inhibition during the first days after treatment. (**Figure 18**).

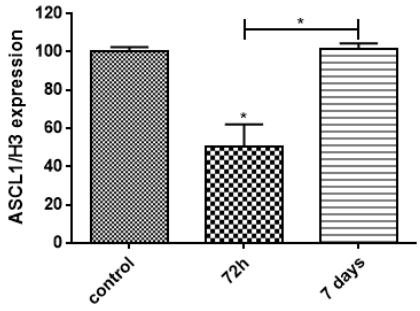

Figure 18. Expression of ASCL1J protein mRNA at 72 hours and 7 days using 16 nM of Rbpj siRNA as treatment. RBPJ expression was relativized to Histone3 expression and normalized to the expression in control cells. Data are show as mean ± SEM. *P<0.05; using 1-way ANOVA followed by the post hoc Bonferroni test (n=3 per group).

4.4.3.3.2. Hes1 siRNA treatment

Hes1 siRNA treatment induced a statistic overexpression of *Ascl1* mRNA at 72 h (2.36 ± 0.2-fold-increase) and 7 days (2.5 ± 0.28-fold-increase) when compared to control treated cells. Interestingly, *Hes1* seemed to achieve a higher *Ascl1* mRNA expression at than *Rbpj* siRNA treatment. Even though that *Rbpj* siRNA was more effective in silencing its *Rbpj* mRNA target, it led to a lower increase of *Ascl1* mRNA expression when compared to *Hes1* siRNA. In fact, *Hes1* siRNA achieved a 2.5 ± 0.28 fold-increase of *Ascl1* mRNA expression after only reducing *Hes1* mRNA expression by less than a 60% (43.02 ± 9.5%) (**Figure 19**).

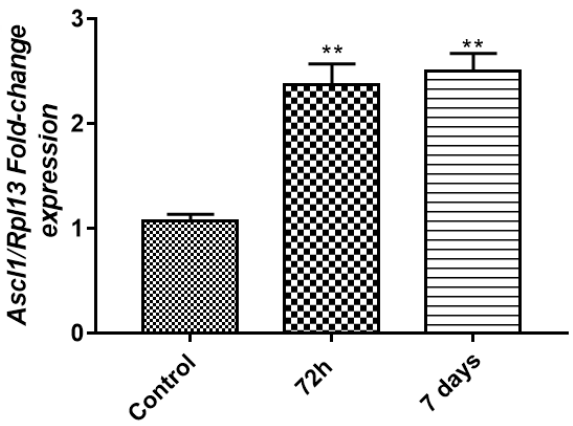

Figure 19. Expression of Ascl1 mRNA after Hes1 siRNA treatment. Ascl1 expression was relativized to Rpl13 expression and normalized to the expression in control cells. Data are show as mean ± SEM. **P<0.01; using 1-way ANOVA (n=3 per group).

However, the highly efficient *Hes1*-mediated increase in *Ascl1* mRNA expression did not correlate with an increase in ASCL1 protein expression. These data reflect a mismatch between mRNA and protein levels for ASCL1 expression. A similar phenomenon was observed in the case of *Rbpj* siRNA treatment. Nevertheless, *Hes1* treatment seems to led ASCL1 protein levels closer to the control cultures than *Rbpj* siRNA treatment (**Figure 20**). It is possible than ASCL1 protein expression started to increase after 7 days in the same way than *Ascl1* mRNA increase at 72 hours and remains high at least until day 7. Further studies are necessary to explore this possibility. However, the knockdown of the NOTCH1 pathway (*Rbpj* and *Hes1*) linked to the overexpression of *Ascl1* justify of hypothesis. Thus, we tried to evaluate the effectivity of the treatment in a cortex astrocyte culture.

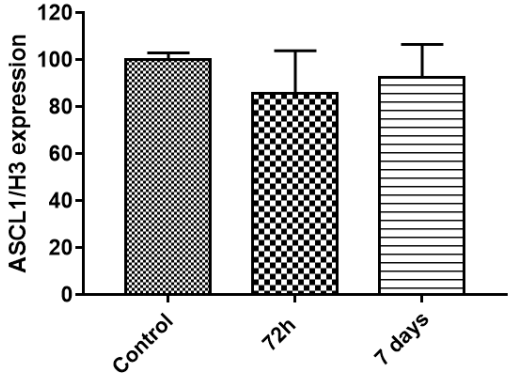

Figure 20. Expression ASCL1 protein using 32 nM of Hes1 siRNA as treatment. ASCL1 expression was relativized to Histone3 expression and normalized to the expression in control cells. Data are show as mean ± SEM.

4.4.4. In vitro reprogramming

4.4.4.1. Neurosphere forming experiments

In previous experiments, we have demonstrated that the *Rbpj* and *Hes1* siRNA treatments can increase the expression of Ascl1 mRNA for at least 7 days. Thus, a weekly dose was administered to cultures of cortical astrocytes. After 14 DIV, the formation of round cell aggregates (similar to neurospheres) was observed both in control and treated wells. Unlike neurospheres, these aggregates remain attached to the bottom of the plate (**Figure 21**). To further elucidate whether these structures were truly neurospheres, the aggregates were immunocytochemically

analysed using the classical neurosphere markers GFAP, Nestin and nuclear marker Hoesch. A clear colocalization of both markers was observed inside these spheres (**Figure 22**).

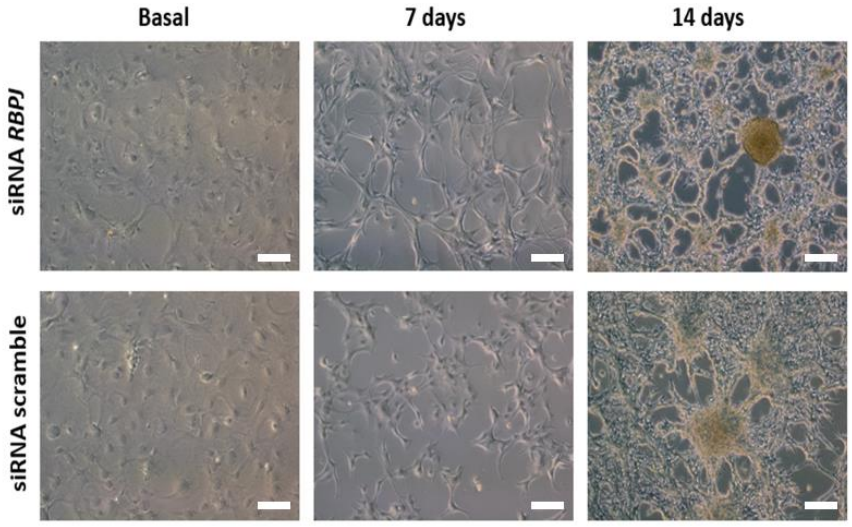

Figure 21. Images of treated cell with siRNA *Rbpj* and control wells at basal, 7 and 14 days. Scale bar 200µm

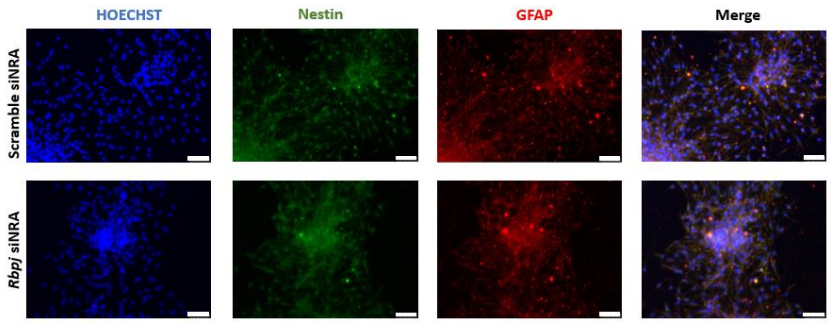

Figure 22. Images of a neurosphere with positive signal for GFAP and Nestin. Scale bar 50µm.

GFAP and nestin markers can be also presented by other cell types. Therefore, we performed a cell differentiation study to determine whether the spheres observed in culture were able to give rise to different cell types belonging to the neural lineage (i.e. neurons, astrocytes, oligodendrocytes). In fact, a positive signal was obtained for the astrocytic marker GFAP and for the neuronal marker β-III-tubulin. Therefore, these spheres were susceptible to be differentiated into several cell types, at least astrocytes and neurons (**Figure 23**). Nevertheless, other immature cell types as neurosphere forming cells or astrocyte progenitor cells present a positive signal for GFAP. Thus, we tested a standard marker for mature astrocytes, S100β and a marker for neuron precursors, DCX. A positive signal for S100β was detected in contrast to the negative signal for DCX so that it seems reasonable to conclude that we have obtained real

neurospheres from an adult astrocyte culture both in control and siRNA treated wells (**Figure 24**).

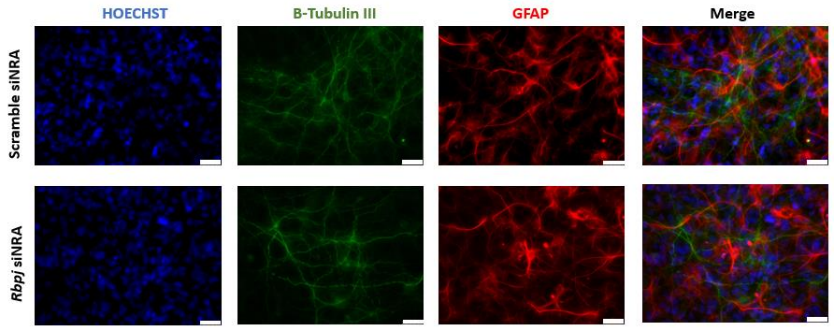

Figure 23. Images of differentiated cells from neurospheres. Positive signal for astrocyte (GFAP) and neuron (B-Tubulin III) markers were detected. There is no colocalization between these markers, so there are two different differentiated type of cells in this culture. Scale bar 25µm.

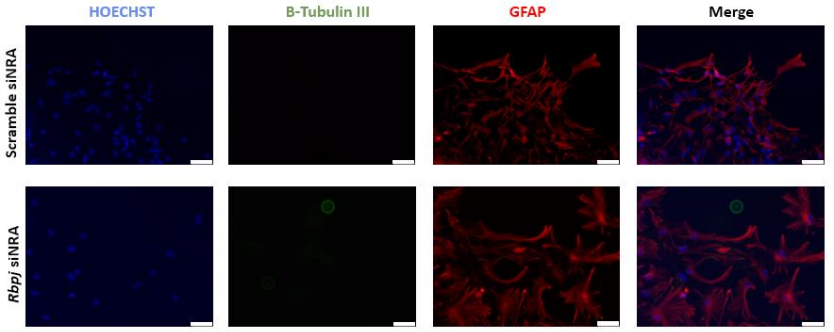

Figure 24. Astrocyte cells expressing GFAP marker. There is no presence of neuron (B-Tubulin III) in the differentiated culture. Scale bar 50µm.

Since the formation of neurospheres was evident in both groups, we assessed the neurosphere forming potential of each experimental group (i.e. number of generated

neurospheres/100 seeded cells in control vs siRNA treated wells). Unexpectedly, there was no statistical difference between the *Rbpj* siRNA treated group (7.62 ± 0.24 neurospheres per 100 seeded cells) and control group (6.85 ± 0.9) neurospheres per 100 seeded cells) (**Figure 25**).

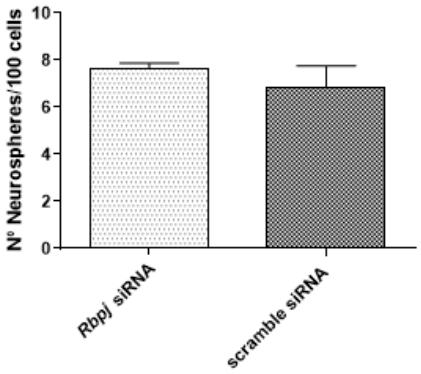

Figure 25. Neurosphere forming potential for treated cells with *Rbpj* siRNA and control groups. Results are showed in number of neurospheres per 100 cells. Data are show as mean ± SEM.

The treatment with *Hes1* siRNA presented a similar effect compared with *Rbpj* siRNA treatment. No statistical differences were found between treated (13.2 ± 4.1) and control group (7.8 ± 2.6) after the weekly administration of *Hes1* siRNA (**Figure 26**).

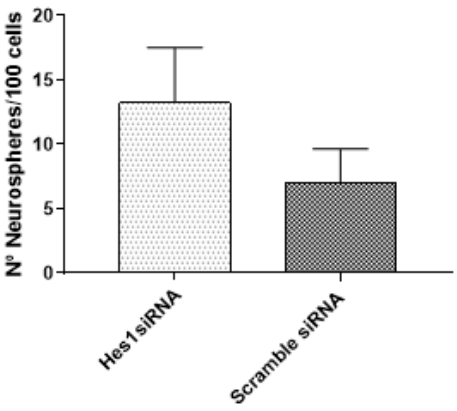

Figure 26. Neurosphere forming potential for treated cells with *Hes1* siRNA and control groups. Results are showed in number of neurospheres per 100 cells. Data are show as mean ± SEM.

These results showed that there is a trend in the neurosphere forming potential of the treatment. However, this tendency did not show statistical significance with control groups. The weekly treatment with the lipofectamine transfection reagent, which showed some toxicity in past studies, plus the limitations of the fetal astrocyte culture, which have the intrinsic capacity of forming neurospheres in the presence of proneurogenic factors, could influence these results.

5. Section II. Using viral vectors for *in vivo* reprogramming

5.1. Hypothesis

Having demonstrated the *Rbpj* and *Hes1* siRNAS capacity for modulating *Ascl1* expression *in vitro*, we postulated that the glial scar could be an interesting source of reprogrammable astrocytes for an *in vivo* approach based on the usage of viral vectors expressing siRNAs. We also hypothesized that this strategy could mediate functional recovery in a mice model of cerebral ischemia.

5.2. Objectives

Our main goal was to study the *in vivo* reprogramming ability of viral vectors expressing siRNAs to silence the Notch-1 pathway in the glial scar developed in the peri-infarct area. This main objective can be itemised in the specific objectives detailed below:

- To study the evolution of glial scar during the first days after the injury in a mice model of ischemic stroke.
- To study whether the expression of siRNAS contained in a viral vector could lead to the *in vivo* silencing of NOTCH1 signaling and to the modification of ASCL1 expression.
- To further elucidate whether this siRNA-based strategy could lead to an improved recovery in animal models of cerebral ischemia.

5.3. Material and Methods

5.3.1. Animal management

Male adult C57BL/6 mice (25-30 g) from Central Animal House of Universidade de Santiago de Compostela (USC), Spain) were used in each culture. In this regard, experimental protocols and animal handling were approved by the chief of the Servizo provincial da Gandaría of the territorial department of Consellería de medio Rural e do Mar of province of A Coruña, being the main responsible PhD Francisco Campos Pérez. The animal experiments were conducted under the procedure number: 15010/2019/004 according to the Spanish and EU rules (86/609/CEE, 2003/65/CEE, 2010/63/EU, RD 1201/2005 and RD

53/2013). All procedures were carried out in the Health Research Institute of Santiago de Compostela (IDIS), with the registration number: ES1507802928[01]. Mice were granted free access to water and pellets of "Aliment complet pour rat/souris (stadeentretien)" (SAFE, France). They were maintained at a room temperature of 20 ± 1 ºC, humidity of 60 ± 5% and light/dark cycle of 12 h/12 h, and were housed one week before any procedure.

For all surgical procedures and MRI acquisitions, mice were anesthetized with sevoflurane (Sevorane, AbbVie, US) in a mix of O2:N2O at 30:70, inducted with 4% and maintained with 3-4% of sevoflurane. Rectal temperature was maintained at 37 °C when anesthetized. The animal status was checked daily after the surgical procedure.

5.3.2. Mouse model of cerebral ischemia

Transient focal ischemia (35 min) was induced by transitory middle cerebral artery (MCA) occlusion (tMCAO), following the method described by Longa and Koizumi[146]. Briefly, a midline incision was made in the neck, exposing the carotidal system: the right common carotid artery (CCA) and the external ramification of the CCA (ECA). The internal ramification of the CCA (ICA) was

provisionally ligated while the right common carotid artery (CCA) and the ECA were permanently occluded**.** A small cut was done in the CCA to introduce a commercial suture with a silicon-rubber coated head (Doccol, USA). The suture was introduced in the CCA and through the ICA by removing temporarily the ICA ligature. The suture was placed in the origin of the (MCA) blocking the blood flow.

During surgery, cerebral blood flow (CBF) was monitored with a Periflux 5000 laser-Doppler system (Perimed AB, Sweden).

5.3.3. Viral injection

AAV5 virus was used for the vectorizarion of the *Hes1* siRNA (treated group n=3 animals) and scramble siRNA (control group n=3 animals) to the peri-infarct area. The viral particles were provided by Tebu-bio (France) with a viral tittering of 10^{13} vg/mL. The virus was constructed with a GFAP promoter to limit the viral expression to the astrocyte cell. Viral particles also presented a tdTomato sequence as report protein.

Three days after the tMCAO, animals were place in the stereotaxic device for the injection of 1.5 µL of AAV5 in the peri-infarct lesion[147]. The stereotaxic coordinates for the injection

were extrapolated using the T2 MRI image at 72 h to perform the injection near the damage area (**Figure 27**).

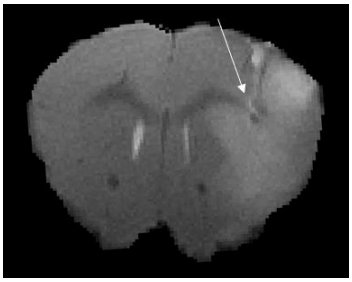

Figure 27. Rare T2 image. White arrow signaling the injection area.

5.3.4. MRI assessment and MRI data analysis

MRI studies were conducted on a 9.4 T horizontal bore magnet (BrukerBioSpin, Ettligen, Germany) with 12 cm wide actively shielded gradient coils (440 mT/m). Radiofrequency (RF) transmission was achieved with a birdcage volume resonator; signal was detected using a two-element arrayed surface coil (RAPID Biomedical, Germany), positioned over the head of the animal, which was fixed with a teeth bar, earplugs and adhesive tape. Respiratory frequency and body temperature were monitored throughout the experiment. Transmission and reception coils were actively decoupled from each other. Gradient-echo pilot scans were performed at the beginning of

each imaging session for accurate positioning of the animal inside the magnet bore.

To analyse the glial scar progression, T2 weighted images were acquired at 24 hours, 72 hours and 7 days after the induction of ischemia (n=3 animals per group). Whereas for the viral injection experiments, images were acquired at 72 hours and 21 days.

The progression of ischemic lesions, and infarct volumes were determined from T2-maps calculated from T2-weighted images. T2-weighted images were acquired using a multi-slice multi-echo (MSME) sequence with a 11 ms echo time (TE), 2.8 s repetition time (TR), 12 echoes with 11 ms echo spacing, flip angle (FA) of 180º, 2 averages, 50 KHz spectral bandwidth (SW), 16 slices (axial) of 0.5 mm, 19.2 × 19.2 mm^2 field of view (FOV) with saturation bands to suppress signal outside this FOV, a matrix size of 256 × 256 (isotropic in-plane resolution of 75 µm/pixel × 75 µm/pixel) and implemented without fat suppression option.

The injection site was checked using RARE (Rapid Acquisition with Refocused Echoes) T2 image with the following acquisition parameters: 33 ms echo time (TE), 2.5 s repetition time (TR), flip angle (FA) of 180º, 4 averages, 50 KHz spectral bandwidth (SW), 14 slices (axial and coronal) of 0.5 mm, 20 × 20 mm^2 field of view (FOV), a matrix size of 256 × 256 (isotropic in-plane resolution of

78 µm/pixel × 78 µm/pixel) and implemented without fat suppression option.

MRI post-processing was performed using ImageJ software (W. Rasband, NIH, USA) on independent workstation.

5.3.5. Behavioural test

An automated 4-lane rotarod unit was used to assess the functional improvement of mice after tMCAO. The system software allows pre-programming of session protocols with varying rotational speed. The system logs the fall as the end of the experiment for that subject, and the total running time on the rotarod is recorded. For training, the animals were placed on the rotarod 3 consecutive days before the surgery and for another 3 consecutive days before the end of the follow-up period (21 days after the viral injection). Only animals with a minimum basal time of over 180 s before the surgery were included in further experiments. [148]

A modified version of Konziela's Inverted Screen Test was used to assess muscle strength and endurance in tMCAO mice (AAV5-scramble vs. AAV5-Hes1) at a final point of follow-up period (21 days post-tMCAO). The novel inverted screen constructed in our laboratory was a 160 cm^2 grid of wire mesh placed above a

plastic cylinder which prevented mice form escaping the apparatus. The mice were placed in the centre of the wire mesh screen before the screen was rotated to an inverted position with the mouse's head declining first. When the screen was stable and the mice standing on all four legs, the timer was started. The time when the mouse fell off was noted, or the mouse was removed when the criterion time of 2 min maximum was reached. [148]

5.3.6. Immunohistochemical analysis

After the last follow-up, animals were sacrificed by overdose of anesthesic and transcardially perfused with 20 mL of PBS 0.1M pH 7.4 and 20 mL of 4% formaldehyde (VWR, U.S.A.). Brains were carefully removed from the skull and were post-fixed by immersion in 4% formaldehyde overnight. Then, the slices were washed in PBS and cryoprotected in a 30% sucrose (AppliChem. U.S.A.) solution in PBS containing a 0.05% of sodium azide.

Brains were sectioned to 30 µm thickness in the cryostat (Tissue-Tek, Japan). For the immunohistochemistry, the distance between each slice was 200 µm. The slices were stored in antifreeze solution at -20ºC. They were mounted in gelatine

(Sigma-Aldrich, U.S.A.) coated microscope slides before starting the immunochemistry.

The microscope slides with the brain slices were dried in the heater for30 min. After that time, the slides were washed with PBS (2x 5 min) and tissue was permeabilized in PBSt for 1 hour. The immunohistochemical procedure was developed in a similar way as it was described above for the immunofluorescence (see section I). Primary antibody incubation was done overnight at 4°C in PBSt whereas secondary antibodies were added in PBSt for 1 h at RT. Streptavidin was added for 30 min and for nuclear staining, Hoechst (1:6,000) was incubated 10 min. Between incubation steps, slides were washed with PBS (2 x 5 min) (**Table 7**).

The slides were observed under Leica CTR6000 (Leica Microsystems, Germany) inverted microscope. Images were obtained using LAS X Life Science software (Leica Microsystems).

Table 7. Antibodies used for the immunohistochemical analysis

Antibody	Dilution	Reference	Commercial
Rabbit anti-DCX	1:400	Ab15364	Abcam, U.K.
Goat anti-Rabbit biotinylated	1:200	Ba-1100	Vector, U.S.A.
Streptavidin 488	1:200	Custom	Immunostep, Spain

5.3.7. Western blot

A piece of tissue of 1 mm wide around the injection zone was used for the protein studies. It was digested in 150 µL of cold RIPA buffer using a TissueLyser II machine (QiaGen, U.S.A.) at 30 Hz for 3 min. Protein was quantified using the BCA protein assay kit as was described in section I.

The Western blot protocol was developed as was described in section I. Necessary volume of cell lysate containing a total amount of 30 µg of protein were subjected to SDS PAGE using Criterion gels 4-15% with a fixed voltage of 140V, 180 mA. Proteins were then transferred to a PVDF membrane using a Trans-Blot semi-dry system with a limited voltage of 25 V and 180 mA for 2 h. After blotting, membranes were blocked for 1h with 5% BSA in Tris-Chloride Buffer with a 0.1% of TBST. Once

blocked, primary antibodies (diluted in TBST with a 5% of BSA) were used overnight in agitation following manufacturer instructions. Secondary antibodies were diluted as the primary antibodies and they were incubated for 1 h at RT in agitation (**Table 8**). Finally, after washing in TBST, the HRP activity was revealed with Pierce™ ECLWestern Blotting Substrate and detected using the ChemiDoc machine. WB results were analysed using ImageJ. The relative expression of proteins compare to Histone 3 expression was calculated for each sample, and the average of samples for each group was normalized to the control.

Table 8. Antibodies used for the western blot experiment.

Antibody	Dilution	Reference	Commercial
Rabbit anti-Hes1	1:200	Ab1749	Abcam, U.K.
Mouse anti-ASCL1	1:400	sc-390794	Santa-Cruz, U.S.A.
Rabbit anti-Histone3	1:400	ab93157	Abcam, U.K.
Rabbit anti Mouse-HRP	1:200	P0260	Dako, U.S.A.
Goat anti Rabbit-HRP	1.200	P0448	Dako, U.S.A.

5.3.8. Statistics

All data are presented as the mean and standard error of the mean (mean ± SEM). One-way analysis of variance (ANOVA) followed by post-hoc Bonferroni evaluation was used for multiple groups to determine significant differences. Student´s t-test was used to test the differences between two groups. Statistical significance was set as *P<0.05; **P<0.01; ***P<0.001. The statistical analysis was conducted using GrapPad Prism 7.0.

5.4. Results

5.4.1. Glial scar progression

In order to evaluate the glial scar progression, the evolution of GFAP expression was assessed at 24h, at 72h and at day 7 after tMCAO (n=3 animals per group) (**Figure 28**). The intensity of GFAP signal, in arbitrary units (AU), was used as an indicator of GFAP expression levels in the tissue. A significative increase of GFAP signal was observed at 72h (6901.3 ± 1014.8 AU) and 7 days (7350 ± 1788.1AU) after ischemia, compared to 24h (1066.6 ± 702.3AU) (**Figure 29**) (all p<0.0001). These data suggested that the glial scar exhibits a fast progression pattern after the

ischemic damage that, remains uniform between 72 h and 7 days. These results suggest that the optimal time window for a targeted treatment against reactive astrocytes would be between 72h and 7 days after ischemic damage, when the expression of GFAP has reached its maximum levels.

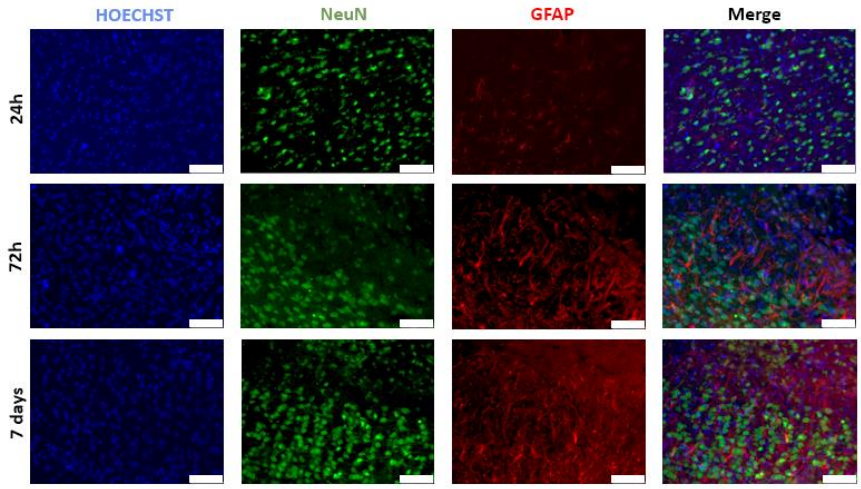

Figure 28. Immunofluorescence stain for mature astrocytes marker (GFAP) neurons (NeuN) of the glial scar in mouse histological sections of cerebral cortex 24h, 72h and 7 days. Scale bar 75µm

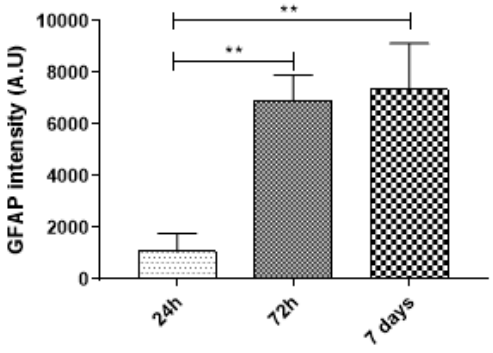

Figure 29. Intensity in arbitrary units of GFAP marker at 24h, 72h and 7 days after the ischemic damage. Data are show as mean ± SEM. **P<0.01 (n=3 per group).

5.4.2. In vivo reprogramming

5.4.2.1 Infarct volume

Based on our *in vitro* results, we tested the effective siRNA treatment, *Hes1* siRNA, but using viral vectors instead of lipofectamine as carriers for the siRNA. Intracerebral administration of the AAV5 virus (10^{13} vg/mL) was performed in the ipsilateral hemisphere. Initially, smaller infarct volumes, although no statistical different, were appreciated in the AAV5-*Hes1* treated animals (6.63 ± 2.47%) and the AAV5-Scramble control group (7.16 ± 2.04%) at 21 days after tMCAO (**Figure 30**)

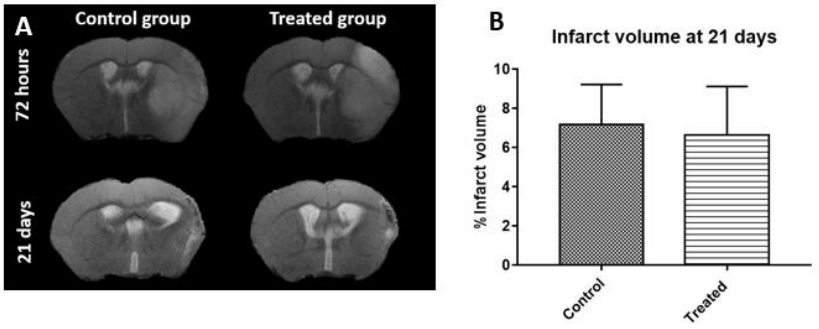

Figure 30. (A) T2 images of the infarct progression in control and treated animals. **(B)**. Percentage of the ipsilateral volume affected by the infarct at 21 days after the ischemic event.

5.4.2.2 Behavioural test

Behavioral tests were performed to determine possible differences in functional outcome between experimental groups. Rotarod test did not show any statistical differences between AAV5-Hes1 (138.3 ± 47.2s) and AAV-scramble (102.75 ± 16.9s), although a clear trend in fuctional recovery was found for the AAV5-Hes1 animals. Similar results were observed when the mice strength and endurance were assessed with the inverted screen test (66.1 ±41s in control animals vs. 86.6 ± 65.9s in AAV-Hes1 animals) (**Figure 31**).

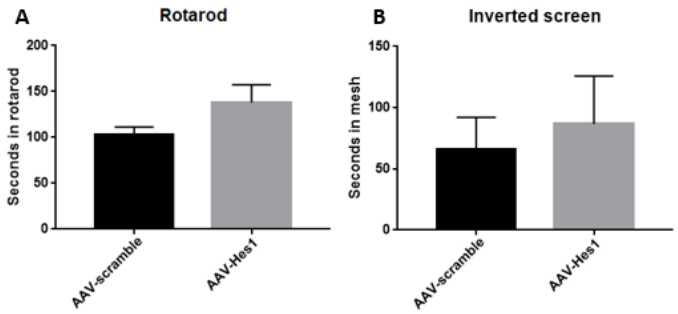

Figure 31. **(A)** Rotarod test at 21 days after the ischemic insult. **(B)** Inverted screen test at 21 days. Data are show as mean ± SEM

5.4.2.3. Protein expression

In order to evaluate whether the injection of viral vectors with siRNAs produce effects on the astrocytes of the glial scar, neural progenitor DCX and ASCL1 markers were measured by western blot at 21 days after tMCAO in the injection area. No statistical differences were found between control and treated animals for DCX (115.7±9.8 relativized to control) or for ASCL1 (112.3s±8.5 relativized to control) (all $p>0.05$) (**Figure 32**). The expression of Hes1 protein was also evaluated in order to check the effectivity of the virus. However, no specific bands were detected (data not shown).

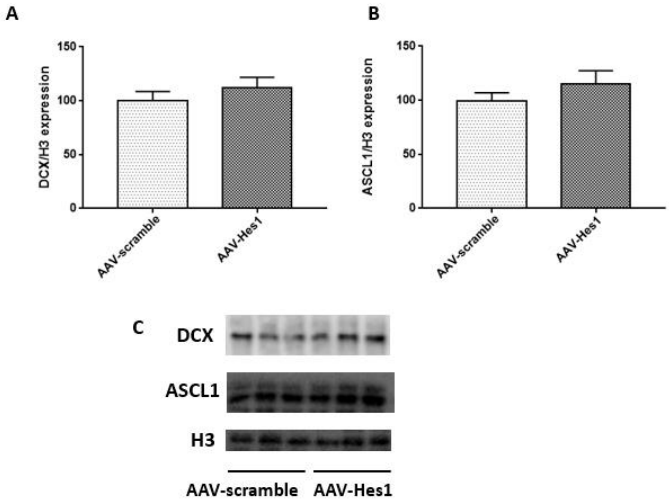

Figure 32. **(A)** DCX protein expression at 21 days in control and treated animals relativized to Histone 3 protein. **(B)** ASCL1 protein expression at 21 days in control and treated animals normalized to Histone 3 protein. **(C)** Western blot bands of DCX, ASCL1 and Histone 3 proteins. Data are show as mean ± SEM (n=3)

5.4.2.4. Neural progenitor markers

The expression of the neural progenitor marker was assessed at 21 days by immunohistochemical analysis of the brain to determine whether infected cells (former astrocytes) correlate with DCX expression, as a marker of neuroblast. Effective transfection of astrocytes by the AAV5 was confirmed by the expression of tdTomato protein (virus reporter) around the injured area. Although infected cells were indeed within next to

the initial injured area, they did not showed significant DCX expression (**Figure33**).

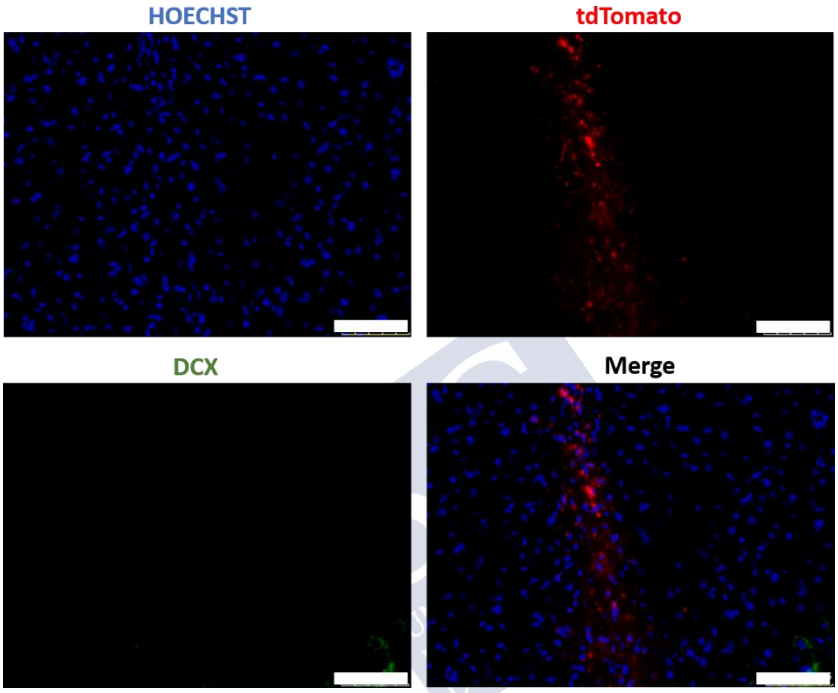

Figure 33. Virus reported positive cells (tdTomato+ cells) showed the tissue area infected with the AAV. No colocalization was observed between infected cells and neural progenitor markers. Scale bar 75µm.

6. Section III. Using nanoparticles as vectors for in vitro reprogramming

6.1. Hypothesis

The way siRNA transfection is performed plays a pivotal role in the effectiveness of reprogramming, as they must reach the target cell specifically and safely. Nanoparticles emerged as a versatile and optimal tool to carry out this function. For this reason, we postulate the use of nanoparticles as a possible translational way to deliver the treatment into astrocyte cells *in vitro*.

6.2. Objectives

The main objective is to synthetize a nanoparticle with the ability to cross the cell membrane and deliver its cargo in the cytosol, as the main target for siRNA treatments. To this aim, the principal objective was structured in three specific sections:

- To synthesize and characterize the nanoparticle with the ability to be internalized by the astrocytes.
- To check its ability to deliver the cargo inside the astrocytes.
- To study the effect of the treatment delivered by the nanoparticle.

6.3. Material and Methods

6.3.1. Biodegradable SiO_2 capsule synthesis

Nanometer sized capsules were prepared by a modification of well-established methods. The protocol followed for the synthesis is briefly described below. [149] [150].

First step was the synthesis of sub-micrometer sized $CaCO_3$ cores, produced by adding 193 µL of Na_2CO_3 (Sigma-Aldrich, U.S.A.) solutions (0.33M) dropwise into of 1 mL of CaCl2·2H2O (Sigma-Aldrich, U.S.A.) (0.33M) under magnetic stirring at 1100 rpm for 20 minutes. Solutions were prepared in an 5:1 (v:v) ethylene glycol (ROTH, Germany) water mixture. The synthesis of the core was performed in the presence of the molecules which should form the cargo inside capsules, that were dissolved in the CaCl2 solution before the addition of Na_2CO_3. As cargo,

dextran functionalized with Cascade Blue (Thermo-Scientific, U.S.A) or siRNA *Gapdh* positive control (Thermo-Scientific, U.S.A.) were used (**Table 9**). Core synthesis was performed by mixture the compound under magnetic stirring at 1100 rpm for 20 minutes.[151]

Table 9.Amounts of molecules (volume V and concentration C of stock solution) added as cargo for later encapsulation to the initial CaCl2·2H2O solution.

Cargo molecule	**V**	**C**
Dextran Cascade Blue	50 µL	6.5 (mg/mL)
siRNA *Gapdh*	50 µL	10 (µM)

The formed $CaCO_3$ cores were transferred into Eppendorf tubes (2 mL), centrifuged at 8,000 rpm and washed twice with 2 mL of ethanol and once time with MilliQ water, supernatants were discarded, washing buffer (ethanol or MilliQ water) was added and pellet was dispersed using sonication. The characterization of the CaCO3 particles containing the desired cargo were finally dispersed in 300 µL of MilliQ water for measuring size and Z potential using the Dynamic Light Scattering (DLS) and Laser Doppler Anemometry using a commercial set-up (Zetasizer Nano ZS, ZEN3600, Malvern; 173° backscatter settings, 633 nm laser).

$CaCO_3$ cores were washed twice with 2 mL MilliQ water and once with 1 mL of ethanol (centrifuging at 8,000 rpm for 3 min). For the coating with polyethylene glycol (PEG), the nanoparticles were precipitated by centrifugation at 8,000 rpm for 3 min, then 1.5 mL of a 5 kDa CH3O-PEG-SH solution (6 mg/mL) was added to resuspend the $CaCO_3$ cores. Suspension was sonicated for 5 min and kept under orbital shaker for 1 hour. The cores were then washed twice with 2 mL MilliQ water and one time with 2 mL ethanol (centrifuging at 14,800 rpm for 3 minutes). Finally, cores were dispersed in 2 mL of ethanol. The cores were then sonicated for 5 min and added to a glass beaker containing 16.1 mL of ethanol, 4 mL of MilliQ water, 230 µL of NH_4OH (Sigma-Aldrich, U.S.A), and 70 µL of TEOS (Sigma-Aldrich, U.S.A). The mixture was stirred at 500 rpm for 3 h.

After coating, the particles were washed one time with ethanol and twice with MilliQ water. Finally, capsules were resuspended at 200 µL of MilliQ water and sonicated until a full dispersion was observed. Then, 1.8 mL of 0.2 M EDTA (Sigma-Aldrich, U.S.A) at pH 6 were added, to dissolve the inorganic $CaCO_3$ cores, and the sample was kept overnight at 4 ºC.

After core dissolution, the capsules were washed twice with MilliQ water (centrifugation speed 1500 rpm for 45 min), capsules were resuspended in 300 µL of MilliQ water for

measuring size and z potential using the DLS. A final positive PARG layer was then deposited onto the capsule surface by adding 500 µL of an aqueous solution of PARG (Sigma-Aldrich, U.S.A) (5 mg/mL, pH 6.5, 0.05 M in NaCl). The mixture was sonicated for 2 s, shaken for 30 min, and finally washed again twice with MilliQ water, as described above. The capsules were finally dispersed in 300 µL of MilliQ water.

Capsules were characterized by measuring its hydrodynamic size in each step of the synthesis: $CaCO_3$ core synthesis, PEG coating, SiO_2 capsule synthesis and PARG coating. In addition, Z potential was measured in the SiO_2 capsules and in the capsules coated with PARG to evaluate the effectivity of the PARG coating.

6.3.2. Capsule quantification

Due to the smaller size of the sub-micrometer sized capsules an estimation of the capsule concentration number by counting capsules with a hemocytometer was not possible. For this reason, all the concentrations of capsules in the experiments described in this work were quantified by the amount of the encapsulated cargo. In this way, cascade-blue dye was used as cargo for the quantification of capsules used in toxicity cell uptake experiments. Whereas siRNA quantification was used to

estimate a relative capsule amount for the knockdown experiments.

For cascade blue quantitation, the encapsulation efficiency of the dye in the $CaCO_3$ core was calculated after the core synthesis. They were centrifugated 10 minutes at 14.800 rpm and cascade blue concentration was measured in the supernatant using a fluorometer (wavelengths of excitation/emission = 400 nm/420 nm).

In addition, cascade blue concentration in the SiO_2 capsule at the end of the reaction was also calculated by digesting the capsules with the enzyme Pronase (Merck, U.S.A.) (2 mg/mL) overnight at 37ºC in a ¼ capsule/pronase mixture proportion **(Figure 34)**. This enzyme induced the digestion of the capsules and allow the liberation of the cargo. The digested capsules were centrifugated 10 minutes at 14.800 rpm to eliminate resto of the capsules. Supernatant was measured in the fluorometer with the parameter described above.

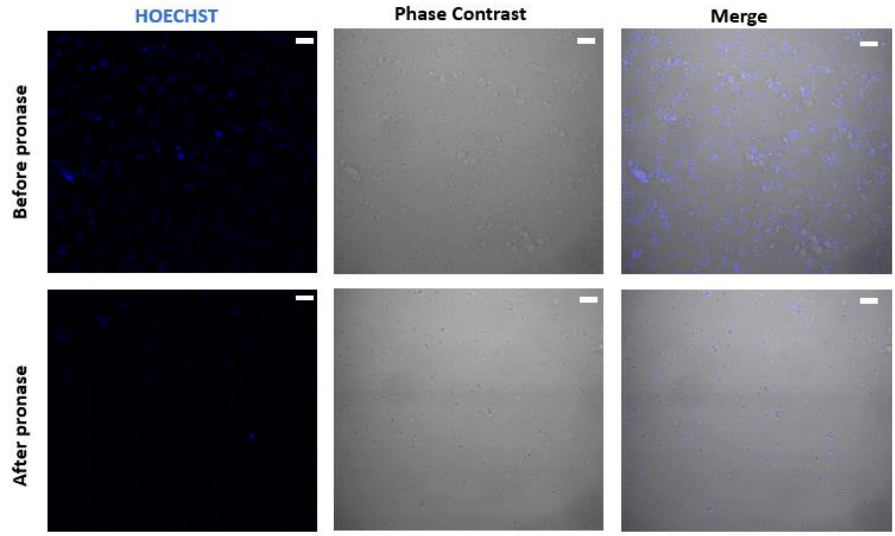

Figure 34. Cascade blue dye encapsulated in SiO_2 capsules before **(A)** and after **(B)** pronase digestion. Scale bar 5 µm.

For both $CaCO_3$ core and SiO_2 capsule, the intensity value obtained was compared to a standard curve to obtain a concentration of cascade blue per mL of capsules. Toxicity and cell uptake experiments were performed using this value as an indirect way to measure capsule concentration.

For the quantification of the capsules with siRNA, the measurements were only done in the final capsules and not in the $CaCO_3$ core because the ethylene glycol used in the core synthesis interfere in the measurement. For the siRNA quantification of the capsules, they were digested as was described above. The RNA was quantified using the commercial

kit Ribogreen. Two dilutions of the sample (1:5 and 1:10) were prepared to dilute possible interferences and its RNA concentration was measured and compared to a standard curve. Toxicity and mRNA silencing experiments were performed using this value as an indirect way to measure capsule concentration.

6.3.3. Cell culture

For toxicity assays, cell uptake and mRNA silencing experiments astrocyte cell line C8-D1A (ATCC) were used. The cells were culture in DMEM with 10% FBS.

6.3.4. Cytotoxicity assays

Cell viability studies were performed with a fluorescence-based approach using resazurin. Resazurin is a non-toxic non-fluorescent compound, which in living cells is converted into fluorescent resorufin [152]. For the toxicity assay 5,000 astrocytes C8-D1A cells were seeded per well in 96-well plates. Each well contained 100 µL medium per well and 0.32 cm^2 of surface area. After 24 h, the growth medium was replaced by medium with different capsule concentrations. Capsule concentration was estimated by the quantification of the cargo.

Therefore, a range of concentrations of cascade blue and RNA were tested (10^{-4} to 10^{3}). In addition, different percentages of batch capsules were used as a way to detect capsule concentration toxicity. A range between 0,08 and 5 % of the total capsules was evaluated.

Cells were then incubated with serial dilutions of capsules for 24 hours. After incubation, cells were washed with PBS and 10% of fresh resazurin solution in pure growth media was added. After 6 hours of incubation with resazurin the samples were analysed with a fluorometer (wavelengths of excitation/emission = 560 nm/585 nm). For the evaluation the background-corrected maximum of the fluorescence emission was used, since this emission correlates with the viability of cells. Each measurement was performed using triplicates to obtain the mean value and the standard deviation. The mean value of the fluorescence intensity was normalized to the fluorescence of cell which had not been exposed to capsules and was plotted against the concentration of the capsules.

6.3.5. Cell uptake experiments

Cell uptake experiments were performed with C8-D1A astrocyte cell line. For the experiment, 10,000 were seeded in 8 well plate

(ibidi, U.S.A.). After 24 hours, cells were incubated with a capsule's concentration of 10pg cascade blue/cell. After 20 hours of incubation with the capsules, LysoTraker (Thermo-Scientific, U.S.A.) was added to the wells to detect lysosomes. Cells were washed with PBS 24 hours after adding the capsules.

6.3.6. Silencing experiments

Sub-micrometer sized biodegradable capsules were synthetized using *Gapdh* siRNA as cargo for the treatment group whereas the control group capsules were synthetized using Scramble siRNA. C8-D1A astrocytes were seeded at a concentration of 5,000 cells per well and after 24 hours, they were incubated with a non-toxic capsule concentration of 16nM of RNA per well (three wells per condition). For these experiments two different batches of capsules with *Gapdh* siRNA as cargo were evaluated, each one with its corresponding siRNA scramble in capsules control.

As a positive control of transfection, 5 µL of Lipofectamine 2000 (Thermo-Scientific) was incubated with 16nM of siRNA. Cells were washed 24 hours after adding the capsules and the knockdown efficiency was evaluated after 48 hours through the evaluation of GAPDH activity using the KDalert™ GAPDH Assay Kit (Thermo-Scientific).

6.3.7. Statistics

All data are presented as the mean and standard error of the mean (mean ± SEM). One-way analysis of variance (ANOVA) followed by post-hoc Bonferroni evaluation was used for multiple groups to determine significant differences. Statistical significance was set as *P<0.05; **P<0.01; ***P<0.001. The statistical analysis was conducted using GrapPad Prism 7.0.

6.4. Results

6.4.1. Biodegradable SiO_2 capsule synthesis

Capsules were synthetized and characterized in a four step process: $CaCO_3$ core synthesis, PEG coating, SiO_2 layer synthesis and PARG coating.

6.4.1.1. $CaCO_3$ core synthesis

The hydrodynamic size of the $CaCO_3$ core was measured by DLS right after the synthesis and purification. The measured hydrodynamic diameter was 642±28 nm (n=4) with a polydispersity index of 0,640 (**Figure 35**).

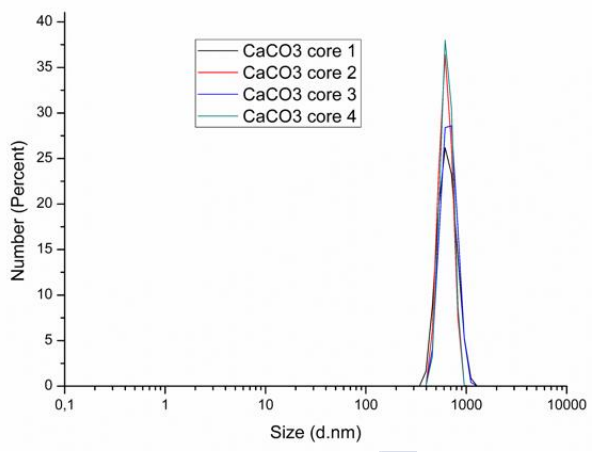

Figure 35. Hydrodynamic size of the $CaCO_3$ core.

6.4.1.2. PEG coating

Cores coated with polyethylene glycol showed a hydrodynamic diameter of 678,9±122nm with a polydispersity index of 0,235 (**Figure 36**).

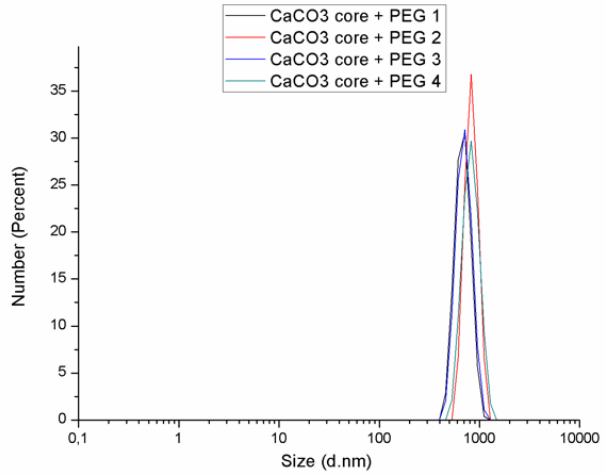

Figure 36. Hydrodynamic size of the pegylated $CaCO_3$ core.

6.4.1.3. SiO_2 layer synthesis

After the SiO_2 layer synthesis, the hydrodynamic size was quantified with the DLS obtaining a diameter of 738±84,3 nm (n=4) with a polydispersity index of 0,4 whereas the Z potential was -39,8±6,44mV, a good indicative of the presence of the silica coating (**Figure 37**).

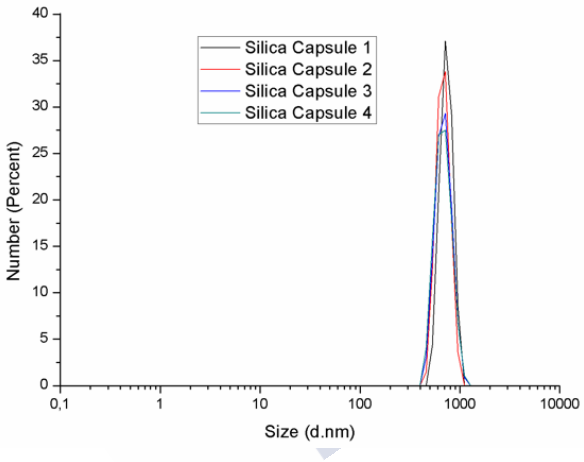

Figure 37. Hydrodynamic size of the SiO_2 capsules.

6.4.1.4. SiO_2 layer with PARG coating

SiO_2 layer was coated with PARG and hydrodynamic size was quantified with the DLS, obtaining a diameter of 815±52,1 nm (n=4) with a polydispersity index of 0,254 **(Figure 38)** whereas the Z potential was 34,2±7,71mV, confirming the presence of the

polycation on the particle surface. The capsules showed nor or little aggregation under the TEM **(Figure 39).**

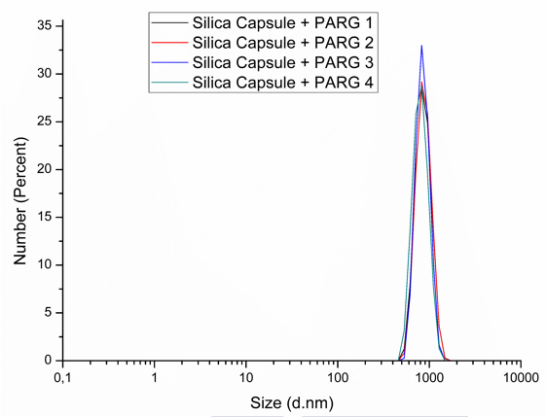

Figure 38. Hydrodynamic size of the SiO_2 capsules coated with PARG.

To summarize, the hydrodynamic diameter of the nanoparticles was increasing in every step, starting in 642 nm for the CaCO3 cores, 679 nm for the CaCO3 coated with PEG, 738 nm for the SiO2 coated nanoparticles and finally 815 nm for the PARG coated nanoparticles. The final nanoparticles showed a positive Z potential that is beneficial for the aimed future transfection studies.

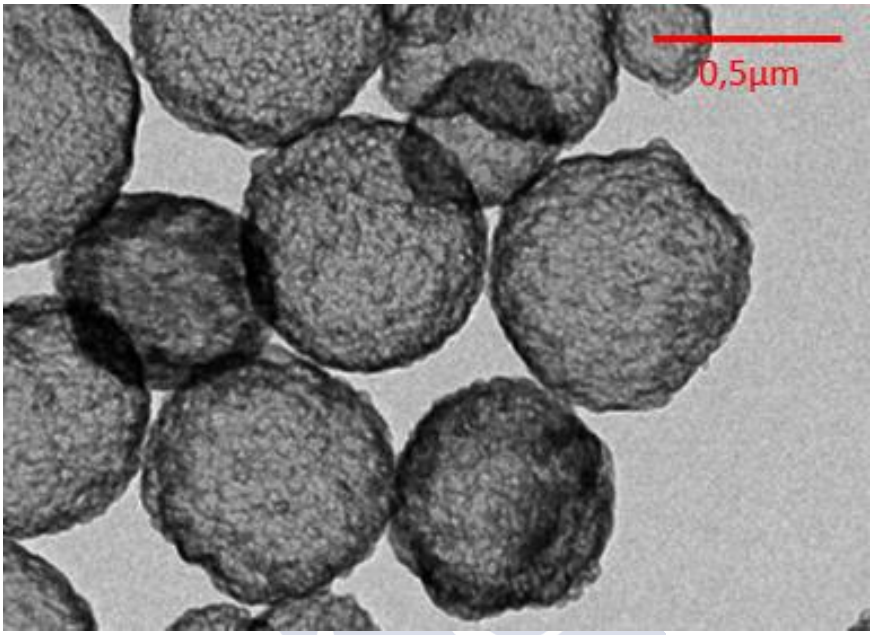

Figure 39. TEM image of SiO_2 silica capsules coated with PARG

6.4.2. Capsule quantitation

For the capsule quantitation, the dye encapsulation efficiency in the CaCO3 cores with cascade blue was 74.9±10.2% (n=3) whereas in the final capsules was 12.2±7.4% (n=3). Some of the encapsulated dye was lost in the coating process, probably due to the washing steps. Regarding the final concentration, we achieved a cascade blue concentration of 104.9±64.2 ng/µL in 300 µL of water (n=3).

For siRNA loaded nanocapsules, the capsules quantitated with siRNA, the encapsulation efficiency in the final capsules was 54.9±19.1% (n=3), whereas the final concentration was 27.5±12.4 ng/µL in 300 µL of water (n=3), corresponding to a concentration of 2067nM, much higher than the dose needed for the silencing experiments. The encapsulation efficiency of the siRNA in the CaCO3 cores was impossible to asses due to the background signal of ethylene glycol.

6.4.3. Toxicity experiments

The capsules toxicity was evaluated in regard with the amount of cascade blue, in regard with the amount of RNA and using the percentage of the total batch capsules.

A very low toxicity was observed for the tested capsules, with the lowest viability value measured for cascade blue capsules of 60,9±9,1% compared to control for the 1,000pg dose **(Figure 40)**. Whereas, the viability measured for cells treated with 1,000 pg of RNA per cell, corresponding to a siRNA concentration of 1880 nM, was 71,1±8,4%. This concentration was 100x higher than the dose needed for the transfection studies, indicating the low toxicity profile of the capsules **(Figure 41)**.

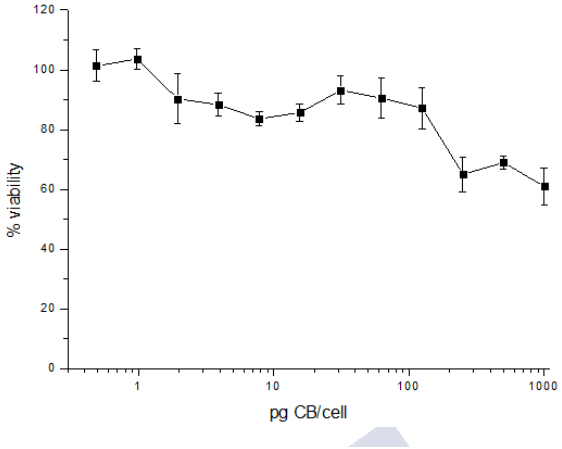

Figure 40. Viability of capsules quantified with cascade blue. The toxicity was determined in a range of 0.5-1,000pg of cascade blue per well.

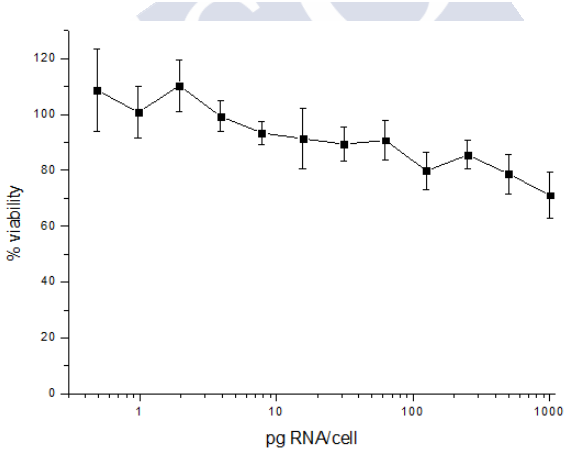

Figure 41. Viability of capsules quantified with RNA. The toxicity was determined in a range of 0.5-1,000pg of RNA per well.

6.4.4. Cell uptake experiments

Cell uptake experiments were carried out for nanocapsules in astrocytes. Cells were incubated 24 hours with the capsules, and LysoTracker Green was used to label lysosomes. Confocal microscopy showed the internalization of the capsules in the cells, and it could be seen some colocalization between the cascade blue used as cargo and the lysosome staining LysoTracker-green **(Figure 42)**, although some the capsules are also in the cytosol and not in the lysosome, suggesting an internalization of the capsules through the endocytosis pathway and a possible lysosomal escape, although this later must be confirmed by other means.

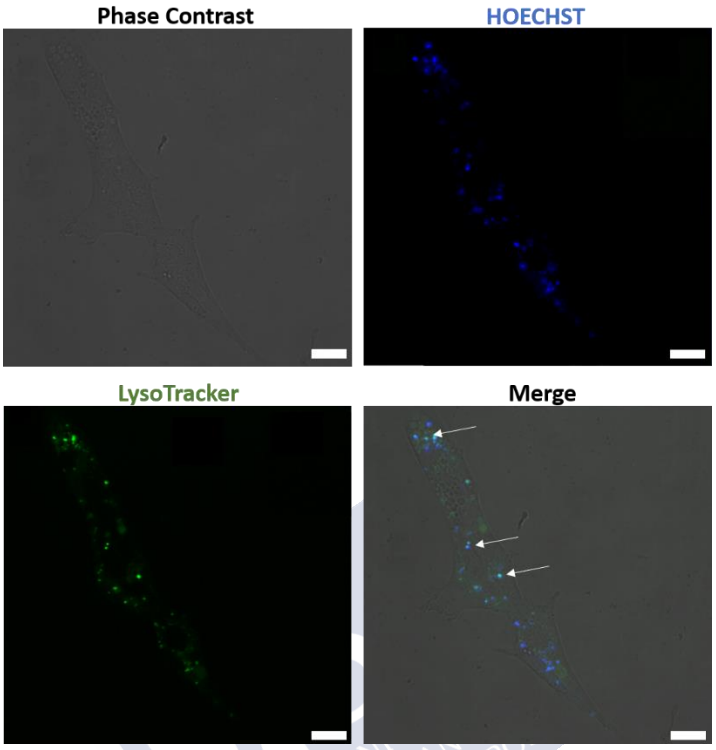

Figure 42. The colocalization of capsules synthetized with cascade blue and the lysosome marker LysoTracker showed that capsules are internalized by the cell membrane. Scale bar 20 µm.

6.4.5. Silencing experiments

Gapdh siRNA loaded capsules were used for the in vitro knockdown experiments at a siRNA concentration of 16 nM, that has shown low cytotoxicity in the previous experiments. Capsule treatment reduces the GAPDH expression to the 71,28%±10,6

(n=3) compare to control. Positive control wells using 16 nM of siRNA with lipofectamine induces reduce the expression of GAPDH to an expression of 53,1%±15,2 (n=3) (**Figure 43**).

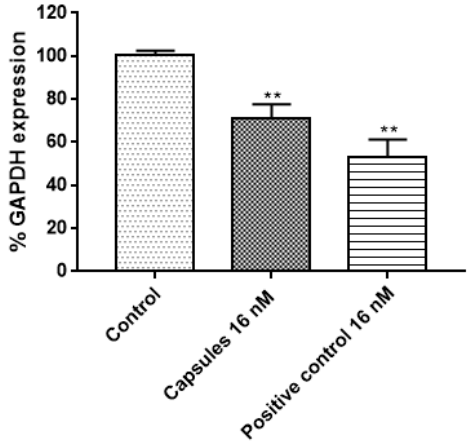

Figure 43. Percentage of GAPDH protein expression in astrocytes after its incubation with capsules containing siRNA and siRNA + lipofectamine (positive control). Data are show as mean ± SEM. **P<0.01; using 1-way ANOVA (n=3 per group).

7. Discussion

According to the WHO, stroke is the second leading cause of death in the world and the first cause of permanent disability in the developed countries. Therefore, stroke has become a major social and economic problem that consume an important percentage of the national budgets for health care and personal assistance services [4-8]. Nevertheless, there are only a few treatments, based on recanalization, able to slow the cell death and loss of function associated to the ischemic damage. However, the use of these treatments is limited by its short therapeutical window[78]. Hopefully, the better understanding of the disease unravels the underlying molecular pathways and opens new therapeutical possibilities.

In recent years, several neuroprotective strategies have been tested in clinical trials but failed in the demonstration of its effectivity. In the last twenty years, cell therapy and the endogenous neurorepair mechanism have emerged as promising alternative for the ischemic stroke[45][89]. However, there are no conclusive results in preclinical models and there are few information about clinical trials using these therapies. In this context it is necessary to develop new alternative therapies to overcome the limitations in the ischemic stroke treatments.

Among this therapies, cell reprogramming is gaining in prominence due to its higher translational potential in recent years [91][94]. This strategy could circumvent some of the technical (i.e. immunogenicity, tumorigenesis, low survival rate of the graft) and ethical issues (i.e. the use of tissue from fetal or embryonic origins) concerning cell transplants [79]. Increasingly powerful and sophisticated reprogramming techniques have been developed for a great number of diseases such as stroke, Alzheimer's disease or spinal cord damage. Evolving therapeutic approaches to treating acute ischemic stroke [142][153][154].

In ischemic stroke, the reactive astrocytes which form the glial scar during the subacute phase seem to be a potential source for reprogrammable cells. Their relative abundance, their proximity to the injured area and their plasticity make them ideal for cell reprogramming approaches. Different studies even indicate that these reactive astrocytes may exhibit a stem cell-like behavior which would enable the reprogramming process [66][67][138]. Moreover, the activation of NOTCH1 signalling pathway induces the translocation of NCID which, in combination with *Rbpj* transcription factor, promotes the expression of Hes transcription factors. HES1 protein inhibits the expression of the neurogenic ASCL1 protein, thus determining cell fate [143][145]. In fact, a recent study by Magnusson and collaborators suggest

the existence of a latent neurogenic program mediated by the overexpression of ASCL1 in reactive astrocytes. It should be noted that Magnusson and colleagues opted for a knockout animal model to abolish Notch-1 signaling, which is not a suitable alternative for translational approaches [143][144].

Therefore, it seems reasonable to suggest that the inhibition of the NOTCH-1 signaling pathway in astrocytes could lead to ASCL1 overexpression with the cell fate leaning towards a neuronal phenotype. Thus, our first goal was to determine the effect of knocking down NOTCH-1 pathway on ASCL1 expression. Among the available reprogramming techniques, siRNA mediated silencing provides for a tighter control of the silenced pathway and reduced side effects of the treatment in comparison to other approaches [115][116]. We aimed at blocking NOTCH1 pathway at two different points, using *Rbpj* and *Hes1* siRNAs.

Our *in vitro* results showed that both *Rbpj* and *Hes1* siRNAs induced a downregulation of the NOTCH1 pathway linked to an *Ascl1* mRNA overexpression. Surprisingly, *Hes1* mRNA knockdown had a higher impact on *Ascl1* mRNA upregulation even when *Rbpj* siRNA was more efficient in reducing *Rbpj* mRNA expression when compared to *Hes1* siRNA. Paradoxically, the upregulation of *Ascl1* mRNA expression by silencing *Rbpj*, correlated with a significant decrease of ASCL1 protein levels at

72h. However, using the *Hes1 siRNA* we didn´t observe a downregulation of ASCL1 protein at 72h. These results may suggest a different response in the NOTCH1 molecular pathway depending which point of the pathway is being inhibited. Nevertheless, the ASCL1 protein levels are close to the control group for both treatments. This data may suggest that the ASCL1 protein renewals itself at a very slow rate. Therefore, the upregulation of Ascl1 mRNA could take more than 7 days in giving rise to upregulated levels of ASCL1 protein. We also hypothesised that ASCL1 may have a strong posttranscriptional regulation so that other molecule pathways could be blocking ASCL1 synthesis. For example, it has been demonstrated that neuroinflammation plays a key role in dedifferentiation processes undergone by astrocytes. In neurosphere forming experiments, neither *Rbpj* siRNA nor *Hes1* siRNA were able to induce a higher percentage of neurospheres in cultures of cortical astrocytes. Nevertheless, the transfection agent may have a toxic effect on culture, thus masking the stimulating neurosphere formation effects of silencing *Rbpj* and *Hes1* mRNAs. It should be also noted that astrocytes in culture are from fetal origin so that it is possible that they retain some intrinsic neurogenic properties. Their immature state would easily enable their spontaneous dedifferentiation in serum-free conditions *in vitro.* During this PhD we have tried to develop

several adult astrocytes protocols without success (data not shown). It is imperative to develop a mouse adult astrocyte culture to assess the neurosphere formation potential of *Rbpj* and *Hes1* silencing.

In vivo reprogramming studies are underpinned by the use of viral vectors as the preferential delivery method for the reprogramming agent (i.e. miRNAs, transcription factors, siRNAs). AAV5 vectors allow for reduced genotoxicity, long-term and stable expression of the inserts in post-mitotic cells and for great tropism for astrocytes [131][129][127]. Thus, after having demonstrated the capability of *Rbpj* and *Hes1* siRNAs to reduce Ascl1 expression *in vitro*, we tested the effect of silencing *Hes1* mRNA on an *in vivo* adult mouse model of stroke using an AAV5 viral vector for siRNA delivery. However, at 21 days post-tMCAO, it was not observed a reduction in the infarct volume in the AAV5-*Hes1* treated animals. However, although no significant differences were found, a clear trend to better functional recovery was observed by behavioral tests in treated animals in comparison to control animals. The neurogenic markers DCX and ASCL1 did not significantly increase in treated animals. Nonetheless, the viral vector effectively infected the target area nearby the ischemic injury. Probably, the infection area was not sufficiently large to have a measurable effect on the infarct

volume and thus, to a much lesser extent on behavioral tests and neurogenic protein levels. Consistently, no DCX expression was observed in the immunohistochemical study. This could be explained by the short follow-up period of choice which was insufficient to detect DCX expression in infected astrocytes. In further studies, the analysis of earlier neurogenic markers such as ASCL1 could lead to more robust results.

To further improve the obtained results with translational perspectives, our final goal was to design a feasible delivery method which could improve the siRNA efficiency *in vitro.* Nanoparticles are known to be extremely adaptable delivery methods with target vectorization and even enable of reduce drug doses and thus, their side-effects [133][134]. We synthetized biodegradable silica capsules which were able to deliver their cargo inside an astrocyte cell line. These nanoparticles were tested for the *in vitro* transfection of *Gapdh* siRNA. Despite the treatment showed an effective knockdown of the *Gapdh* mRNA, more studies are required to reduce *in vitro* toxicity of the nanoparticles and to improve their effectivity.

Taken together, our results suggest that an approach based on siRNA silencing of the NOTCH1 signalling pathway could be a promising alternative for astrocyte reprogramming to the neural phenotype. This is the first time, to our knowledge, that *Rbpj* and

Hes1 silencing strategy is attempted aiming at stroke therapy with *in vivo* reprogramming purposes. Furthermore, the deeper understanding of the molecular pathways involved in cell fate determination is essential to improve these methods as well as longer follow-up periods to accurately determine the changes occurring in reprogrammed cells.

USC
UNIVERSIDADE
DE SANTIAGO
DE COMPOSTELA

8. Conclusions

1. The treatment with *Rbpj* siRNA induces the upregulation of *Ascl1* through the NOTCH1 inhibition for 7 days.
2. The treatment with *Hes1* siRNA induces the upregulation of *Ascl1* through the NOTCH1 inhibition for 7 days.
3. The *Hes1* siRNA has demonstrated to be more effective than the *Rbpj* siRNA in the upregulation of *Ascl1*.
4. The treatment with siRNA did not demonstrate a reprogramming of the cortex astrocytes.
5. The reactive astrocyte development of the glial scar reaches its maximum expression at 72h and it is maintained for 7 days.
6. The treatment with AAV5 vector did not reveal any reduction in the infarct volume or improvement in the behavioral test.
7. The biodegradable silica capsules are able to enter the cell through the endocytic pathway.
8. The biodegradable silica capsules are able to encapsulate the siRNA treatment and induce the knockdown expression of the target gen, opening a new possible translational approach for the ischemic stroke.

USC
UNIVERSIDADE
DE SANTIAGO
DE COMPOSTELA

9. Bibliography

[1] N. authors Listed, “The World Health Organization Monica Proyect (Monitoring trends and determinats in cardiovascular international disease): A major international collaboration,” *J. Clin. Epidemiol.*, vol. 41, no. 2, 1988.

[2] G. J. Hankey, “Stroke,” *Lancet*, vol. 389, pp. 641–654, 2017.

[3] R. L. Sacco *et al.*, “AHA / ASA Expert Consensus Document An Updated Definition of Stroke for the 21st Century,” *Stroke*, pp. 2064–2089, 2013.

[4] A. Di Carlo, “Human and economic burden of stroke,” *Age Ageing*, vol. 38, pp. 4–5, 2009.

[5] R. A. Grysiewicz, K. Thomas, and D. K. Pandey, “Epidemiology of Ischemic and Hemorrhagic Stroke : Incidence , Prevalence , Mortality , and Risk Factors,” *Neurol. Clin. NA*, vol. 26, no. 4, pp. 871–895, 2008.

[6] M. G. George, L. Fischer, W. Koroshetz, C. Bushnell, and M. Frankel, “CDC Grand Rounds : Public Health Strategies to Prevent and Treat Strokes,” *Morb. Mortal. Wkly. Rep.*, vol. 66, no. 18, pp. 479–481, 2017.

[7] E. Stevens, E. Emmett, Y. Wang, C. Mckevitt, and C. Wolfe, “The burden of stroke in Europe,” 2017.

[8] E. Rodríguez-castro *et al.*, “Trends in stroke outcomes in the last ten years in a European tertiary hospital,” *BioMed Cent. Neurol.*, vol. 18, no. 1, 2018.

[9] J. Castillo, J. Zarranz, and I. Rouco, “Enfermedades vasculares cerebrales (EVC),” in *Neurología*, III., Madrid: Elsevier, 2003, pp. 357–436.

[10] X. Ustrell-roig and J. Serena-leal, “Stroke . Diagnosis and Therapeutic Management of Cerebrovascular Disease,” *Rev. española Cardiol.*, vol. 60, no. Vi, pp. 753–769, 2007.

[11] L. Calandre *et al.*, “Risk Factors for Spontaneous Cerebral Hematomas . Case-Control Study,” *Stroke*, vol. 176, pp. 1126–1128, 196AD.

[12] V. L. Feigin, B. Norrving, and G. A. Mensah, “Global Burden of Stroke,” *Circ. Res.*, pp. 439–448, 2017.

[13] B. White *et al.*, “Global Brain Ischemia and Reperfusion,” *Ann. Emerg. Med.*, no. May, pp. 588–594, 1996.

[14] S. Arias-rivas, J. Vivancos-mora, J. Castillo, and D. Los, “Epidemiología de los subtipos de ictus en pacientes hospitalizados atendidos por neurólogos : resultados del

registro EPICES (I),” *Neurología*, vol. 54, no. I, pp. 385–393, 2012.

[15] A. Harold *et al.*, “Classification of Subtype of Acute Ischemic Stroke,” *Stroke*, vol. 24, no. 1, pp. 35–41, 1992.

[16] B. R. S. Broughton, D. C. Reutens, and C. G. Sobey, “Apoptotic Mechanisms After Cerebral Ischemia,” *Stroke*, vol. 40, pp. 331–339, 2009.

[17] B. R. S. Broughton, D. C. Reutens, and C. G. Sobey, “Apoptotic Mechanisms After Cerebral Ischemia,” 2009.

[18] J. Astrup, L. Symon, N. Branston, and N. Lassen, “Cortical Evoked Potential and Extracellular K + and H + at Critical Levels of Brain Ischemia,” *Stroke*, vol. 8, 1977.

[19] J. O. N. Hansen, “Effect of Anoxia on Ion Distribution in the Brain,” *Physiolgical Rev.*, vol. 65, no. 1, 1985.

[20] W. Blank and H. Kirshner, “The kinetics of extracellular potassium changes during hypoxia and anoxia in the cat cerebral cortex,” *Brain Res.*, vol. 123, no. 123, pp. 113–124, 1977.

[21] W. Choi, “Ionic Dependence of Glutamate Neurotoxicity,” *Th J. Neurosci.*, vol. 7, no. 2, pp. 369–379, 1987.

[22] W. Choi and M. Rothman, “The role of glutamate

neurotoxicity in hypoxic-ischemic neuronal death," *Annu. Rev. Neurosci.*, vol. 13, pp. 171–182, 1990.

[23] B. C. White, J. M. Sullivan, D. J. Degracia, B. J. O. Neil, R. W. Neumar, and L. I. Grossman, "Brain ischemia and reperfusion : molecular mechanisms of neuronal injury," *J. Neurol. Sci.*, vol. 179, pp. 1–33, 2000.

[24] D. W. Choi, "Excitotoxic Cell Death," *J. Neurobiol.*, vol. 23, no. 9, pp. 1261–1276, 1972.

[25] K. Schiene *et al.*, "Neuronal Hyperexcitability and Reduction of GABAA-Receptor Expression in the Surround of Cerebral Photothrombosis," *J. Cereb. bloof flow Metab.*, no. 16, pp. 906–914, 1996.

[26] B. C. White, J. M. Sullivan, D. J. Degracia, B. J. O. Neil, R. W. Neumar, and L. I. Grossman, "Brain ischemia and reperfusion: molecular mechanisms of neuronal injury," *J. Neurol. Sci.*, vol. 179, no. 1–2, pp. 1–33, 2000.

[27] K. J. Banasiak, Y. Xia, and G. G. Haddad, "Mechanisms underlying hypoxia-induced neuronal apoptosis," *Prog. Neurobiol.*, vol. 62, pp. 215–249, 2000.

[28] M. Grandati *et al.*, "Calcium-independent NO-synthase activity and nitrites / nitrates production in transient focal cerebral ischaemia in mice," *Br. J. Pharmacol.*, vol. 122,

pp. 625–630, 1997.

[29] S. Nogawa, F. Zhang, M. E. Ross, and C. Iadecola, “Cyclo-Oxygenase-2 Gene Expression in Neurons Contributes to Ischemic Brain Damage,” *J. Neurosci.*, vol. 17, no. 8, pp. 2746–2755, 1997.

[30] E. S. Mcdonald and A. J. Windebank, “MECHANISMS OF NEUROTOXIC INJURY AND CELL DEATH,” *Clin. Neurobehav. Toxicol.*, vol. 18, no. 3, pp. 525–540, 2000.

[31] A. Rami, R. Agarwal, and G. Botez, “m -Calpain activation , DNA fragmentation , and synergistic effects of caspase and calpain inhibitors in protecting hippocampal neurons from,” *Brain Res.*, vol. 866, pp. 299–312, 2000.

[32] W. M. Pardridge, “The Blood-Brain Barrier : Bottleneck in Brain Drug Development,” *NeuroRx*, vol. 2, no. January, pp. 3–14, 2005.

[33] N. J. Abbott, A. A. K. Patabendige, D. E. M. Dolman, S. R. Yusof, and D. J. Begley, “Neurobiology of Disease Structure and function of the blood – brain barrier,” *Neurobiol. Dis.*, vol. 37, no. 1, pp. 13–25, 2010.

[34] V. Muoio, P. B. Persson, and M. M. Sendeski, “The neurovascular unit – concept review,” *Acta Physiol.*, pp. 790–798, 2014.

[35] B. Obermeier, A. Verma, and R. M. Ransohoff, “The blood – brain barrier,” in *Handbook of Clinical Neurology*, 3rd ed., vol. 133, Elsevier B.V., 2016, pp. 39–59.

[36] J. Keaney and M. Campbell, “The dynamic blood – brain barrier,” *FEBS J.*, vol. 282, pp. 4067–4079, 2015.

[37] X. Jiang *et al.*, “Blood-brain barrier dysfunction and recovery after ischemic stroke,” *Prog. Neurobiol.*, pp. 144–171, 2019.

[38] K. E. Sandoval and K. A. Witt, “Neurobiology of Disease Blood-brain barrier tight junction permeability and ischemic stroke,” *Neurobiol. Dis.*, vol. 32, no. 2, pp. 200–219, 2008.

[39] R. Rodrigo *et al.*, “Oxidative Stress and Pathophysiology of Ischemic Stroke : Novel Therapeutic Opportunities,” *CNS Neurol. Disord. - Drug Targets*, no. 12, pp. 698–714, 2013.

[40] N. R. Sims, “Energy metabolism and selective neuronal vulnerability following global cerebral ischemia,” *Neurochem. Res.*, vol. 17, no. 9, pp. 923–931, 1992.

[41] N. R. Sims and H. Muyderman, “Mitochondria, oxidative metabolism and cell death in stroke,” *Biochim. Biophys. Acta - Mol. Basis Dis.*, vol. 1802, no. 1, pp. 80–91, 2010.

[42] S. E. Khoshnam, W. Winlow, M. Farzaneh, Y. Farbood, and H. F. Moghaddam, “Pathogenic mechanisms following ischemic stroke,” *Neurol. Sci.*, vol. 38, no. 7, pp. 1167–1186, 2017.

[43] M. Song and S. P. Yu, “Ionic Regulation of Cell Volume Changes and Cell Death after Ischemic Stroke,” *Transl. Stroke Res.*, vol. 5, no. 1, pp. 17–27, 2014.

[44] A. B. Gillentine, LN Berry, RP Goin-Kochel, MA Ali, J Ge, D Guffey, JA Rosenfeld, V Hannig, P Bader, M Proud, M Shinawi, BH Graham1, A Lin, SR Lalani, J Reynolds, M Chen, T Grebe, CG Minard, P Stankiewicz and C. Schaaf, “Neuropathophysiology of Brain Injury,” *J Autism Dev Disord*, vol. 47, no. 3, pp. 549–562, 2017.

[45] H. Prentice, J. P. Modi, and J.-Y. Wu, “Mechanisms of Neuronal Protection against Excitotoxicity, Endoplasmic Reticulum Stress, and Mitochondrial Dysfunction in Stroke and Neurodegenerative Diseases,” *Oxid. Med. Cell. Longev.*, vol. 2015, pp. 1–7, 2015.

[46] S. Manzanero, T. Santro, and T. V. Arumugam, “Neuronal oxidative stress in acute ischemic stroke: Sources and contribution to cell injury,” *Neurochem. Int.*, vol. 62, no. 5, pp. 712–718, 2013.

[47] Á. Chamorro, U. Dirnagl, X. Urra, and A. M. Planas, “Neuroprotection in acute stroke: Targeting excitotoxicity, oxidative and nitrosative stress, and inflammation,” *Lancet Neurol.*, vol. 15, no. 8, pp. 869–881, 2016.

[48] Q. Chen, S. Moghaddas, C. L. Hoppel, and E. J. Lesnefsky, “Ischemic defects in the electron transport chain increase the production of reactive oxygen species from isolated rat heart mitochondria,” *Am. J. Physiol. Physiol.*, vol. 294, no. 2, pp. C460–C466, 2008.

[49] D. J. DeGracia, “Regulation of mRNA following brain ischemia and reperfusion,” *Wiley Interdiscip. Rev. RNA*, vol. 8, no. 4, pp. 1–25, 2017.

[50] D. Chen, E. L. Thomas, and P. Kapahi, “HIF-1 modulates dietary restriction-mediated lifespan extension via IRE-1 in Caenorhabditis elegans,” *PLoS Genet.*, vol. 5, no. 5, 2009.

[51] N. Riaz, S. L. Wolden, D. Y. Gelblum, and J. Eric, “Targeting hypoxia signalling for the treatment of ischaemic and inflammatory diseases,” *Nat. Rev. Drug Discov.*, vol. 13, no. 11, pp. 852–869, 2014.

[52] M. E. Lindholm and H. Rundqvist, “Skeletal muscle

hypoxia-inducible factor-1 and exercise," *Exp. Physiol.*, vol. 101, no. 1, pp. 28–32, 2016.

[53] I. Ünal-Çevik, M. Kilinç, A. Can, Y. Gürsoy-Özdemir, and T. Dalkara, "Apoptotic and necrotic death mechanisms are concomitantly activated in the same cell after cerebral ischemia," *Stroke*, vol. 35, no. 9, pp. 2189–2194, 2004.

[54] E. Susan, "Apoptosis: A Reveiw of Programmed Cell Death," *Toxicol. Pathol.*, vol. 35, no. 4, pp. 496–516, 2007.

[55] D. R. Schultz and W. J. Harrington, "Apoptosis: Programmed cell death at a molecular level," *Semin. Arthritis Rheum.*, vol. 32, no. 6, pp. 345–369, 2003.

[56] J. Zhaoyu and S. E.-D. Wafik, "Overview of cell death signaling pathways, Cancer Biology & Therapy," *Cancer Biol. Ther.*, vol. 4, no. 2, pp. 139–163, 2005.

[57] D. V. and M. R. Antoine Drieu, Damien Levard, "Anti-inflammatory treatments for stroke: from bench to bedside," *Ther. Adv. Neurol. Disorde*, vol. 9, no. 6, pp. 259–261, 2018.

[58] S. C. Zhao, L. S. Ma, Z. H. Chu, H. Xu, W. Q. Wu, and F. Liu, "Regulation of microglial activation in stroke," *Acta Pharmacol. Sin.*, vol. 38, no. 4, pp. 445–458, 2017.

[59] J. Anrather and C. Iadecola, “Inflammation and Stroke: An Overview,” *Neurotherapeutics*, vol. 13, no. 4, pp. 661–670, 2016.

[60] M. Ahmad *et al.*, “Inflammation in Ischemic Stroke: Mechanisms, Consequences and Possible Drug Targets,” *CNS Neurol. Disord. - Drug Targets*, vol. 13, no. 8, pp. 1378–1396, 2014.

[61] S. Zhang, “Microglial activation after ischaemic stroke,” *Stroke Vasc. Neurol.*, 2019.

[62] R. Jin, L. Liu, S. Zhang, A. Nanda, and G. Li, “Role of inflammation and its mediators in acute ischemic stroke,” *Mol. Neurobiol.*, vol. 71, no. 2, pp. 233–236, 2013.

[63] L. Gu, Z. Jian, C. Stary, and X. Xiong, “T Cells and Cerebral Ischemic Stroke,” *Neurochem. Res.*, vol. 40, no. 9, pp. 1786–1791, Sep. 2015.

[64] M. V. Sofroniew, “Molecular dissection of reactive astrogliosis and glial scar formation,” *Trends Neurosci.*, vol. 32, no. 12, pp. 638–647, Dec. 2009.

[65] J. Cregg, M. A. DePaul, A. R. Filous, B. T. Lang, and A. Tran, “Functional Regeneration Beyond Glial Repair,” *Exp. Neurol.*, vol. 0, pp. 197–207, 2014.

[66] H. Kawano and J. Kimura-kuroda, “Role of the lesion scar in the response to damage and repair of the central nervous system,” *Cell Tissue Res.*, vol. 349, pp. 169–180, 2012.

[67] F. Fernández-klett and J. Priller, “The Fibrotic Scar in Neurological Disorders Astroglial scar,” vol. 24, no. 36, pp. 404–413, 2014.

[68] K. L. Adams and V. Gallo, “The diversity and disparity of the glial scar,” *Nat. Neurosci.*, vol. 21, no. 1, pp. 9–15, 2018.

[69] S. Sakai and T. Shichita, “Inflammation and neural repair after ischemic brain injury.,” *Neurochem. Int.*, 2018.

[70] T. Hayashi *et al.*, “Cerebral Ischemia and Angiogenesis,” *Curr. Neurovasc. Res.*, vol. 3, no. 2, pp. 119–129, 2006.

[71] J. Altman and G. D. Das, “Autoradiographic and histological evidence of postnatal hippocampal neurogenesis in rats,” *J. Comp. Neurol.*, vol. 124, no. 3, pp. 319–335, 1965.

[72] P. S. Eriksson *et al.*, “Neurogenesis in the adult human hippocampus.,” *Nat. Med.*, vol. 4, no. 11, pp. 1313–7, 1998.

[73] B. Machalinski, “Tissue regeneration in stroke: cellular and trophic mechanisms,” *Expert Rev. Neurother.*, vol. 14, no. 8, pp. 957–967, Aug. 2014.

[74] M. Kreuzberg, E. Kanov, O. Timofeev, M. Schwaninger, H. Monyer, and K. Khodosevich, “Increased subventricular zone-derived cortical neurogenesis after ischemic lesion,” *Exp. Neurol.*, vol. 226, no. 1, pp. 90–99, 2010.

[75] A. Arvidsson, T. Collin, D. Kirik, Z. Kokaia, and O. Lindvall, “Neuronal replacement from endogenous precursors in the adult brain after stroke,” *Nat. Med.*, vol. 8, no. 9, pp. 963–970, 2002.

[76] X.-Y. Xiong, L. Liu, and Q.-W. Yang, “Functions and mechanisms of microglia/macrophages in neuroinflammation and neurogenesis after stroke,” *Prog. Neurobiol.*, vol. 142, pp. 23–44, 2016.

[77] A. Schmidt and J. Minnerup, “Promoting recovery from ischemic stroke,” *Expert Rev. Neurother.*, vol. 16, no. 2, pp. 173–186, Feb. 2016.

[78] M. Lahr, G. Luijckx, P. Vroomen, D. Van der Zee, and E. Buskens, “The chain of care enabling tPA treatment in acute ischemic stroke: a comprehensive review of organisational models,” *J. Neurol.*, vol. 260, no. 4, pp.

960–968, 2012.

[79] J. M. Weinberger, “Evolving therapeutic approaches to treating acute ischemic stroke,” *J. Neurol. Sci.*, vol. 249, no. 2, pp. 101–109, Nov. 2006.

[80] M. D. Ginsberg, “Neuroprotection for ischemic stroke: Past, present and future,” *Neuropharmacology*, vol. 55, no. 3, pp. 363–389, Sep. 2008.

[81] J. L. Saver *et al.*, “Prehospital Use of Magnesium Sulfate as Neuroprotection in Acute Stroke,” *N. Engl. J. Med.*, vol. 372, no. 6, pp. 528–536, Feb. 2015.

[82] M. Pérez-Mato *et al.*, “Blood glutamate EAAT2-cell grabbing therapy in cerebral ischemia,” *EBioMedicine*, vol. 39, pp. 118–131, Jan. 2019.

[83] A. da Silva-Candal *et al.*, “Clinical validation of blood/brain glutamate grabbing in acute ischemic stroke,” *Ann. Neurol.*, vol. 84, no. 2, pp. 260–273, Aug. 2018.

[84] D. B. Mangus, L. Huang, P. M. Applegate, J. W. Gatling, J. Zhang, and R. L. Applegate, “A systematic review of neuroprotective strategies after cardiac arrest: from bench to bedside (Part I – Protection via specific pathways),” *Med. Gas Res.*, vol. 4, no. 1, p. 9, 2014.

[85] G. A. Matchett, M. W. Allard, R. D. Martin, and J. H. Zhang, “Neuroprotective effect of volatile anesthetic agents: molecular mechanisms,” *Neurol. Res.*, vol. 31, no. 2, pp. 128–134, Mar. 2009.

[86] Á. Chamorro *et al.*, “Safety and effi cacy of uric acid in patients with acute stroke (URICO-ICTUS): a randomised , double-blind phase 2b / 3 trial,” pp. 453–460.

[87] M. I. Ayuso and J. Montaner, “Advanced neuroprotection for brain ischemia: an alternative approach to minimize stroke damage,” *Expert Opin. Investig. Drugs*, vol. 24, no. 9, pp. 1137–1142, Sep. 2015.

[88] P. Venkat, M. Chopp, and J. Chen, “New insights into coupling and uncoupling of cerebral blood flow and metabolism in the brain,” *Croat. Med. J.*, vol. 57, no. 3, pp. 223–228, Jun. 2016.

[89] R. Veltkamp and D. Gill, “Clinical Trials of Immunomodulation in Ischemic Stroke,” *Neurotherapeutics*, vol. 13, no. 4, pp. 791–800, Oct. 2016.

[90] P. Dassan, M. M. Brown, S. M. Gregoire, G. Keir, and D. J. Werring, “Association of Cerebral Microbleeds in Acute Ischemic Stroke With High Serum Levels of Vascular Endothelial Growth Factor,” *Arch. Neurol.*, vol. 69, no. 9,

Sep. 2012.

[91] L. O. Kokaia Z, Tornero D, “Transplantation of reprogrammed neurons for improved recovery after stroke,” *Prog. Brain Res.*, vol. 231, pp. 245–263, 2017.

[92] S. S. Andrabi, S. Parvez, and H. Tabassum, “Melatonin and Ischemic Stroke: Mechanistic Roles and Action,” *Adv. Pharmacol. Sci.*, vol. 2015, pp. 1–11, 2015.

[93] E. Ramos *et al.*, “Ischemic brain injury: New insights on the protective role of melatonin,” *Free Radic. Biol. Med.*, vol. 104, pp. 32–53, Mar. 2017.

[94] L. Fang *et al.*, “Potentials of Cellular Reprogramming as a Novel Strategy for Neuroregeneration,” *Front. Cell. Neurosci.*, vol. 13, no. November, pp. 1–10, 2019.

[95] K. Takahashi, “Cellular Reprogramming,” *Cold Spring Harb. Perspect. Biol.*, pp. 1–2, 2014.

[96] L. A. Davis RL, Weintraub H, “Expression of a single transfected cDNA converts fibroblasts to myoblasts.,” *Cell*, pp. 987–1000, 1987.

[97] J. Ankshita Prasad, S. M. C. Manivannan, Daniel TB Loong, P. M. Gharibani, and & A. H. All, “A review of induced pluripotent stem cell , direct conversion by

reprogramming and oligodendrocyte differentiation," *Regen. Med.*, vol. 11, pp. 181–191, 2016.

[98] D. Srivastava and N. DeWitt, "In Vivo Cellular Reprogramming: The Next Generation," *Cell*, vol. 166, no. 6, pp. 1386–1396, 2016.

[99] A. Grath and G. Dai, "Direct cell reprogramming for tissue engineering and regenerative medicine," *J. Biol. Eng.*, vol. 9, pp. 1–15, 2019.

[100] C. Jopling, S. Boue, and I. Juan Carlos Belmonte, "Dedifferentiation, transdifferentiation and reprogramming: three routes to regeneration," *Nat. Rev. Mol. cell Biol.*, vol. 12, no. 2, pp. 79–89, 2011.

[101] A. Romito and G. Cobellis, "Pluripotent Stem Cells: Current Understanding and Future Directions," *Stem Cell Int.*, 2016.

[102] K. Takahashi and S. Yamanaka, "Induction of Pluripotent Stem Cells from Mouse Embryonic and Adult Fibroblast Cultures by Defined Factors," *Cell*, vol. 2, no. 126, pp. 663–676, 2006.

[103] T. Hamazaki, N. El Rouby, N. C. Fredette, K. E. Santostefano, and N. Terada, "Concise Review: Induced Pluripotent Stem Cell Research in the Era of Precision

Medicine Takashi," *Stem Cells*, vol. 35, no. 3, pp. 545–550, 2017.

[104] A. Guhr, S. Kobold, S. Seltmann, A. E. M. S. W. A. Kurtz, and P. LÖser, "Recent Trends in Research with Human Pluripotent Stem Cells: Impact of Research and Use of Cell Lines in Experimental Research and Clinical Trials," *Stem Cell Reports*, vol. 11, pp. 485–496, 2018.

[105] S. Margariti, K. Amy, and A. Cochrane, "Direct reprogramming of adult cells : avoiding the pluripotent state," *Stem Cells Cloning Adv. Appl.*, pp. 19–29, 2014.

[106] X. Xie, Y. Fu, and J. Liu, "Chemical reprogramming and transdifferentiation," *Curr. Opin. Genet. Dev.*, vol. 46, no. M, pp. 104–113, 2017.

[107] N. An, H. Xu, W. Gao, and H. Yang, "Direct Conversion of Somatic Cells into Induced Neurons," *Mol. Neurobiol.*, 2016.

[108] A. Cieślar-Pobudaa *et al.*, "Transdifferentiation and reprogramming: Overview of the processes, their similarities and differences," *BBA - Mol. Cell Res.*, vol. 1864, no. March, pp. 1359–1369, 2017.

[109] J. S. Mattick and I. V. Makunin, "Small regulatory RNAs in mammals," *Hum. Mol. Genet.*, vol. 14, pp. 121–132, 2005.

[110] P. N. Pushparaj, J. J. Aarthi, J. Manikandan, and S. D. Kumar, “siRNA, miRNA, and shRNA: In vivo applications,” *J. Dent. Res.*, vol. 87, no. 11, pp. 992–1003, 2008.

[111] G. C. Shukla, J. Singh, and S. Barik, “MicroRNAs: Processing, Maturation, Target Recognition and Regulatory Functions,” *Mol. Cell. Pharmacol.*, vol. 3, no. 3, pp. 83–92, 2012.

[112] J. Luginbühl, D. M. Sivaraman, and J. W. Shin, “Non-coding RNA Research The essentiality of non-coding RNAs in cell reprogramming,” *Non-coding RNA Res.*, vol. 2, no. 1, pp. 74–82, 2017.

[113] Y. Lu and A. S. Yoo, “Mechanistic Insights Into MicroRNA-Induced Neuronal Reprogramming of Human Adult Fibroblasts,” *Front. Neurosci.*, vol. 12, no. August, pp. 1–9, 2018.

[114] E. A. Jayawardena, Tilanthi M. J Egemnazarov, Bakytbek Finch *et al.*, “MicroRNA-mediated in vitro and in vivo Direct Reprogramming of Cardiac Fibroblasts to Cardiomyocytes,” *Circ. Res.*, vol. 110, no. 11, pp. 1465–1473, 2012.

[115] R. W. Carthew and E. J. Sibtgeuner, “Origins and Mechanisms of miRNAs and siRNAs Richard,” *Cell*, vol.

136, no. 4, pp. 642–655, 2010.

[116] J. Kazantseva, H. Sadam, T. Neuman, and K. Palm, “Targeted alternative splicing of TAF4: A new strategy for cell reprogramming,” *Sci. Rep.*, vol. 6, no. July, pp. 1–11, 2016.

[117] S. Dal-Pra, C. P. Hodgkinson, M. Mirotsou, I. Kirste, and V. J. Dzau, “Demethylation of H3K27 Is Essential for the Induction of Direct Cardiac Reprogramming by MIR Combo,” *Circ. Res.*, vol. 120, no. 9, pp. 1403–1413, 2017.

[118] X. Ma, L. Kong, and S. Zhu, “Reprogramming cell fates by small molecules,” *Protein Cell*, vol. 8, no. 5, pp. 328–348, 2017.

[119] H. Qin, A. Zhao, and X. Fu, “Small molecules for reprogramming and transdifferentiation,” *Cell. Mol. Life Sci.*, vol. 74, no. 19, pp. 3553–3575, 2017.

[120] T. Lin and S. Wu, “Reprogramming with small molecules instead of exogenous transcription factors,” *Stem Cells Int.*, vol. 2015, 2015.

[121] L. Zhang *et al.*, “Small Molecules Efficiently Reprogram Human Astroglial Cells into Functional Neurons,” *Cell Stem Cell*, vol. 17, no. 6, pp. 735–747, 2015.

[122] M. F. Naso, B. Tomkowicz, W. L. Perry, and W. R. Strohl, “Adeno-Associated Virus (AAV) as a Vector for Gene Therapy,” *BioDrugs*, vol. 31, no. 4, pp. 315–332, 2017.

[123] C. Elsner and J. Bohne, “The retroviral vector family: something for everyone,” *Virus Genes*, 2017.

[124] B. Kantor *et al.*, “Methods for Gene Transfer to the Central Nervous System,” *Adv. Genet.*, pp. 1–67, 2015.

[125] C. J.Burrell, C. R.Howard, and F. A.Murphy, “Chapter 23 - Retroviruses,” in *Fenner and White’s Medical Virology (Fifth Edition)*, 2017, pp. 317–344.

[126] T. Athanasopoulos, M. M. Munye, and R. J. Yáñez-muñoz, “Nonintegrating Gene Therapy Vectors,” *Hematol. Clin. NA*, vol. 31, no. 5, pp. 753–770, 2017.

[127] M. J. E. Havenga *et al.*, “Exploiting the Natural Diversity in Adenovirus Tropism for Therapy and Prevention of Disease,” *J. Virol.*, vol. 76, no. 9, pp. 4612–4620, 2002.

[128] Y. Yamamoto, M. Nagasato, T. Yoshida, and K. Aoki, “Recent advances in genetic modification of adenovirus vectors for cancer treatment,” *Cancer Sci.*, vol. 108, no. 5, 2017.

[129] K. Shimizu *et al.*, “Suppression of leaky expression of

adenovirus genes by insertion of microRNA-targeted sequences in the replication-incompetent adenovirus vector genome," *Mol. Ther. — Methods Clin. Dev.*, no. April, pp. 1–13, 2014.

[130] S. Daya and K. I. Berns, "Gene Therapy Using Adeno-Associated Virus Vectors," *Clin. Microbiol. Rev.*, vol. 21, no. 4, pp. 583–593, 2008.

[131] N. J. Philpott and A. J. Thrasher, "Use of Nonintegrating Lentiviral Vectors for Gene Therapy," *Hum. Gene Ther.*, vol. 489, no. June, pp. 483–489, 2007.

[132] J. Jeevanandam, A. Barhoum, Y. S. Chan, A. Dufresne, and M. K. Danquah, "Review on nanoparticles and nanostructured materials : history , sources , toxicity and regulations," *J. Nanotechnol.*, pp. 1050–1074, 2018.

[133] A. Z. Wilczewska, K. Niemirowicz, K. H. Markiewicz, and H. Car, "Nanoparticles as drug delivery systems," *Pharmacol. Reports*, vol. 64, no. 5, pp. 1020–1037, 2012.

[134] S. Tammam, P. Malak, D. Correa, O. Rothfuss, and M. E. Hassan, "Nuclear delivery of recombinant OCT4 by chitosan nanoparticles for transgene-free generation of protein-induced pluripotent stem cells," *Oncotarget*, vol. 7, no. 25, 2016.

[135] R. A. Barker, M. Götz, and M. Parmar, “New approaches for brain repair — from rescue to reprogramming,” *Nature*, pp. 3–8, 2018.

[136] A. Popa-wagner, D. Hermann, and A. Gresita, “Genetic conversion of proliferative astroglia into neurons after cerebral ischemia : a new therapeutic tool for the aged brain ?,” *Geroscience*, pp. 0–5, 2019.

[137] C. Heinrich *et al.*, “Directing astroglia from the cerebral cortex into subtype specific functional neurons,” *PLoS Biol.*, vol. 8, no. 5, 2010.

[138] J. M. Qi, L. Z. Kou, P. Yang, and X. C. F. Sun, “MicroRNA-365 modulates astrocyte conversion into neuron in adult rat brain after stroke by targeting Pax6,” *Glia*, no. January, pp. 1346–1362, 2018.

[139] C. Lin *et al.*, “Direct conversion of astrocytes into neuronal cells by drug cocktail,” *Cell Res.*, pp. 1269–1272, 2015.

[140] Y. Yu, Y. Ping, X. Bian, L. Shen, and G. Pei, “Direct Generation of Human Neuronal Cells from Adult Astrocytes by Small Molecules,” *Stem Cell Reports*, vol. 8, no. 3, pp. 538–547, 2017.

[141] W. Niu *et al.*, “In vivo reprogramming of astrocytes to neuroblasts in the adult brain,” *Nat. Cell Biol.*, vol. 15, no.

10, pp. 1–23, 2014.

[142] Z. Guo, L. Zhang, W. Zheng, Y. Chen, W. Fan, and C. Gong, “In vivo direct reprogramming of reactive glial cells into functional neurons after brain injury and in an Alzheimer’s disease model,” *Cell Stem Cell*, vol. 14, no. 2, pp. 188–202, 2014.

[143] J. P. Magnusson *et al.*, “A latent neurogenic program in astrocytes regulated by Notch signaling in the mouse,” *Science (80-.).*, vol. 346, no. 6206, pp. 237–241, 2014.

[144] J. P. Magnusson and J. Frise, “Stars from the darkest night : unlocking the neurogenic potential of astrocytes in different brain regions,” *Development*, pp. 1075–1086, 2016.

[145] E. R. Andersson and U. Lendahl, “Therapeutic modulation of Notch signalling-are we there yet?,” *Nat. Rev. Drug Discov.*, vol. 13, no. 5, pp. 357–378, 2014.

[146] G. P. Morris, A. L. Wright, R. P. Tan, and A. Gladbach, “A Comparative Study of Variables Influencing Ischemic Injury in the Longa and Koizumi Methods of Intraluminal Filament Middle Cerebral Artery Occlusion in Mice,” *PLoS One*, pp. 1–34, 2016.

[147] R. L. Lowery and A. K. Majewska, “Intracranial Injection of

Adeno-associated Viral Vectors," *Jove*, pp. 14–16, 2010.

[148] R. M. J. Deacon, "Measuring Motor Coordination in Mice," *J. Vis. Exp.*, no. May, pp. 1–8, 2013.

[149] G. B. Sukhorukov, E. Donath, S. Davis, H. Lichtenfeld, V. I. Popov, and H. Mo, "Stepwise Polyelectrolyte Assembly on Particle Surfaces: a Novel Approach to Colloid Design," *Polym. Adv. Technol.*, vol. 9, pp. 759–767, 1998.

[150] A. Ott *et al.*, "Light-addressable and degradable silica capsules for delivery of molecular cargo to the cytosol of cells," *Chem. Mater.*, vol. 27, no. 6, pp. 1929–1942, 2015.

[151] B. V. Parakhonskiy, A. Haase, and R. Antolini, "Sub-micrometer vaterite containers: Synthesis, substance loading, and release," *Angew. Chemie - Int. Ed.*, vol. 51, no. 5, pp. 1195–1197, 2012.

[152] J. O. Brien, I. Wilson, T. Orton, and Ë. Pognan, "Investigation of the Alamar Blue (resazurin) fluorescent dye for theassessment of mammalian cell cytotoxicity," *Eur. J. Biochem.*, vol. 267, pp. 5421–5426, 2000.

[153] G. Chen, M. Wernig, B. Berninger, M. Nakafuku, and M. Parmar, "In Vivo Reprogramming for Brain and Spinal Cord Repair," *eNeuro*, vol. 20, no. October, pp. 1–6, 2015.

[154] T. Yamashita, J. Shang, Y. Nakano, R. Morihara, and K. Sato, “In vivo direct reprogramming of glial linage to mature neurons after cerebral ischemia,” *Sci. Rep.*, pp. 1–7, 2019.

USC
UNIVERSIDADE
DE SANTIAGO
DE COMPOSTELA

Annexed

XUNTA DE GALICIA
CONSELLERÍA DO MEDIO RURAL

Departamento Territorial
Edificio Administrativo de Servizos Múltiples
Vicente Ferrer, 2
15071 – A Coruña

RESOLUCIÓN DE AUTORIZACIÓN DE PROXECTOS DE EXPERIMENTACIÓN ANIMAL

Expediente núm.: 15010/2019/004 **Data de inicio:** 05.02.2019
Persoa interesada: Francisco Campos Pérez **Procedemento:** resolución de autorización
Forma de inicio: solicitude da persoa interesada

ANTECEDENTES

A persoa interesada, como representante do centro CIMUS (Universidade de Santiago de Compostela), presentou con data 05.02.2019 unha solicitude para a realización do proxecto de experimentación animal (entrada no Rexistro Electrónico da Xunta de Galicia 2019/246024), cuxos datos se detallan a continuación:

Denominación do proxecto: *Nanopartículas biomiméticas para a administración dirixida de nanomedicinas*
Nome do centro usuario: Animalario do CIMUS
Persoa responsable do proxecto: Francisco Campos Pérez
Establecemento onde se realizarán os procedementos do proxecto (ou lugar xeográfico no caso de traballos de campo): Animalario do CIMUS
Clasificación do proxecto : Tipo I ☐ Tipo II ☐ Tipo III ☒

CONSIDERACIÓNS LEGAIS E TÉCNICAS

1 O Real decreto 53/2013, de 1 de febreiro (BOE 34, do 8 de febreiro), polo que se establecen as normas básicas aplicables para a protección dos animais utilizados en experimentación e outros fins científicos, incluíndo a docencia, establece no seu artigo 33 as condicións de autorizacións dos proxectos con animais de experimentación.

2 O artigo 88 da Lei 39/2015, de 1 de outubro, do procedemento administrativo común das administracións públicas (BOE 236, do 2 de outubro de 2015) establece que a resolución que poña fin o procedemento decidirá todas as cuestións expostas polos interesados e aquelas outras derivadas deste.

3 O Servizo de Gandaría da Coruña revisou a documentación achegada na solicitude e o resultado favorable da avaliación do proxecto, realizada polo órgano habilitado da Sección de Experimentación Animal do Comité de Bioética da Universidade de Santiago de Compostela.

Esta xefatura territorial é competente para ditar unha resolución, de conformidade co Decreto 149/2018, do 5 de decembro, polo que se establece a estrutura orgánica da

Departamento Territorial
Edificio Administrativo de Servizos Múltiples
Vicente Ferrer, 2
15071 – A Coruña

Consellería do Medio Rural e se modifica parcialmente o Decreto 177/2016, do 15 de decembro, polo que se fixa a estrutura orgánica da Vicepresidencia e das consellerías da Xunta de Galicia (DOG 235, do 11 de novembro).

De acordo con todo o indicado, RESOLVO:

1 Autorizar o proxecto solicitado.
2 O mencionado proxecto precisa someterse a unha avaliación retrospectiva tras finalizar a súa autorización.
3 A autorización deste proxecto terá unha duración de dous anos e unha vez transcorrido este tempo deberá ser autorizado de novo.

A citada autorización é unicamente válida nas condicións que figuran no expediente. Ante calquera cambio significativo no proxecto que poida ter efectos negativos sobre o benestar dos animais, deberá solicitar a confirmación da autorización ao Servizo Provincial de Gandaría.

Esta autorización poderá ser suspendida, no caso de que o proxecto non se leve a cabo de acordo coas condicións de autorización e retirala, previo expediente tramitado ao que se lle dará audiencia.

Contra a presente resolución, que non lle pon fin á vía administrativa, poderá interpoñer un recurso de alzada ante o conselleiro de Medio Rural. O prazo comezará a contar dende o día seguinte ao da recepción desta resolución. Todo isto, segundo o disposto nos artigos 121 e 122 da citada Lei 39/2015.

Mediante este escrito notifícaselle ao CIMUS da USC esta resolución segundo o esixido no artigo 40.1 da antedita Lei 39/2015.

VICERREITORÍA DE INVESTIGACIÓN
E INNOVACIÓN
Oficina de Investigación e Tecnoloxía
Servizo de Convocatorias e Recursos Humanos de I+S
Edificio CACTUS – Campus Vida
15782 Santiago de Compostela
Tel. 981 547 040 - Fax 981 547 077
Correo electrónico: cittinfo@usc.es
http://imaisd.usc.es

JOSÉ MANUEL CIFUENTES MARTÍNEZ, PRESIDENTE DEL COMITÉ DE BIOÉTICA DE LA UNIVERSIDAD DE SANTIAGO DE COMPOSTELA, cuya Sección de Experimentación animal ha sido designada como Órgano Habilitado para la evaluación de proyectos de experimentación animal por resolución de la Xunta de Galicia, con fecha 11 de noviembre de 2013, de acuerdo con lo exigido por el RD 53/2013 de 1 de febrero, por el que se establecen las normas básicas aplicables para la protección de los animales utilizados en experimentación y otros fines científicos, incluyendo la docencia,

INFORMA:

Que el proyecto de investigación titulado: **"Nanopartículas biomiméticas para la administración dirigida de nanomedicinas"** del que es investigador responsable **D. Francisco Campos Pérez,** ha sido examinado por el Comité de Bioética de esta Universidad, Sección de Experimentación Animal, llegando a las siguientes conclusiones:

Con respecto a su finalidad, se trata de un proyecto de investigación traslacional o aplicada cuyo objetivo fundamentale el desarrollo de nanosistemas biomiméticos basados en cubiertas celulares (extraídas de células madre mesenquimales y/o plaquetas) para dirigir nanomedicinas a su lugar de acción (diana).

- Con respecto a los requisitos de las 3Rs,
    - No cabe la posibilidad de reemplazo ya que no se han encontrado otros métodos o estrategias de ensayo que permitan llevar a cabo los experimentos propuestos en este trabajo.
    - La experimentación se realizará en un centro registrado como usuario de animales de experimentación por lo que la manipulación, manejo y supervisión de los animales durante todo el proyecto será llevada a cabo por personas capacitadas. El grupo investigador lo componen personas con capacitaciones A, B y C, lo que asegura su preparación para garantizar el bienestar animales durante todos los procedimientos (requisito de refinamiento).
    - Finalmente, con respecto al requisito de reducción, se considera que el número de animales a utilizar es el mínimo imprescindible para la obtención de los resultados.

- La clasificación de los procedimientos en función de su grado de severidad es de "leve pa ra los procedimientos 1, 3 y "severo" para los procedimiento 2 y 4.
- Con respecto al balance de los daños y los beneficios, los procedimientos se efectúan bajo analgesia y anestesia previa a la administración de sustancias e intervenciones quirúrgicas por lo que se minimiza el dolor, angustia y sufrimiento. Los métodos de sacrificio descritos (sobredosis de anestesia) se encuentran entre los indicados por el propio RD 53/2013.
- Se han examinado las situaciones y excepciones previstas en el punto e) del artículo 34. 2 encontrando que ninguna de ellas es aplicable en este proyecto.
- El el proyecto se clasifica como tipo III y por tanto debe ser sometido a evaluación retrospectiva. Este Comité considera que dicha evaluación debería efectuarse a los dos años de la concesión de la autorización.

VICERREITORÍA DE INVESTIGACIÓN
E INNOVACIÓN
Oficina de Investigación e Tecnoloxía
Servizo de Convocatorias e Recursos Humanos de I+S
Edificio CACTUS – Campus Vida
15782 Santiago de Compostela
Tel. 981 547 040 - Fax 981 547 077
Correo electrónico: cittinfo@usc.es
http://imaisd.usc.es

Por todas estas razones, este Comité acordó emitir un **INFORME FAVORABLE.**

En la evaluación de este proyecto NO HA EXISTIDO CONFLICTO DE INTERESES.

Lugo, 17 de abril de 2018

CONSEJERÍA DE MEDIO AMBIENTE,
ADMINISTRACIÓN LOCAL
Y ORDENACIÓN DEL TERRITORIO
Comunidad de Madrid

Ref.: CAP-1129-18

RESOLUCIÓN DE RECONOCIMIENTO DE LA CAPACITACIÓN E INCLUSIÓN EN EL REGISTRO DE PERSONAL QUE MANEJA ANIMALES UTILIZADOS, CRIADOS O SUMINISTRADOS CON FINES DE EXPERIMENTACIÓN Y OTROS FINES CIENTÍFICOS, INCLUYENDO LA DOCENCIA (Orden ECC/566/2015, de 20 de marzo)

Vista la solicitud formulada por D./DÑA. IGNACIO JOSÉ LÓPEZ LOUREIRO, con DNI/NIE 32705349Q, para obtener el reconocimiento de la capacitación para realizar las funciones de CUIDADO DE LOS ANIMALES, EUTANASIA DE LOS ANIMALES, REALIZACIÓN DE LOS PROCEDIMIENTOS en ROEDORES .

Visto el informe favorable del Área de Protección Animal.

Considerando que el solicitante cumple los requisitos para estimar su solicitud, por lo dispuesto en la Orden ECC/566/2015, de 20 de marzo, por la que se establecen los requisitos de capacitación que debe cumplir el personal que maneje animales utilizados, criados o suministrados con fines de experimentación y otros fines científicos, incluyendo la docencia.

Esta Dirección General ha resuelto: reconocer la capacitación a D./ DÑA. IGNACIO JOSÉ LÓPEZ LOUREIRO, con DNI/NIE 32705349Q, para realizar las funciones de CUIDADO DE LOS ANIMALES, EUTANASIA DE LOS ANIMALES, REALIZACIÓN DE LOS PROCEDIMIENTOS en ROEDORES.

El mantenimiento de esta capacitación se debe demostrar al menos cada ocho años, en los términos que establece el artículo 20 de la Orden ECC/566/2015, de 20 de marzo, a partir de la fecha de esta Resolución.

Contra esta Resolución, que no agota la vía administrativa, cabe interponer recurso de alzada en el plazo de un mes, contado desde el día siguiente a la recepción de esta notificación, ante el Viceconsejero de Medio Ambiente, Administración Local y Ordenación del Territorio, conforme a lo establecido en el artículo 121 y siguientes de la Ley 39/2015, de 1 de octubre, del Procedimiento Administrativo Común de las Administraciones Públicas.

EL DIRECTOR GENERAL DE AGRICULTURA Y GANADERÍA
(P.D.F Resolución de 2 de noviembre de 2015)
EL SUBDIRECTOR GENERAL DE RECURSOS AGRARIOS

Firmado digitalmente por JESUS CARPINTERO HERVAS
Organización: COMUNIDAD DE MADRID
Fecha: 2018.02.14 17:58:20 CET
Huella dig.: 0a123a0176468983b88e62727815b4012135b8ae

Fdo.: Jesús Carpintero Hervás

CONSEJERÍA DE MEDIO AMBIENTE,
ADMINISTRACIÓN LOCAL
Y ORDENACIÓN DEL TERRITORIO
Comunidad de Madrid

Ref.: CAP-1129-18

Vista la solicitud formulada por D./DÑA. IGNACIO JOSÉ LÓPEZ LOUREIRO, con DNI/NIE, 32705349Q para obtener el reconocimiento de la capacitación para realizar las funciones de CUIDADO DE LOS ANIMALES, EUTANASIA DE LOS ANIMALES, REALIZACIÓN DE LOS PROCEDIMIENTOS en ROEDORES, en base a lo señalado en la Orden ECC/566/2015, de 20 de marzo, por la que se establecen los requisitos de capacitación que debe cumplir el personal que maneje animales utilizados, criados o suministrados con fines de experimentación y otros fines científicos, incluyendo la docencia.

Revisada la documentación, se procede a informar favorablemente del reconocimiento de la capacitación para realizar las funciones de CUIDADO DE LOS ANIMALES, EUTANASIA DE LOS ANIMALES, REALIZACIÓN DE LOS PROCEDIMIENTOS en ROEDORES .

ÁREA DE PROTECCIÓN ANIMAL
La Técnica Veterinaria
Firmado digitalmente por MARIA JOSEFA MORENO MELLADO
Organización: COMUNIDAD DE MADRID
Fecha: 2018.02.14 09:40:03 CET
Huella dig.: 0a123a0176468983b88e62727815b4012135b8ae

Fdo. Mª Josefa Moreno Mellado

CONSEJERÍA DE MEDIO AMBIENTE,
ADMINISTRACIÓN LOCAL
Y ORDENACIÓN DEL TERRITORIO

Comunidad de Madrid

Certificado de reconocimiento de la capacitación para manejar animales utilizados, criados o suministrados con fines de experimentación y otros fines científicos, incluyendo la docencia. Orden ECC/566/2015, de 20 de marzo

D./Dña. IGNACIO JOSÉ LÓPEZ LOUREIRO, con DNI/NIE 32705349Q ha obtenido el reconocimiento de la capacitación para realizar las funciones de:

CUIDADO DE LOS ANIMALES

EUTANASIA DE LOS ANIMALES

REALIZACIÓN DE LOS PROCEDIMIENTOS

en los siguientes grupos de especies animales:

ROEDORES

Nº de certificado: CAP-1129-18

ORGANISMO QUE EXPIDE EL CERTIFICADO

Dirección General de Agricultura y Ganadería. Consejería de Medio Ambiente, Administración Local y Ordenación del Territorio. Comunidad de Madrid

El reconocimiento de la capacitación para la realización de las funciones relacionadas en este certificado surtirá efecto en todo el territorio nacional.

Fecha	**Sello**

EL DIRECTOR GENERAL DE AGRICULTURA Y GANADERÍA

(P.D.F Resolución de 2 de noviembre de 2015)

EL SUBDIRECTOR GENERAL DE RECURSOS AGRARIOS

Firmado digitalmente por JESUS CARPINTERO HERVAS
Organización: COMUNIDAD DE MADRID
Fecha: 2018.02.14 18:02:47 CET
Huella dig.: 0a123a0176468983b88e62727815b4012135b8ae

Fdo: Jesús Carpintero Hervás